Design and Numerical Analysis of Hydrokinetic Turbine System for Small Scale Irrigation; A Case Study of Tedecha Village in Awash River Basin

Gera Worku Gelaneh

A Thesis Submitted to the Department of Mechanical Engineering,

School of Mechanical, Chemical and Materials Engineering

Presented in Partial Fulfillment of the Requirement for the Degree of Master of Science in Thermal Engineering

Office of Graduate Studies

Adama Science and Technology University

May,2024

Adama, Ethiopia

Design and Numerical Analysis of Hydrokinetic Turbine System for Small Scale Irrigation; A Case Study of Tedecha Village in Awash River Basin

Gera Worku Gelaneh

Advisor Dr. Addisu Bekel (Associate Professor in Thermal Engineering)

A Thesis Submitted to the Department of Mechanical Engineering,

School of Mechanical, Chemical and Materials Engineering

Presented in Partial Fulfillment of the Requirement for the Degree of Master of Science in Thermal Engineering

Office of Graduate Studies

Adama Science and Technology University

May, 2024

Adama, Ethiopia

DECLARATION

I hereby declare that this Master Thesis entitled "Design and Numerical Analysis of Hydrokinetic Turbine System for Small Scale Irrigation; A Case Study of Tedecha Village in Awash River Basin" is my original work. That is, it has not been submitted for the award of any academic degree, diploma or certificate in any other university. All sources of materials that are used for this thesis have been duly acknowledged through citation.

Gera Worku Gelaneh	__________	__________
Name of student	Signature	Date

RECOMMENDATION OF ADVISOR

I, the advisor of this thesis, hereby certify that I have read the revised version of the thesis entitled “Design and Numerical Analysis of Hydrokinetic Turbine System for Small Scale Irrigation; A Case Study of Tedecha Village in Awash River Basin” prepared under my guidance by Gera Work Gelaneh submitted in partial fulfillment of the requirements for the degree of Master of Science in Thermal Engineering. Therefore, I recommend the submission of the thesis to the department following the applicable procedures.

Dr. Addisu Bekele	______________________	_______________
Advisor	Signature	Date

APPROVAL PAGE

I, the advisor of the thesis entitled "Design and Numerical Analysis of Hydrokinetic Turbine System for Small Scale Irrigation; A Case Study of Tedecha Village in Awash River Basin" by Gera Worku Gelaneh, hereby certify that the recommendation and suggestions made by the board of examiners are appropriately incorporated into the final version of the thesis.

Dr. Addisu Bekele ________	____________________	______________
Advisor	Signature	Date

We, the undersigned, members of the Board of Reviewers of the thesis by Gera Worku Gelaneh have read and evaluated the thesis entitled "Design and Numerical Analysis of Hydrokinetic Turbine System for Small Scale Irrigation; A Case Study of Tedecha Village in Awash River Basin" and examined the candidate during open defense. This is, therefore, to certify that the thesis is accepted for partial fulfillment of the requirement of the degree of Master of Science in Thermal Engineering.

Chairperson	Signature	Date
Internal Examiner	Signature	Date
External Examiner	Signature	Date

Final approval and acceptance of the thesis is contingent upon submission of its final copy to the Office of Postgraduate Studies (OPGS) through the Department Graduate Council (DGC) and School Graduate Committee (SGC).

Department Head	Signature	Date
School Dean	Signature	Date
Office of Postgraduate Studies, Dean	Signature	Date

ACKNOWLEDGEMENT

First of all, I would like to address my deepest gratitude for the almighty God, whom have never stop his mercy upon me and gives strength to finish this thesis. Next to God, I would like to express my deepest and sincere gratitude to my thesis advisor Dr. Addisu Bekele for his providing guidance, unwavering support and supervision from the beginning to the ending of the study. I would like to thanks my friends lemi jambo and habitamu Shambel for their immeasurable support during the hard time of the site assessments in awash river and also I would like to said thanks to my parents and friends for their all indispensable supports during the journey of the study.

The last but not the list, I would like to express my sincere gratitude for all maintenance staffs of koka hydroelectric power plants gives advice and supports in many aspects and specially the maintenance in charge Mr, Yafet Tesfaye contribution was higher.

ABSTRACT

Renewable energy is the best source of energy generation now a day across the globe. Ethiopia has a plenty of flowing rivers throughout the country. Agriculture is the backbone of the country economy. Awash River is one of the main rivers that used widely for irrigation but it has no power supply access for irrigation purpose. Due to this, reason the site assessments takes place at tedecha in Awash River and get average flow velocity 1.92m/s. This velocity is too low to get the required power supply for the purposes of irrigation pumps. Due to this reason design the flow accelerator rectangular duct that changes the velocity from 1.92m/s to 4.6m/s. Based on this flow velocity designing the curtain hydrokinetic savonuis turbine technology designed for the selected site and 3D modeling of ducted hydrokinetic savonius turbine with curtain system is modeled. From the designed the output power of the turbine is 13.6KW generated. Based on this power output three-phase AC synchronous STC generator with the rated output power of 15KW, apparent power of 18.8KVA with 1500RPM selected and pump type of electric high flow rate centrifugal water pump with maximum power rating of 10KW were selected.

From the numerical analysis of the turbine blade with and without curtain are analyzed by power coefficient of without curtain is maximum at TSR=0.8 with C_P *=0.15 and the maximum power coefficient for curtain blade is at TSR=1 with* C_P *=0.28. Therefore, from those above values can be concluded that the Awash River at Tedecha has higher hydrokinetic potential for irrigation and the savonius blade with curtain design is more efficient than without the curtain blade.*

Key words*: - Renewable Energy, Hydrokinetic Turbine, Synchronous Generator, Power Coefficient, 3D Modeling*

TABLE OF CONTENT

LIST OF TABLES

LIST OF FIGURE

ACRONMYS

AC	Alternative current
AR	Aspect Ratio
CFD	Computational fluid dynamics
DC	Direct current
DEM	Digital Elevation Model
FDC	Flow Duration Curve
GHG	Greenhouse Gas
GIL	Grid Independence Limit
GR	Gap Ratio
HKT	Hydrokinetic turbine
KW	Kilowatt
MW	Mega watt
OR	Overlap Ratio
PD	Power Density
RANS	Reynolds-averaged Navier–Stokes
STC	Serial Transfer Complete
TSR	Tip Speed Ratio

CHAPTER ONE

INTRODUCTION

1.1 Background of the Study

The world's energy demand is rising sharply due to population growth and industrialization. Even though renewable energy technologies are developing quickly these days, the energy market is still dominated by fossil fuels. Climate change and the emission of greenhouse gases (GHGs) are caused by this. Renewable energy is, however, expected to grow at the fastest rate over the next 20 years, according to the trend forecast for primary energy sources. 69% of the world's net electricity generation is predicted to rise, from 21.6 trillion KWh in 2012 to 36.5 trillion KWh in 2040, with 11 trillion KWh coming from renewable energy sources. Africa, which has one of the world's greatest rates of population growth, will confront a significant energy-related challenge in the years to come. Over 600 million people in sub-Saharan Africa will not have access to consistent electricity by 2030, with the majority relying on conventional energy sources. It arrives in our nation. Ethiopia is making significant efforts to develop renewable energy technologies and leave a green legacy, but traditional fuels like charcoal, fuel wood, dung cakes, and agricultural residues still account for the majority of the country's energy consumption (≈87%). These fuels pose a number of health and environmental risks. Numerous renewable energy sources, including as solar, hydro, wind, and geothermal, are abundant; nevertheless, at now, only 5% of its total hydropower potential is being utilized, while other sources remain underutilized (Tiruye et al., 2021).

Ethiopia is fortunate blessed and gifted with abundant water bodies that can be used to fulfill its continuous growing energy demand, despite being non-oil producing and landlocked country (Abebe, 2014). Thus, for more than a century, energy-related research and analysis have been conducted from an economic perspective. This is because energy plays a crucial role in all areas of economic activity and is essential to economic progress.

Consequently, countries have started to explore and utilize their energy resources in order to maintain economic expansion. Furthermore, achieving energy security and lowering poverty in rural areas of developing nations like Ethiopia requires a shift from traditional to modern energy sources. Moreover, the most popular option for energy sources is conventional energy sources like coal, gas, and oil. However, excessive usage of them increases greenhouse gas emissions and damages to the ecosystem (Bhattacharyya, 2019). It is necessary to use another alternate energy source as a result. Solar, hydropower, these alternative energy sources include biomass, geothermal, wind, and oceanic resources. Compared to traditional energy sources, renewable energy sources provide a number of advantages, such as greater energy security, cleanliness renewability, eco-friendliness, and less facility maintenance (Guta, 2018).

Due to a large amount of investment requirement to construct and build there have been significant complaints leveled at traditional hydropower due to dams, turbine complexity, and the impact on ecosystem disturbance (Gailiusis et al., 2017). Therefore, in comparison to dam-based hydropower technology, hydrokinetic technology is the ideal choice for small-scale power generation, such as use for small-scale irrigation and household in off-grid electricity generation (Tigabu et al., 2019).

1.1.1 Working Principle of HKT

The general operating principle of all HKT systems, whether for tidal or river current applications, is the same: the kinetic energy of freely flowing water streams is extracted and transformed into the mechanical energy of rotating blades, which is then transformed into useable power, mostly electricity. As the water turns the turbine's rotor blades, the kinetic energy of the river current is transformed into mechanical energy. A shaft that is attached to the turbine powers a generator. To transform mechanical energy into electrical energy, a gearbox unit is connected to a generator, usually of the permanent magnet variety.

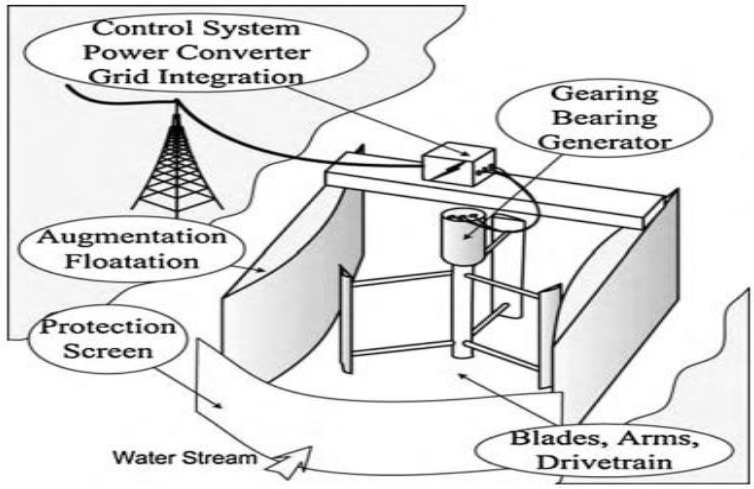

Figure 1.1 The HKT energy converter system outline (Khan, 2008)

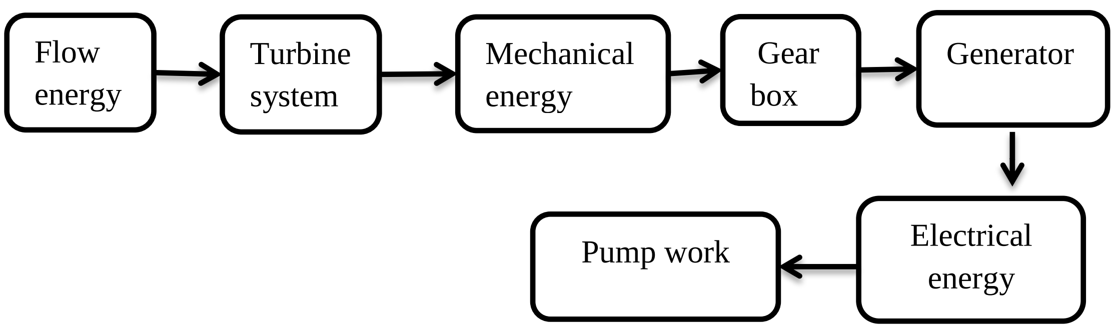

Figure 1.2 Schematic diagram of HKT

The hydrokinetic turbine is working under a flow of river with zero head. The turbine blade starts to rotate due to the energy of the water velocity to create rotational mechanical energy. This created energy on the blade develops rotational moment on the generator shaft and then produce electrical energy by a generator, thereby produce the useable form of electrical energy. This energy used to drive the electrical irrigation pumps

1.1.2 Hydrokinetic technology classification

The general classification hydrokinetic system can be categorized by based on their physical arrangements (Khan et al., 2009) is given below

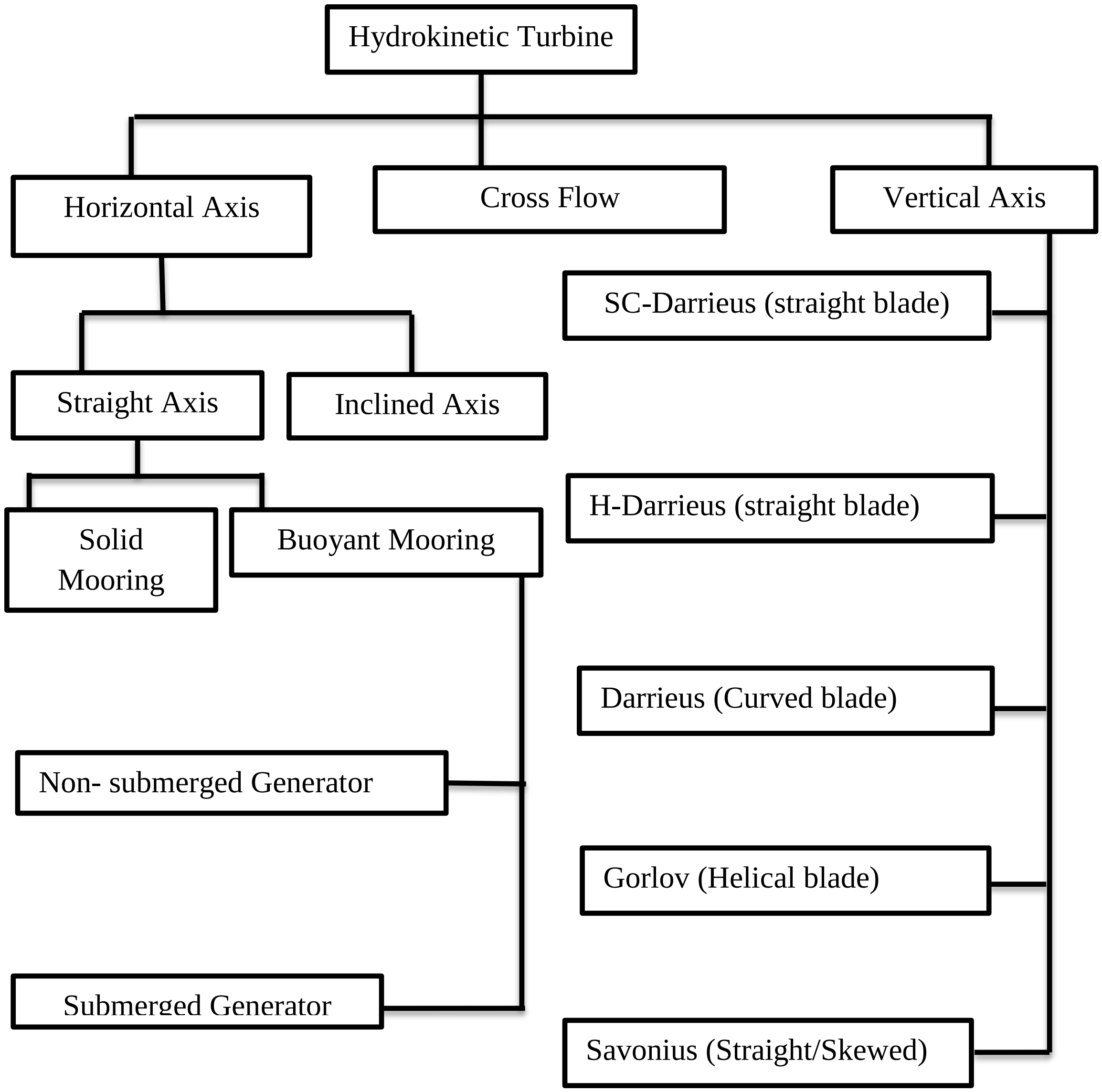

Figure 1.3 Classification of turbine rotors

1.2 Statements of the Problem

The problem of energy is one of the critical issues in our countries. According to World Bank report, only 54.19% of Ethiopians have access of electrification currently (World Bank, 2023). The remote rural communities have no access of grid electricity due to these many social-economic problems are existed.

In Ethiopia economic policy is agricultural lead industry due to this reason agriculture is the backbone of the country economy but power supply for irrigational activity is very low due to many reason. Most of peoples live near to Awash River basin are farmers and irrigation is one of the best activities of generating income. Currently the farmers live in around Tedecha village in Awash River basin uses fuel operated water pumps for irrigation, but now days the cost of diesel is rapidly increasing, the cost of maintenance on diesel generator pump system is expensive and its GHG emission is very high as well as indirectly the cost of agricultural products increased from day today.

Existing hydrokinetic turbine designs is not be optimized for the specific flow characteristics and irrigation requirements of Techada village and also the design approach is not considering local water flow data. The potential of the site remains unused due to the lack of a suitable hydrokinetic turbine system designed for small-scale irrigation needs.

Due to the above critical problems exist on the selected site tedecha using savonius type of hydrokinetic turbine is the best option to use the free flowing river energy. Designing and numerically simulating of the ducted hydrokinetic curtain savonius type of turbine to the site. In order to improve the performance of the turbine, using ducted type for improving the low river flow velocity and using curtain to concentrate the flow in to the advancing blade and covering the returning blade these improve the performance of the blade to produce sufficient amount of energy for small scale irrigation at tedecha.

1.3 Objectives of Research

1.3.1 General objectives of the research

The general objective of the research is site assessment, designing, modeling study of hydrokinetic turbine system for Tedecha village small-scale irrigation in Awash River basin.

1.3.2 Specific objectives of the research

- Analyzing the river flow data of the site and estimate the flow velocity
- Studying hydrokinetic turbine performance improvement techniques
- Design and modeling of HKT blade
- Hydrodynamic performance analysis of the HKT blade
- CFD modeling and analysis of fluid flow over the blade

1.4 Significance of the Study

In this study, the potential of Awash River at Tedecha village in hydrokinetic energy production for irrigation purpose has been investigated and the main contribution of the study is to propose the farmer to use hydrokinetic turbine system to run water pump instead of fuel operated water pump used for irrigation in Awash River. It will act as a cornerstone and the development of hydrokinetic turbines technology in the sites in the free flowing river.

In this study, potential of Awash River at Tedecha village in hydrokinetic energy production for irrigation purpose has studied. The main contribution of the study is designing and modeling of the HKT to the site based on the results of assessments and measurement records taken from the site. It gives encouragement for the farmer to use hydrokinetic turbine system to run water pump instead of fuel operated water pump used for irrigation in Awash River in many aspects. It gives clean; free and sustainable energy supply for Tedecha village farmers, which are far from electric power supply. It will give a clue to other researchers in the area of hydrokinetic turbines technology in Ethiopia.

1.5 Scope of the Study

The main scopes of the study is carried out site assessment, studying the performance improvement techniques and based on the results provided from measurements and historical discharge designing and modeling hydrokinetic turbine system, selecting appropriate water pumps, generators according to the design parameters. CFD performance analyses of the turbine blades with and without curtain are studied.

CHAPTER TWO

LITERATURE REVIEW

2.1 Introduction

A review of the literature was produced using a variety of sources, including books, journals, articles, and more. All significant research and findings from earlier studies conducted by other researchers are included in this chapter. Before conducting any further research, it is crucial to conduct a literature review because the relevant data might provide guidance for future investigations. Understanding the research clearly is aided by reviewing the literature before beginning the thesis study. By reviewing the literature, one can learn enough to ensure that the topic is well grasped and that the research can be completed. An analysis of the paper was done to find studies that were pertinent to the subject.

2.2 Research on Hydrokinetic Technology

In general, in addition to new blade designing, mainly of recent and former research in the hydrokinetic technology mainly focused on,

- ✓ Site assessment
- ✓ Turbine performance improvement

In order to ascertain the energy capacity and guarantee that the site is appropriate for energy harvesting, site assessment is crucial. A duct or shroud, addition, and innovative turbine design can all increase the turbine's performance.

2.2.1 Site Assessment Studies

Lack of proper information resulting from the paucity of research on hydrokinetic resource assessment in Ethiopia is one of the potential issues that could work against hydrokinetic development in that nation. There is need to identify resourceful sites to harness hydrokinetic energy. This would require looking into the large and small-scale site assessment, figuring out the annual energy yield, and analyzing the characteristics of the rivers.

Numerous evaluation and practicability studies have looked into the possibility of using river currents to harvest hydrokinetic energy. Technical resource estimation was done for river segments where the average long-term runoff flow water velocity exceeded 0.4m/s and the depth exceeded 0.5m. These small and medium-sized rivers in Lithuania have an estimated capacity of 13.6MW, and they can produce 79.4GWh of electric energy annually (Sarauskiene, 2017). In the Initial assessment, Canada has 340GW of energy potential in river current (Jenkinson et al., 2014). In the Amazon River basin (Jamari and Curua Ana river) studied collecting basic river data such as depth, sectional area, and velocity 109.5KW and 31.5KW potential powers produce respectively (Santos et al., 2019).

Muluken et al., (2020) study about the potential for hydropower in the Upper Blue Nile Basin. They assessed rivers and canals to see how much power could be generated using small-scale turbines (HKTs). The study found that the Gilgel-Abay River has the highest potential, with a maximum water velocity exceeding 1 meter per second and a power output of 3.4 kilowatts per square meter. This potential is present along more than 32% of the river's length. The Gumara River also showed potential, with suitable conditions for HKTs along 25% of its length, and a maximum power output of 1.4 kilowatts per square meter. Finally, the Bahirdar-Abay River demonstrated potential for HKTs along over 29% of its length, with a maximum power output of 2.6 kilowatts per square meter.

Wee Tan et al., (2021) developed a prototype HKT that generated a decent amount of power (92 watts) from a relatively modest current velocity (1.3 meters per second) in Malaysia. The study found that this prototype could produce about 2.2 kilowatt-hours of energy per day, which is enough to power a household in a remote area. This could mean lighting, charging batteries, and even improving the quality of life for people living off the grid. The researchers also highlighted that these HKTs could be used independently or in combination with solar power systems, which are already popular for remote electrification. This flexibility makes them a promising option for communities in need of reliable energy sources.

2.2.2 Hydrokinetic Turbines Types

Hydrokinetic systems, is a technology in renewable energy, can be categorized based on their energy conversion methods and the fundamental principles governing their operation

1) Horizontal axis hydrokinetic turbines

Horizontal axis turbines designed either with their rotational axis parallel or at an angle to the direction of the flowing water. One key advantage of this design is that the turbine can start spinning even in slow-moving currents. However, a drawback is that they are more susceptible to clogging with debris from the river, and the manufacturing cost tends to be higher.

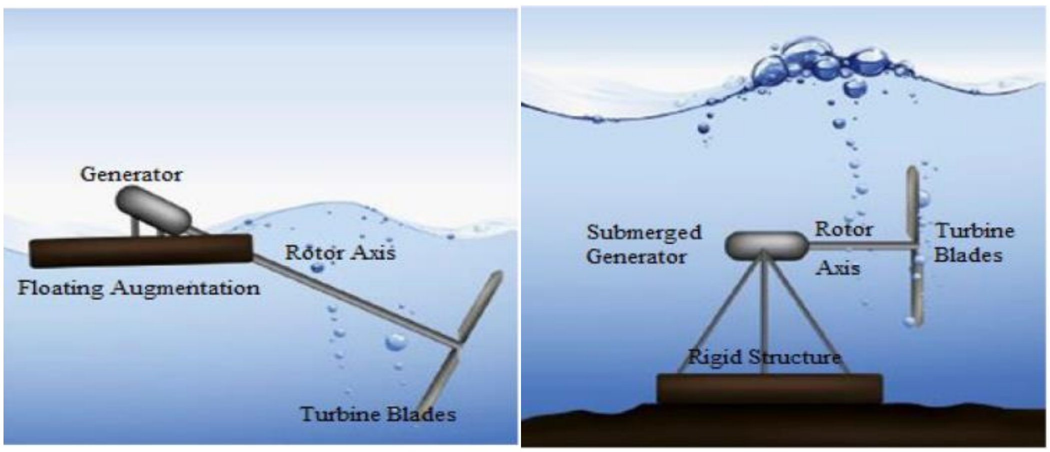

a) Inclined axis b) Rigid Mooring

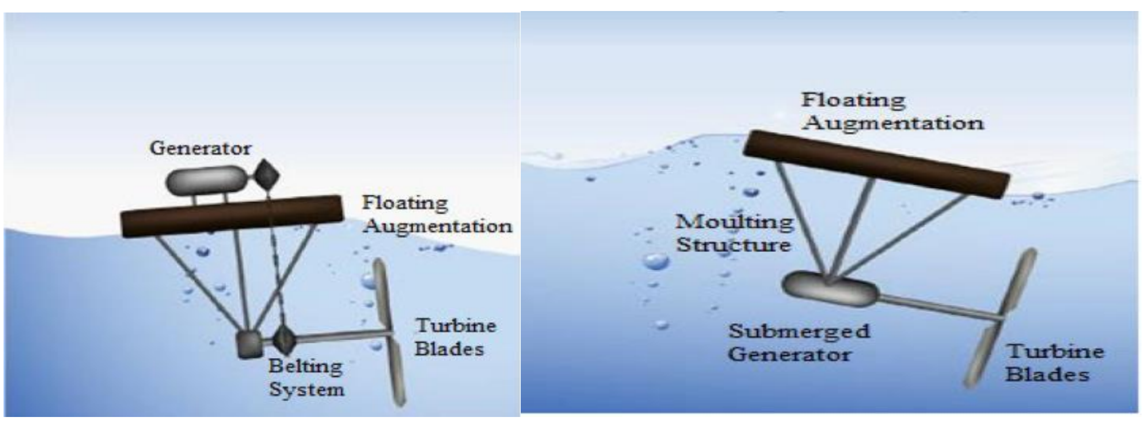

c) Non Submerged Generator d) Submerged Generator

Figure 2.1 Horizontal axis turbines (Ibrahim et al., (2021))

2) Vertical axis hydrokinetic turbines

Vertical axis turbines are a popular choice for harnessing the kinetic energy of rivers. Their unique design, with the rotor's axis of rotation perpendicular to the water's surface, allows them to operate without a yawing device, meaning they can handle water flow from any direction. This design also contributes to their quieter operation and simpler mechanical construction. Additionally, VAHKT don't require gearing, and their placement above the waterline can lead to lower costs.

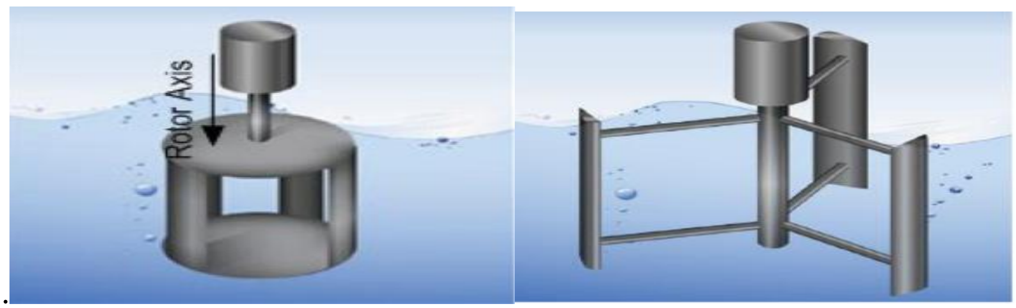

a) Squirrel Cage Savonius b) H- Darrieus

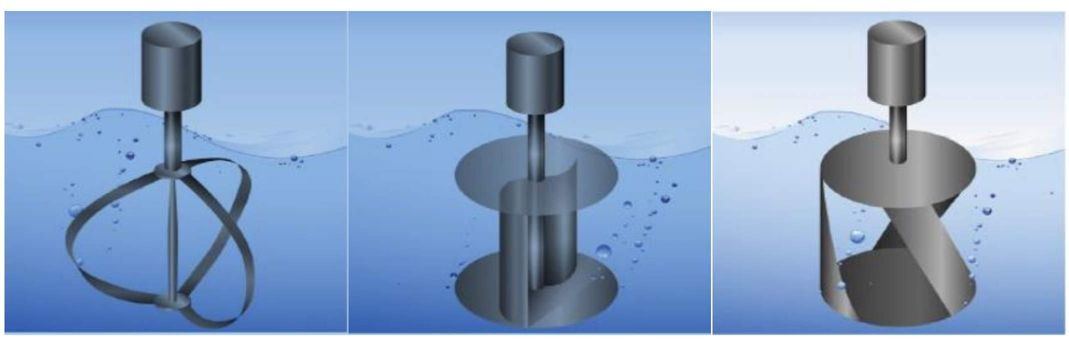

c) Darrieus d) Savonius e) Gorlov

Figure 2.2 Types of Vertical axis turbines (Ibrahim et al., (2021))

3) Cross-flow hydrokinetic turbines

Cross-flow turbines designed with their rotor axis perpendicular to the water flow but parallel to the water's surface. Like vertical axis turbines, they do not need a yawing mechanism to adjust to different flow directions. This makes them ideal for hydrokinetic farms or arrays, as they arranged more efficiently in terms of space, and their rectangular swept area helps maximize power output. Furthermore, operates at lower speeds, reducing cavitation, noise levels, and potential harm to marine life.

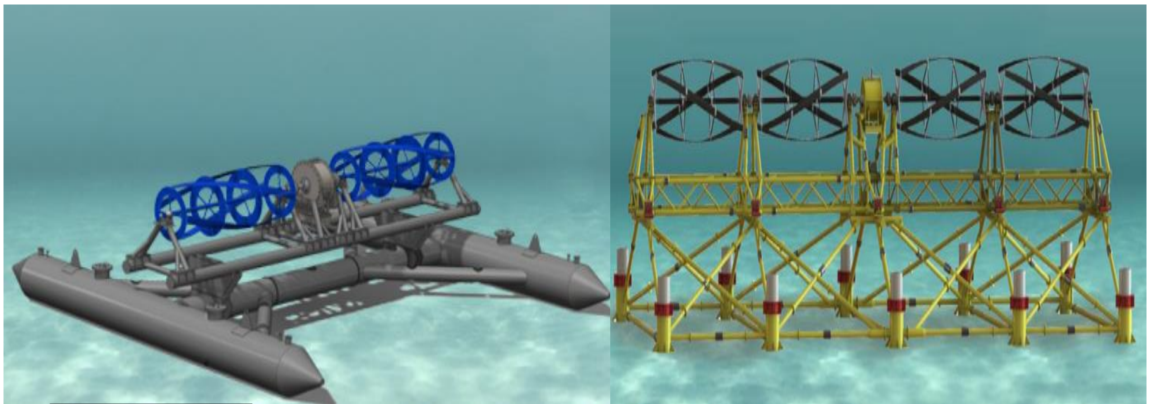

a) RivGen

b) TidGen.

Figure 2.3 the Cross-flow turbine (Ibrahim et al., (2021))

2.2.3 Comparison of the Turbine Type

Salleh et al., (2019) found that horizontal axis hydrokinetic turbine (HKT) systems perform best in high velocity water currents, making hen more suitable for ocean and tidal application.in contrast, vertical axis HKT systems excel in lower flow rates, typically below 1 meter per second ,and are well suited for shallow channels and areas with varying water velocities. These characteristics make them ideal for lower river current applications. Additionally, the simpler and smaller blade designs of vertical axis systems contribute to their lower manufacturing and maintenance costs.

Behrouzi et al., (2016) investigated darrieus turbines, which are lift-based designs with various sub configurations. These turbines generally have higher efficiency compared to savonius turbines. However, they struggle to start on their own. In contrast, savonius turbines, which are drag based, have a better self-staring capability and can operate effectively in lower flow rates.

Akwa et al., (2012) concludes on the research studies about the Savonius turbine, with their simple uniformly thin curved blades have a significant advantage over darrieus turbines, which require more complex airfoil-shaped blades. This simpler design translates to lower manufacturing and maintenance costs of the entire system. Additionally, savonuis turbines perform well in low flow rates, having good starting characteristics, and generate high static torque. These features make them a practical choice for river current hydrokinetic turbine (HKT) systems, especially for providing sustainable power to remote areas and communities lacking access to electricity

According to the above literature reviews on the site assessment and feasibility, the type of turbine comparisons on different parameters the savonius hydrokinetic turbine selected for this research work.

2.2.4 Working Principle of Savonius Turbine

The operating principles of the savonuis turbine is based on the difference in resistance forces between the forward and backwardblades.at the turbine rotates the leading blade collects the incoming free stream in its concave surface while the convex surface of the returning blades deflects the flow. Therefore the advancing blade of the incoming flow experiences a greater drag force than the returning blade. This drag force creates a positive torque on the leading rotor blade (with the counter clockwise direction consider positive) and a negative torque on the retreating rotor blade. This impedes the rotational moment on the turbine. Because the drag force are between the rotor blades, a net positive torque drives the counter clockwise rotational motion of the turbine about the central turbine shaft

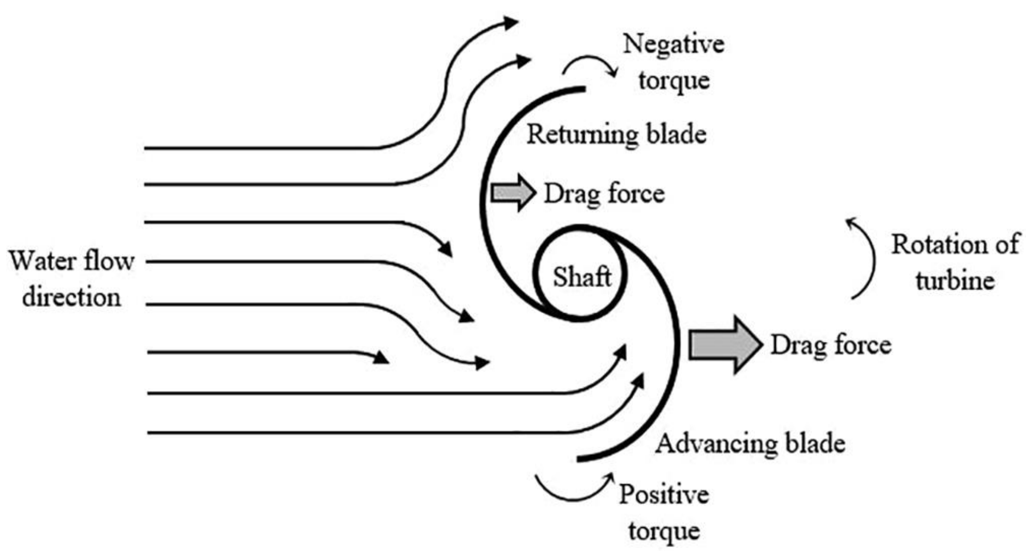

Figure 2.4 Drag forces acting on the blades of the Savonius turbine (Salleh et al., (2019))

All hydrokinetic turbines share certain operating characteristics, such as cut-in, rated and cut-out speeds. Figure below shows the power output schematic for a typical hydrokinetic turbine.

- ✓ Cut-in Speed - river water velocity on the turbine start spinning and producing power
- ✓ Rated Speed - river water velocity at which the generator output reaches its maximum
- ✓ Cut-out Speed – is a very high river water speeds, at which the turbine stop rotating

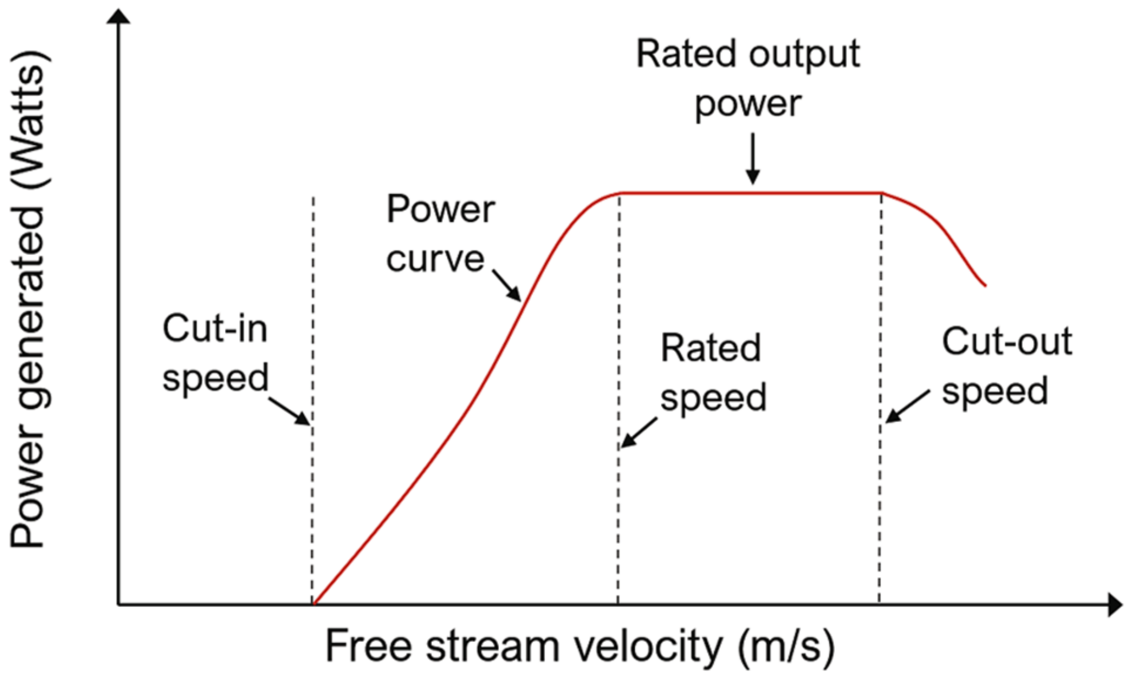

Figure 2.5 Power output schematic for a turbine (Maldar et al., (2020))

2.3 Main Parameters Affecting the Savonius Turbine’s Performance

Due to its simple design, the Savonius turbine's performance is highly dependent on its geometry, as shown in the figure below. Key parameters like the number of blades, stages, and blade profiles significantly influence the turbine's overall effectiveness

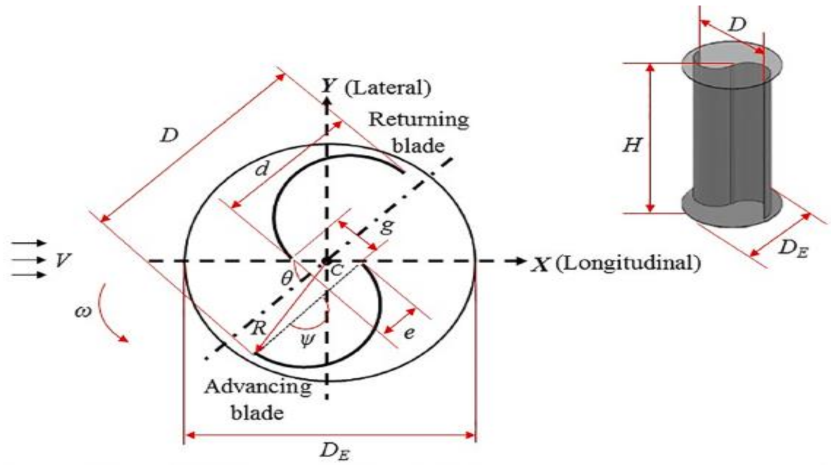

C	Center of turbine	v	Free stream velocity(m/s)
D	Diameter of turbine(m)	θ	Turbine rotor angle(˚)
D_E	End plate diameter(m)	ω	Angular velocity of turbine(rad/s)
d	Diameter of blade(m)	ψ	Blade arc angle(˚)
e	Overlap distance(m)	AR	Aspect ratio(H/D)
g	Gap distance(m)	ER	End plate ratio(D_E/D)
H	Height of turbine(m)	GR	Gap ratio(g/d)
R	Radius of turbine(m)	OR	Overlap ratio(e/d)

Figure 2.6 Main geometric parameters of the Savonius turbine (Salleh et al., (2019))

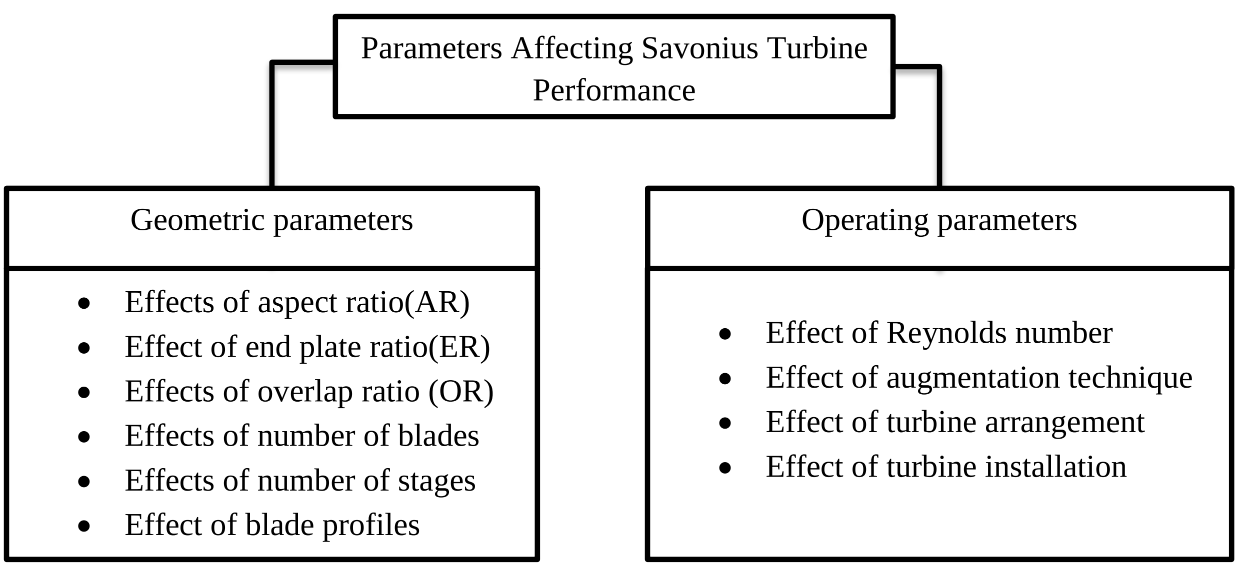

Figure 2.7 various parameters affecting the Savonius turbine's performance

2.3.1 The main geometric parameters affecting the Savonius turbine's performance

a) Effect of aspect ratio (AR)

In Savonius turbines, the aspect ratio (AR), defined as turbine height to diameter (H/D), plays a crucial role in performance. Varying water depths at different sites necessitate adjustments to the turbine's dimensions, and the optimal AR can significantly influence the choice of diameter when shallow water depths limit turbine height.

$$AR = \frac{H}{D}$$

Mabrouki et al., (2014) studied the impact of aspect ratio (AR) on the performance of a straight-bladed Savonius hydrokinetic turbine (SHT) by comparing two models with different blade heights. Their findings suggest that a lower AR of 0.53 leads to significantly better performance, as evidenced by a higher maximum coefficient of power (Cp) of 0.19 compared to a lower Cp of 0.05 for the higher AR of 1.06.

Patel et al., (2017) experimentally studied the impact of aspect ratio (AR) on the performance of a 2-bladed Savonius HKT turbine. Their findings, obtained in a small water tunnel with a flow velocity of 0.46 m/s, demonstrate that a turbine with an AR of 0.401 achieves the highest maximum coefficient of power (C_{Pmax}) of around 0.15, which is a substantial 114.29% improvement compared to the turbine with the lowest AR of 0.211.

b) The effect of end plate ratio (D_E/D)

In a Savonius wind turbine, end plates play a crucial role in preventing fluid leakage to the external flow, thereby maintaining a satisfactory pressure difference across the rotor height. This leads to improved performance, as demonstrated by (Patel et al., 2017) through experiments. Their study showed that with end plates, the coefficient of performance (C_{Pmax}) of the turbine increased significantly from 0.02 to 0.10 at a water velocity of 0.46 m/s, highlighting the substantial benefits of end plates in Savonius turbine design.

c) Overlap ratio (OR) and gap ratio (GR)

Kerikous, (2019) identified an optimal operating range for overlap ratio (OR) between 0.12 and 0.21 and generator ratio (GR) between 0 and 0.1. Their study achieved a maximum power coefficient (Cp) of 0.23 for a turbine configuration with OR =0.161 and GR= 0.033, exceeding the performance of a conventional Savonius turbine by 8%. Velocity analysis revealed that higher OR values create larger vortices around the overlapping area, hindering turbine performance.

d) Effect of number of blade

Salleh et al., (2019) experimentally compared the performance of two- and three-bladed Savonius wind turbines. While adding blades increases drag and reduces net torque, the two-bladed design outperformed the three-bladed turbine, achieving a higher maximum power coefficient (C_{Pmax}) of 0.21 compared to 0.17, both at a tip speed ratio (TSR) of 0.80.

e) Effect of number of stage

Frikha et al., (2016) combined numerical simulations and experiments to evaluate the performance of Savonius wind turbines with varying numbers of stages (single, two, three, four, and five) at a wind speed of 3.0 m/s. Their findings suggest that single-stage turbines achieve the highest velocity. Among three Savonius rotors of the same cross-sectional area used as water current turbines, the single-stage design exhibited superior performance, starting at lower water speeds and generating higher torque compared to two- and three-stage configurations

2.3.2 The Main Operating Parameters Affecting the Savonius Turbine's Performance

a) Effects of Augmentation technique

Savonius turbine performance can be boosted by integrating auxiliary devices either inside or outside the turbine. These devices manipulate the incoming airflow by deflecting, concentrating, or increasing its mass flow rate, ultimately leading to enhanced power output.

This study optimizes the position of an obstacle placed before the Savonius turbine's returning blade, aiming to improve flow orientation towards the advancing blade and enhance overall performance. As demonstrated in the graph, Mohamed et al., (2010) achieved a significant performance improvement using such obstacles, with a power output coefficient increase exceeding 27%.

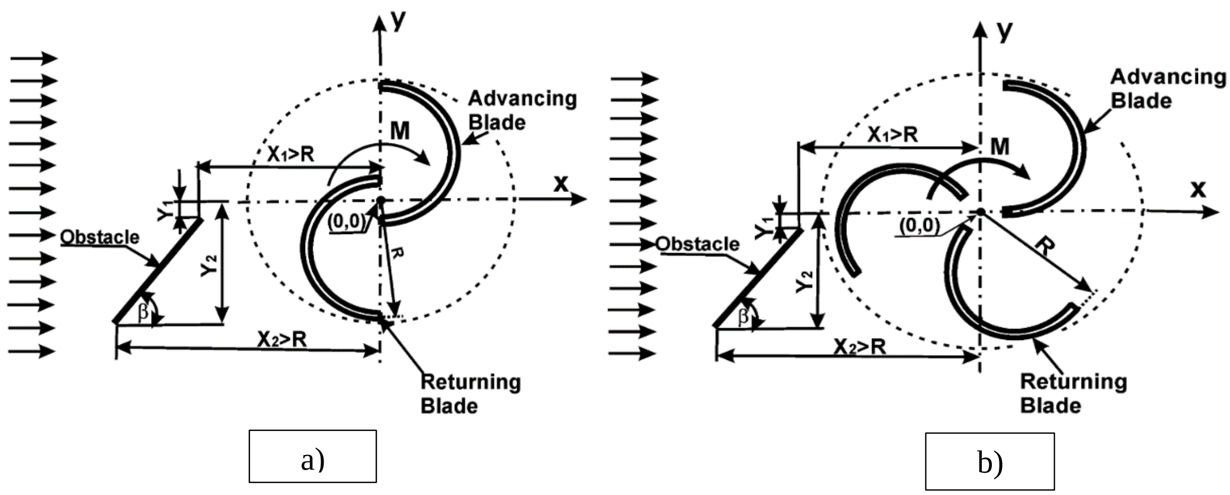

Figure 2.8 Schematic description of the geometry a) two-blade b) three-blade Savonius rotor

Shaughnessy, (2019) study found that a strategically placed deflector can significantly increase wind turbine power output. In their research, a properly positioned deflector boosted power generation by 20% compared to an unblocked rotor at a wind speed of 4m/s. This simple and inexpensive modification demonstrates the significant potential of partially blocking wedges for wind energy harvesting, as illustrated in the figure below. Notably, the optimal deflector position not only maximized power output but also enabled self-starting in wind conditions.

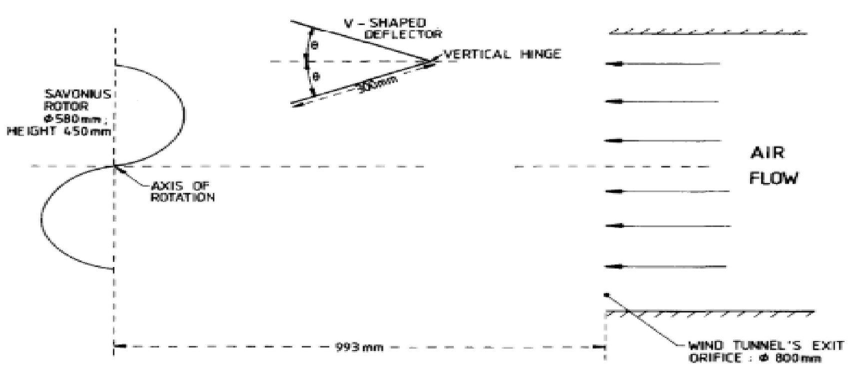

Figure 2.9 schematic diagram of V-shape deflector

Kailash et al., (2012) conducted the research work on comparing the use of the deflection plate and without deflection plate in the improvement of efficiency as shown figure below. By strategically placing two deflector plates at their optimal positions upstream, the coefficient of power can be significantly increased from 0.14 for the rotor without deflectors to 0.35.

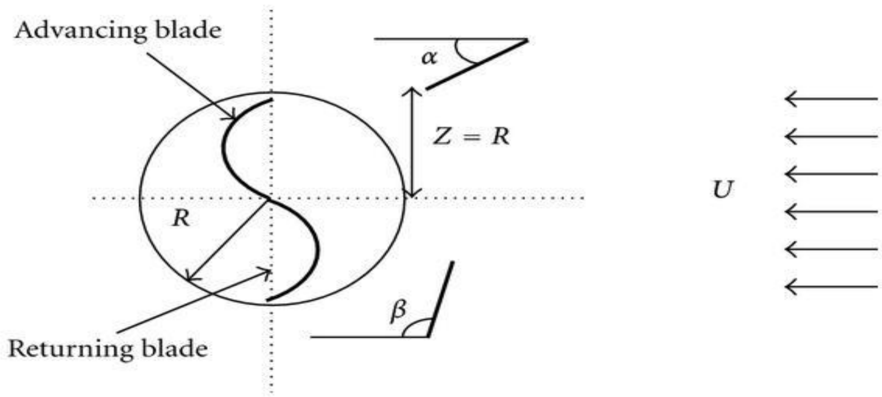

Figure 2.10 Schematic of modified Savonius rotor with space parameters of two-deflector plate

In a study by Singh et al., (2024) a novel combined deflector system significantly enhanced the performance of a Savonius hydrokinetic rotor. The system, consisting of a circular cylindrical deflector and a wedge-shaped triangular deflector, achieved a maximum power coefficient of 0.432 at a tip speed ratio of 1.0. This represents a 73.7% improvement compared to the conventional Savonius rotor, which only reached a maximum power coefficient of 0.248 at a tip speed ratio of 0.7.

b) Effect of turbine arrangement

Golecha et al., (2012) investigated the interaction between two Savonius turbines arranged in series by varying the separation gap between them. They found that increasing the gap ratio from 3 to 8 significantly reduced the interaction and ultimately allowed the turbines to operate independently without affecting each other's performance.

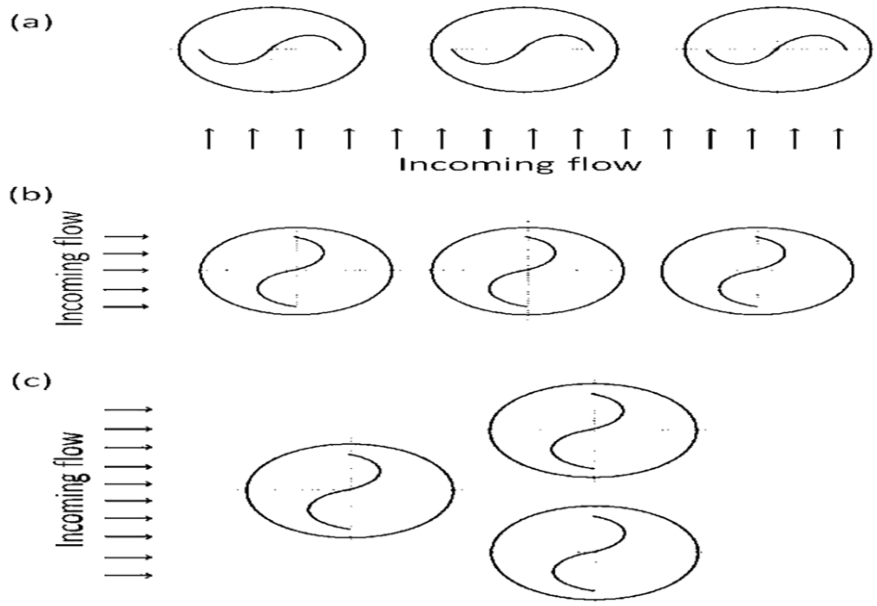

Figure 2.11 various types of turbine arrangement (a) side-by-side arrangement (b) in-line arrangement (c) triangular or V-shape arrangement

Mosbahi et al., (2019) conducted the research work on studies to enhance the performance of rotor blade by designing new optimal deflector system and make a comparison between with deflector and without deflector, finally it gives with deflector higher power coefficient than without deflector system (i.e. power coefficient from 0.125 to 0.14 at 0.7 TSR).

Patel et al., (2019) studies the effect on different geometries of channel on Savonius turbine were studied at Elevated channel bottom (hump) to improve the power output from the turbine by reducing the depth of flow to increasing the kinetic energy flow rate. Experimental results indicate that the power output increase 83% by configuring the turbine on the hump with relative to the turbine placed at the bottom of the channel.

Vaz et al., (2019**)** assessed powertrain resistance for shrouded horizontal axis hydrokinetic turbines. A quasi-steady model based on the rigid-body dynamic equation of the powertrain and BEM theory, modified to account for the effect of a diffuser. Due to an increase in aerodynamic torque Shrouded turbine has a significantly lower starting flow velocity when compared to the same bare turbine. The diffuser turbine has a 27% lower starting torque compared to a bare turbine.

Goundar et al., (2013) demonstrated that a ducted Savonius turbine (DST) with an area ratio of 2.5:1 can operate efficiently at low water velocities and depths. This design significantly increases kinetic energy and improves overall turbine performance, with current research indicating a maximum efficiency of 53% at a tip speed ratio of 3.5 and a corresponding maximum power output of 63.4KW at 2.15m/s.

Park et al., (2023) leveraged computational fluid dynamics (CFD) and a gradient-based optimization approach to design a ducted hydrokinetic turbine, achieving an impressive 54% efficiency across various operating conditions, significantly surpassing the typical 46% efficiency of unducted turbines. By employing a gradient-based optimization approach and leveraging the adjoint method for efficient gradient calculation, researchers achieved a ducted turbine design with an impressive 54% efficiency across diverse operating conditions, significantly exceeding the typical 46% efficiency of unducted turbines

Muluken et al., (2019) analyzed the economic feasibility of using hydrokinetic turbines (HKTs) to provide electricity in rural areas. Their study, focusing on a site on the Gumara River with an average water speed of 2m/s, revealed a positive net present value of $89,764, annual revenue of $161, and a simple payback period of 5.16 years. Additionally, the calculated internal rate of return (IRR) of 17.4% exceeded the inflation rate of 11%, leading the study to conclude that implementing HKTs in the Gumara River is economically viable for rural electrification.

Mosbahi et al., (2021) through numerical simulations and experimental tests, the impact of an upstream deflector system placed ahead of a twisted Savonius rotor in a channel was explored. Results from the numerical analysis revealed that the proposed deflector system enhanced the power coefficient of the Savonius rotor by 14%. Furthermore, experimental studies were conducted to evaluate the performance of a Savonius rotor in an irrigation canal with a flow velocity of V = 0.86 m/s. To enhance efficiency, a deflector system was recommended, and the effects of four different deflector designs were examined through numerical testing on the Savonius rotor.

Khan et al., (2022) studies on new the innovative blade shape is based on the S1048 airfoil section. The structure of the S1048 airfoil section blades consists of both straight and curved segments. The extended straight edge allows for a larger moment arm and gap flow, while the curved section diminishes the impact of negative torque on the rotor. It has been demonstrated that, by utilizing the new blade profile, the maximum power coefficient of the standard design can be enhanced by 14% at a tip speed ratio of 1. Furthermore, the performance of the proposed design was assessed by adding an upstream curtain arrangement to the turbine. Consequently, an extra 13% increase in the power coefficient was achieved compared to the traditional augmented rotor.

Chaudhari, (2023) conducts the research on NACA6409 blades instead of the traditional semi-circular blades in the Savonius hydrokinetic turbine, leading to the creation of the new Airfoil Bladed Savonius Hydrokinetic Turbine (ABSHKT). In order to boost the performance of ABSHKT, a deflector plate is incorporated. The inlet velocity is set at 1 m/s, and the analysis is conducted over a range of Tip Speed Ratios (TSR) from 0.7 to 1.1. The findings of this study reveal that the maximum power coefficient for ABSHKT and SHKT with a deflector is 0.227 at 0.8 TSR and 0.25 at 0.8 TSR respectively. It is evident that the ABSHKT with a deflector exhibits low performance compared to the SHKT with a deflector. It is recommended to implement an advanced augmentation technique to enhance the performance of ABSHKT.

2.4 Research Gap

These literature reviews above summarized as numerous studies show that the performance of the hydrokinetic turbine improved in many ways. Geometrical parameter like number of blades, blade profiles and number of stage and also Operating condition parameter like Reynolds number, augmentation technique, turbine arrangement and installation.

In this studies work based on the above reviewed literatures the research gap is most studies focus on the wind energy system instead of hydrokinetic system and the efficiency of savonius turbine is critically very low to use the turbine for power production, so using the best augmentation technique for performance improvement is designed in power generation. From this study adopting the wind savonius blade into hydrokinetic savonius blade and the type of augmentation used is curtain type for directing the incoming free stream velocity to the advanced blade by shielding the returning blade integrating with the flow accelerating rectangular duct to produce power for irrigation purpose.

CHAPTER THREE

MATERIALS AND METHODS

The primary data of river flow data from minister of water, irrigation and energy, Koka hydroelectric power plant and actual measuring of Awash River flow velocity using different technical methods. Secondary data collects from different related article, books. In order to accomplish the above-mentioned general and specific objectives of this thesis work, the following methodical procedures used throughout the research works.

3.1 Description of the study area

This study area was in Awash River at tedecha, which is located in the upper Awash River. Awash is one of the largest rivers in Ethiopia used for mainly irrigation and fishing. The river stored at koka hydro reservoir dam and travels along the Rift Valley and ends in Lake Abe on the border between Ethiopia and Djibouti. The river has higher discharge and flow velocity this makes compatible for application of HKT. The study area is situated in tedecha village at 8°28'N 39°10'E (latitude and longitude) near to Adama city, North shewa, Oromia regional State of Ethiopia. The Site of tedecha is located almost all 15 km away from the Adama city. The farmers live in around tedecha village, vegetable planting agriculture is the main tasks of the individual’s.

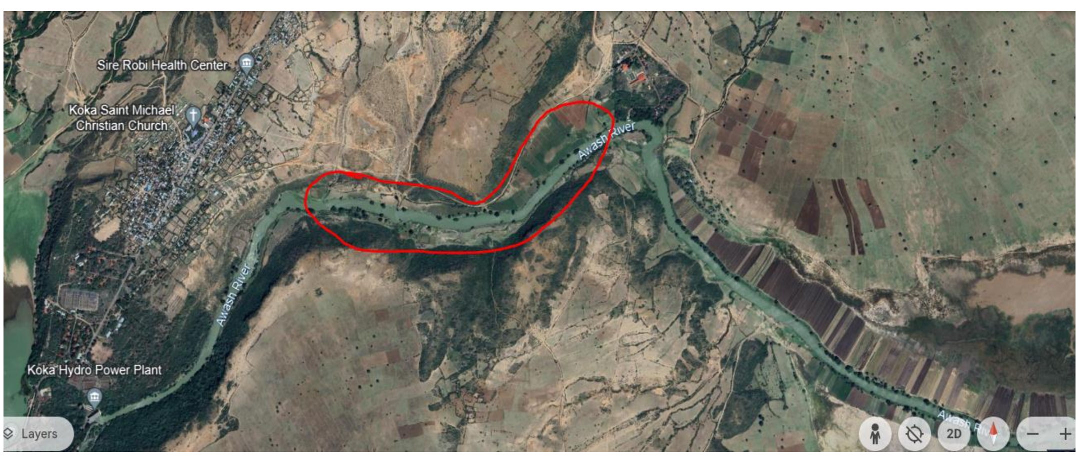

Figure 3.1 Site location of the study area (Google earth map)

Two methods can be formally distinguished for the assessment of HK resources of rivers

1) Hydrological Method: This approach utilizes readily available data from standard stream gauging stations; including discharge, water surface slope, and velocity. It leverages both the conventional potential power expression and the specific hydrokinetic power formula.
2) Hydraulic/Hydrodynamic Modeling: This method relies solely on in-stream velocity data, modeled spatially using flow and river bathymetry information. It requires a digital elevation model (DEM) of the specific river reach under investigation.

3.2 River Flow Velocity Measurement Methods

The floating method offers a simple way to estimate river flow rates by combining the measured velocity of a floating object with the river's cross-sectional area. This velocity is determined by timing the object as it travels a known distance downstream on the water's surface. Since water velocity varies across a river's profile, with slower speeds near the bottom and sides, the object is placed on the surface and timed over a pre-defined distance. This method is most effective for straight rivers with consistent and relatively even water flow.

The floating method utilizes a floating object to gauge the surface velocity of water flow. It involves measuring the time taken for the object to travel a known distance (e.g., 2 meters) along the river surface, which allows for calculating the surface speed in meters per second

$$\text{velocity(m/s)} = \frac{\text{Distance traveled(m)}}{\text{time travel(s)}}$$

Figure (3.7) depicts significant variations in velocity (V) both vertically and horizontally within the water column. The "no slip" condition dictates zero velocity at the flow boundaries and peak velocities near the water's surface, as documented by (Tigabu et al., 2020).

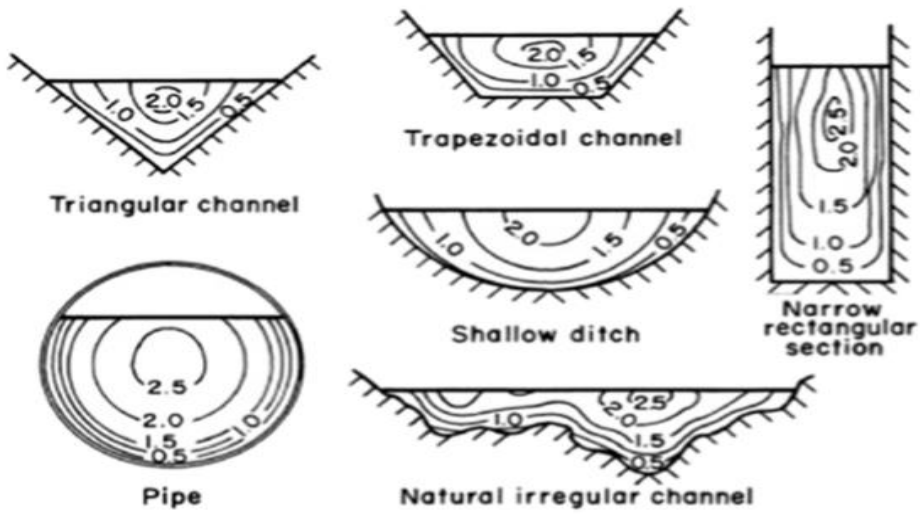

Figure 3.2 Velocity contours in various channel sections given as multiple of average velocity

To accurately estimate the average flow speed (Vm), the measured velocity needs to be adjusted by a correction factor ranging from 0.45 to 0.85 based on the watercourse depth and bottom/riverbank roughness. A value of 0.85 is generally accepted for the given sites.

Then, the mean flow velocity can be calculated as $V_m = 0.85 * V_{surface}$

Then, the flow rate can be calculated as

$$Q = A * V_m \tag{3.1}$$

Where: Q = water flow rate (discharge) of the river or stream

To measure the water's surface flow velocity, a pre-defined flow structure with known dimensions was used. A floating object's travel time from the start point (0 m) to the end (2 m) within this structure was measured, and the flow velocity was calculated as the flow length divided by the travel time, resulting in a velocity in m/s.

Volume = (L x W x H)

$$\text{velocity} = \frac{\text{the distance traveled by floating tennis ball(2m)}}{\text{the time taken for the floating object to reach the length}}$$

The three sites were selected, measuring, and recording of data with comparison selecting the best site for the hydrokinetic turbine installation. The instruments that used to measure the flow river width, depth and velocity by using the floating method are

- ✓ Tape measure
- ✓ Stop-watch (used mobile phone stopwatch)
- ✓ Yard or meter stick to measure depth
- ✓ Floating object (tennis ball)
- ✓ Reading recorder
- ✓ Long string

The field measurement procedures include;

- ✓ Selecting the appropriate sites along the river suitable for HKTs
- ✓ Tie a string line running across the stream,
- ✓ Measuring and recording of the geometry (width and depth) of the river cross-sections;
- ✓ Measuring and recording of the time taken of the floater to move 2m using stopwatch
- ✓ Calculating the velocity and discharge of the river

Figure 3.3 the three-selected site for comparison of river (Google earth map)

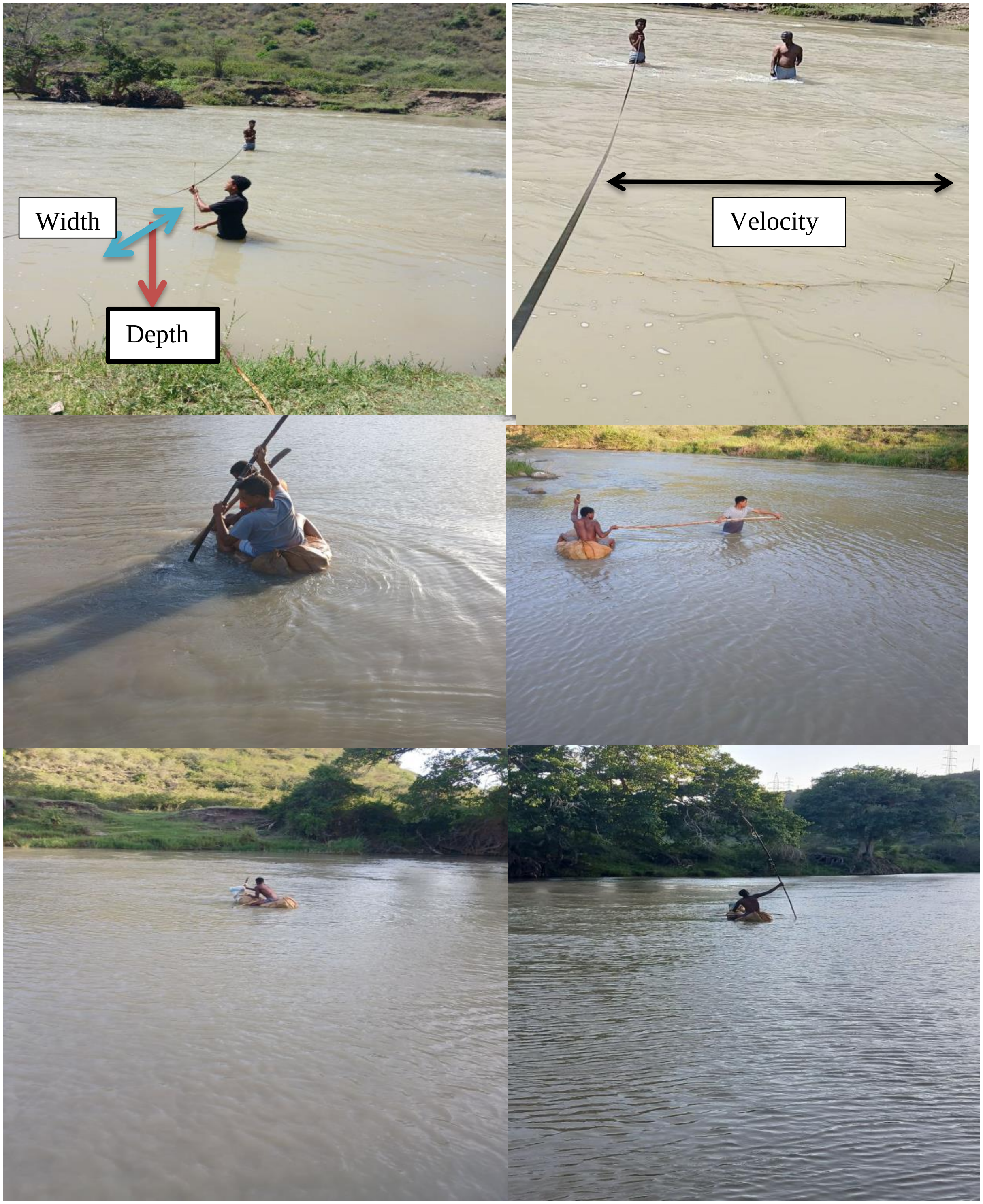

Figure 3.4 the cross section and velocity measurement of the river at sites

3.4 Methodology of the study

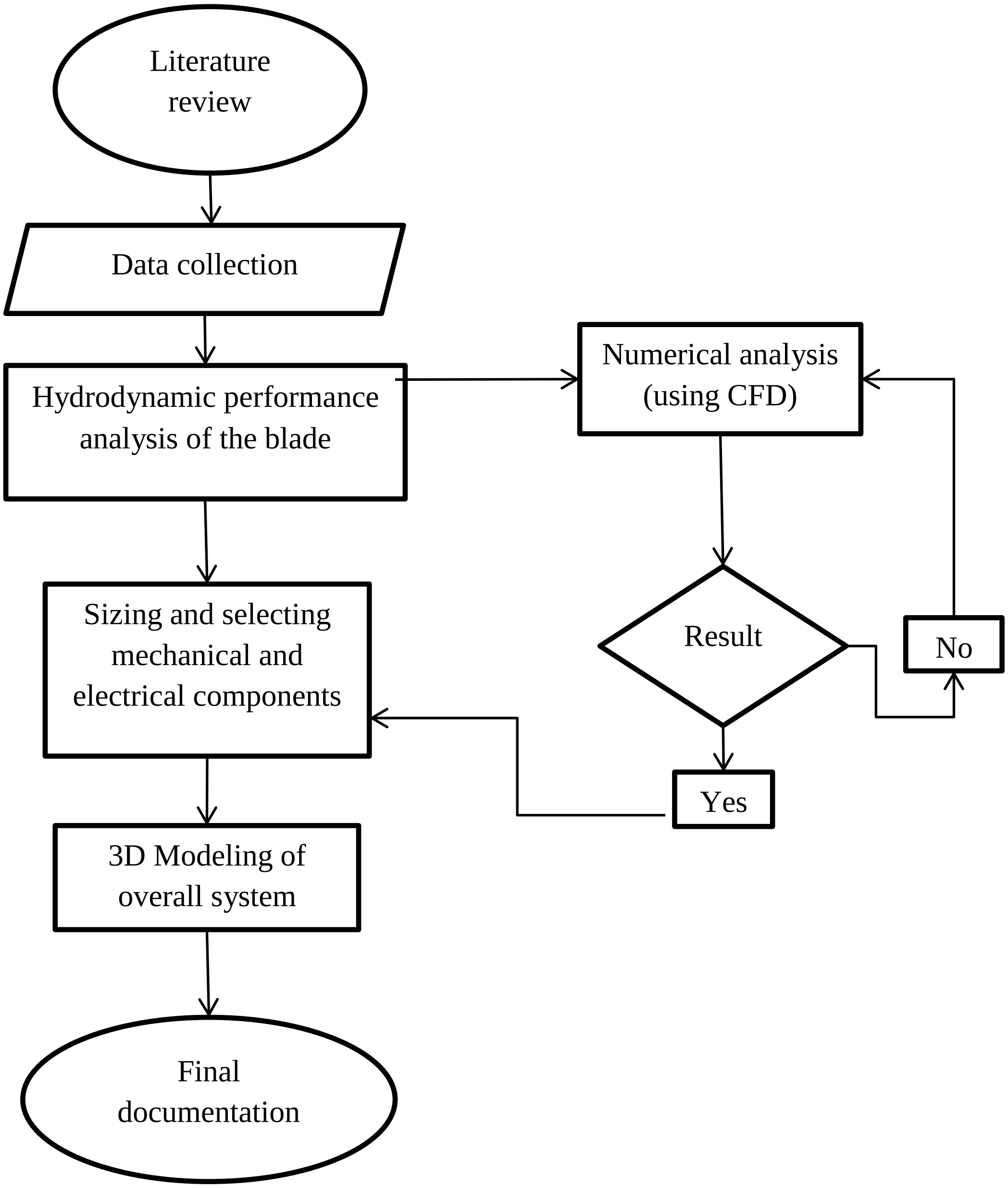

Figure 3.5 Flowchart diagram of the study

3.5 Design of Savonius Hydrokinetic Turbine and Auxiliary Components

The Savonius turbine's inherent design simplicity, low cost, quiet operation, and superior performance under low flow rates, high static torque, and better starting characteristics make it the ideal choice for river current hydrokinetic turbine (HKT) systems aiming to deliver sustainable power to remote areas and communities. These advantages have led to its selection for this study.

The main parameters taken from previous studies are:-

1) Studies have shown that most Savonius turbines achieve a maximum power coefficient (Cp) between 0.15 and 0.30 at a tip speed ratio (TSR) of 0.6 to 0.9, while other turbine types typically reach a maximum Cp of around 0.2 at a TSR between 0.7 and 0.8 (Salleh, 2019). This indicates that Savonius turbines generally have a lower power conversion efficiency compared to other types.

For this design, a power coefficient (Cp) of 0.2 is chosen, as this value represents the optimal performance point for Savonius hydrokinetic turbines, as established by various researchers.

2) The turbine's aspect ratio (AR) plays a crucial role in the performance of Savonius Hydrokinetic Turbines (SHTs). This non-dimensional parameter is often expressed as...

$$\mathrm{AR} = \frac{\mathrm{H}}{\mathrm{D}} \tag{3.2}$$

Where D and H denotes height and diameter of the turbine

In Savonius wind turbines, maintaining a low aspect ratio (AR < 1.5) is often preferred for structural stability. Research (Talukdar, 2018) suggests that increasing the turbine diameter increases generated torque while simultaneously reducing rotational speed. Therefore, an aspect ratio of AR = 1 is a suitable choice.

3) The 2-bladed turbine design outperformed other configurations across all tip speed ratios (TSR) due to a phenomenon called Coanda flow. This flow, occurring on the downstream side of the advancing blade, reverses the flow direction on the following blade, contributing to positive torque. However, in 3-bladed turbines, large vortices closer to the blades destabilize this phenomenon, leading to high-pressure regions downstream and

reduced power extraction as observed in (Maldar, 2020). Therefore, the research focuses on the 2-bladed design for its superior performance.

4) End plates on turbine blades prevent fluid from escaping sideways, leading to increased flow concentration on the concave surface and higher positive torque due to greater resultant pressure. Studies by (Maldar, 2020) confirm that rotors with end plates exhibit higher efficiency compared to those without them.

$$ER = \frac{D_E}{D} = 1.1$$

5) Single stage Savonius rotor has more performed than two stage Savonius rotor with maximum C_p was achieved for single-stage turbine (Kamoji et al., 2008).then the single stage is compatible to the site and the system.
6) Maldar, (2020) study found that turbines with overlapping blades exhibit a wider range of operational tip speed ratios (TSR) and higher efficiency compared to turbines without overlap. However, it's crucial to determine the optimal values for overlap ratio (OR) and gap ratio (GR) to avoid excessive gaps or major blade overlap, which can lead to a decrease in efficiency. In this study, the optimal values for OR and GR were found to be 0.16.
7) The performance of a hydrokinetic turbine, measured by its power coefficient (Cp), is directly influenced by its tip-speed ratio (TSR), which is the ratio of the turbine's blade tip speed to the velocity of the incoming water flow.

$$TSR = \frac{\omega * R}{v} \tag{3.3}$$

Darrieus or the axial propeller type has operating TSR range is higher (4 to 7) but for the Savonius turbine operates at a lower range (0 to 2) in the studies of (Maldar, 2020). The optimum TSR =1

3.5.1 Design power output of the turbine

The power output (p_{out}) in Watts (W) for produced from the flow velocity can be obtained by the equation

$$p_{out} = \frac{1}{2} C_p * \rho * A * v^3 \tag{3.4}$$

Where, ρ is the fluid density (kg/m^3), A is the cross-sectional swept area of the turbine blades (m^2) and V is the incoming flow velocity for the turbine (m/s)

The equation reveals a strong dependence of power (P) on flow velocity; with a cubic relationship meaning even small velocity fluctuations significantly impact power. Additionally, fluid density plays a crucial role, with water's density being roughly 800 times higher than air, further amplifying the power variations due to density differences.

The rotor diameter (D) =1m, From the selected site of the river depth average is in April in the low discharge month is 1.5m due to this reason the height of the turbine must be below this value. Take H=1m, the rotor height (H) =1m, Aspect ratio($\frac{H}{D}$) =1

But the power generated is lower due to the velocity of the river is lower due to this reason the flow accelerator of rectangular duct is used and Savonius turbines significantly benefit from a well-designed duct or shroud, allowing them to operate effectively even at low depths due to their reduced sensitivity to turbulent flow.

To enhance the performance of the energy change the duct was optimized. According to the Goundar et al., (2013) findings the duct area ratio (A_1/A_2) and the tapered angle α is optimized. The area ratio was varied from 2 to 10 and α was varied from 5º to 20º then finally from the results, the best area ratio obtained was 5 and best α come to 15º.

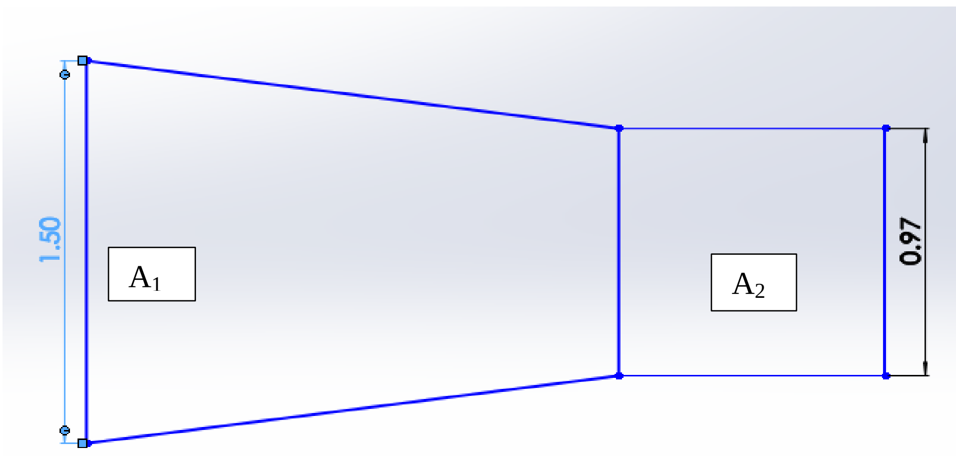

Figure 3.6 flow accelerator rectangular duct

In steady, one-dimensional flow with a single inlet and outlet, the principle of mass conservation leads to the continuity equation. This equation states that the mass flow rate entering the system must equal the mass flow rate exiting it. For more complex scenarios with multiple inlets and outlets, the net mass flow within the control volume must be zero, ensuring that mass is neither created nor destroyed within the system.

$$\dot{M}_{in} = \dot{M}_{out}$$

$$\rho A_1 V_1 = \rho A_2 V_2 \tag{3.5}$$

However, the density of water is constant

Then $A_1 V_1 = A_2 V_2$ the dimension of the duct at the inlet is 2×1.5m and at the outlet is 1.3×0.97m, with the length of 3m then the free stream velocity V_1=1.92m/s therefore the outlet velocity of the duct on the converging side is

$$V_2 = \frac{A_1 V_1}{A_2} = \frac{2 * 1.5 * 1.92}{1.3 * 0.97} = 4.6\text{m/s}$$

The power generated from the ducted rectangular flow accelerator of changing 1.92 to 4.6 m/s and the optimum value of C_p =0.28 at TSR=1 from numerical value of results. Therefore the power generated by the turbine is

$$p_{out} = \frac{1}{2} C_d * \rho * A * v^3$$

$$p_{out} = \frac{1}{2} * 0.28 * 1000 * 1 * 1 * 4.6^3 = 13.6 \text{ Kw}$$

3.5.2 Design torque output of the turbine

$$P_{out} = T_{out} * \omega \tag{3.6}$$

T_{out} The torque output by the turbine (Nm), and is the angular velocity of the blade (rad/s) r - Rotor radius (r =0.5m).if the value of TSR =1 then

$$\text{TSR} = \frac{\omega * r}{V} = 1$$

$$\omega = \frac{2 * V}{r} = \frac{1 * 4.6}{0.5} = 9.2\text{rad/s}$$

$$\text{Therefore, } T_{out} = \frac{P_{out}}{\omega} = \frac{13600}{9.2} = 1481\text{Nm}$$

3.5.3 Design angular and rotational speed of the turbine

We know that, the mechanical power output (P_{out}) is the product of torque output (T_{out}) and angular speed (ω) of the turbine from the above equation,

$$P_{out} = T_{out} * \omega$$

To solve the angular speed in terms of power output and torque output, we obtain the following value on the above calculation.

The rotational speed (N) of the turbine in RPM became as follows:

$$\omega = 2\pi N$$

Where: N in (RPM). Thus, the rotational speed (N) became:

$$N = \frac{60 * \omega}{2 * \pi} = \frac{60 * 9.2}{2 * \pi} = 88\text{RPM}$$

3.5.4 Rotor Shaft design

To ensure optimal performance and safety, the turbine shaft must be as light as possible while remaining robust enough to handle the combined loads of river flow, wind, and the weight of the turbine blades and end plates. Careful material selection for the blades and end plates can minimize their weight, making the river flow the dominant force acting on the shaft. Additionally, the design of the shaft should incorporate the maximum expected peak water speed at the chosen site. The trust force exerted by the water flow on the shaft can be calculated using the following equation:

$$F = \frac{1}{2}\rho_w S V^2 \quad (3.7)$$

Where: - ρ_w –water density (Kg/m^3), S –turbine blades swept area (m^2), V –free stream water speed (m/s) and F – is thrust force of river on shaft (N).

To design the shaft take the maximum velocity of the river velocity for the matter of safety due to reason the design velocity for the shaft is 4.6m/s

$$F = \frac{1}{2} * 1000 * 1 * 4.6^2 = 10.58KN$$

The torque on the shaft will be

$$T = F * r = 10.58 * 0.6 = 6.3KNm$$

With the shaft solely supported by ball bearings at the top and bottom, the reaction forces F1 and F2 at each end are equal, each bearing half the total load of 5.29 KN. Since the shaft lacks central support, the maximum bending moment occurs at the center, necessitating the calculation of the maximum possible bending moment (Mb) for optimal shaft design.

$$M_b = r_1 * F_1 = r_2 * F_2 = 3.2KNm$$

To minimize system weight while maintaining strength, this study employs a hollow circular shaft design. This choice is informed by the ASME code equation for hollow shafts subjected to combined torsion and bending, incorporating factors for shock, fatigue, and column effects, as detailed in (Shigley, 2011).

$$d^3{}_o = \frac{16}{\pi * S_s(1-K^4)} \sqrt{(K_b M_b)^2 + (K_t M_t)^2} \quad (3.8)$$

Where:- S_s = Allowable shear stress (MPa), M_t = Torsional moment (N.m), M_b = bending moment (N.m), d_i = inner diameter of shaft (m), d_o = outer diameter of shaft (m), K_b = combined shock and fatigue factor applied to bending moment, K_t = combined shock and fatigue factor applied to torsional moment

$K = \frac{d_i}{d_o}$ Hence, the load on the shaft is suddenly applied and minor shock the value of K_b and K_t will be: K_b = 2 and K_t = 1.5 with the K = 0.8

$$(d_o)^3 = \frac{16}{\pi * 55 * 10^6(1 - 0.8^4)} \sqrt{(2 * 3200)^2 + (1.5 * 6300)^2}$$

$$d_o = 76.5mm$$

For the matter of safety outer diameter of shafts above the calculated values, $d_o = 80mm$ accordingly a hallow steel shaft the inner diameter of the shaft is

$$K = \frac{d_i}{d_o} = 0.8$$

$$d_i = 64mm$$

3.5.5 Bearing selection

In order to select the standard bearing calculating dynamic load rating (C_{10}) must

$$C_{10} = P_d \left[\frac{L_d}{10^6}\right]^{\frac{1}{k}} \quad (3.9)$$

Where: - C_{10} - dynamic load rating, L_d - design life, P_d - design load and K = 3 for ball bearings.

The bearings should resist radial load from river water speed and thrust load from weight of turbine itself. Therefore the design load (P_d) in above equation have to be corrected as equivalent rating load which given as follows

$$P_d = VXR + YT \quad (3.10)$$

Where: - P_d - is equivalent load, V - is rotational factor and for inner ring rotation (V = 1), R - applied radial load, X - radial factor and Y – is thrust factor.

Calculating the weight of the turbine gives 21kg then the thrust force (T) is weight of rotor time's gravitational constant (g).

$$T = Wg = 21 * 9.81 = 206N$$

Where: W – is weight of rotor (Kg) and g – is gravitational constant (m/s^2), taking g = 9.81 m/s^2

Using X = 0.56 and assuming Y = 2.33 for initial calculation the equivalent effective load (P) will be

$$P_d = 1 * 0.56 * 6300 + 2.33 * 206 = 4KN$$

Using the speed of the shaft calculated above which 36.7 RPM and Take working period as one year is 8760hr. Now the design life and dynamic load rating became

$$L_d = (hr)(rpm)(60\,min/hr) = 8760 * 36.7 * 60 = 1.93 * 10^7 rev$$

$$C_{10} = 4000\left[\frac{1.93 * 10^7}{10^6}\right]^{\frac{1}{3}} = 10.75KN$$

Accordingly the above calculation ball bearings with the following specification are selected from standard table compatible to the shaft. The Bore = 80mm, Outer diameter = 140mm and Width = 26 mm is selected to support shaft at the top and bottom.

3.5.6 Generator selection

Despite potentially higher initial costs compared to DC generators AC generators offer a significant advantage in terms of extended lifespan and reduced maintenance requirements. This contrasts with induction motors, which provide a balance between cost and reliability, making them a viable alternative to DC motors (Singh et al., 2019).

Selection of an electrical generator is heavily dependent on rotor speed and torque. According to the power, produce and the speed of the rotor the types of the generator that fits to the system selected with power factor 0.8. According to the power produce and the speed of the rotor the types of the generator that fits to the system is three phase AC synchronous STC generator with the rated output power of 15Kw, apparent power of 18.8KVA with 1500 rpm, frequency 50Hz without put voltage of 220/380V with power factor 0.8.

Figure 3.7 Three-phase AC synchronous STC generators

3.5.7 Design of Gear Box

Gear drives offer several advantages over belt, rope, and chain drives: they provide precise velocity ratios, handle high power transmission, work well with small center distances, boast high efficiency, offer reliable operation, and require minimal space.

If D_1 and D_2 are the diameters of the two engaging gears having the teeth T_1 and T_2 with the speed of $N_1$and N_2 respectively; then for them to engage correctly,

$$\frac{D_1}{D_2} = \frac{T_1}{T_2} = \frac{N_2}{N_1} \tag{3.12}$$

But N_1=88rpm and let N_2=1500rpm then the velocity ratio (VR) is

$$VR = \frac{N_2}{N_1} = \frac{1500}{88} = 17 \text{ The gear ratio is 17:1}$$

The catalogue number SS1-200 gear selected with number of teeth of the gear is 200, bore =20mm, hub diameter=160mm, pitch diameter=200, outside diameter=202mm, face width=10, hub width=10 according to the table attached on appendix. It can calculate the number of teeth of pinion gear $\frac{T_1}{T_2} = 17$, then T_2=12 with catalogue number SS2-12, bore=10mm, hub diameter 18mm, pitch diameter=24, outside diameter=28, face width=20, hub width=10

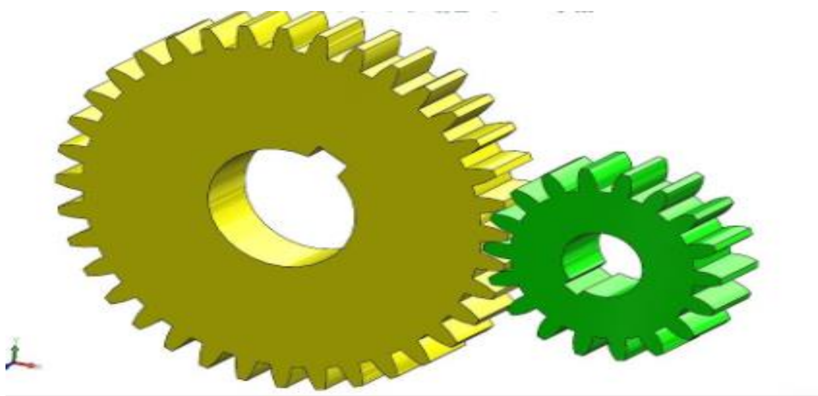

Figure 3.8 Spur gear and pinion modeling

Table 3.1 Geometrical parameters design savonuis turbine

No.	Geometrical parameters	Value	Unit
1	Blade diameter	0.54	m
2	Turbine diameter	1	m
3	Turbine height	1	m
4	Diameter of the end plate	1.1	m
5	End plate thickness	0.003	m
6	The thickness of the turbine blade	0.003	m
7	Aspect Ratio, AR	1	
8	Shaft diameter	0.08	m

3.5.8 Sizing of curtain

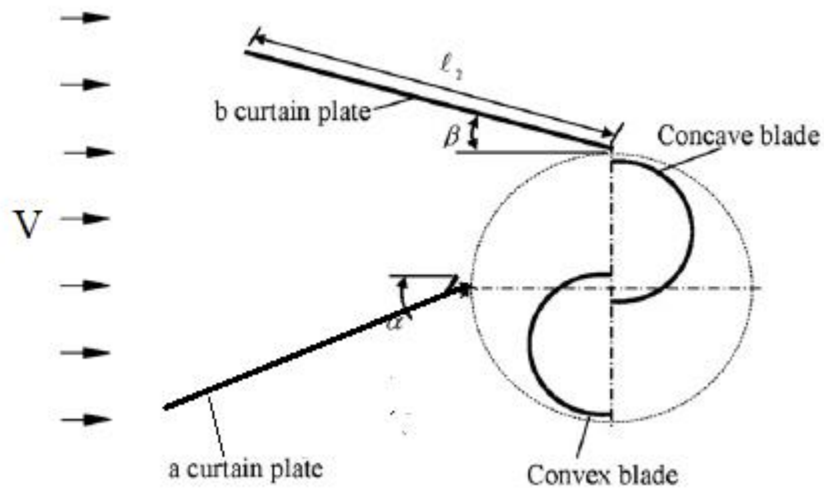

Figure 3.9 design of curtain arrangement

Curtain arrangement was created and implemented in order to remove the moment on the convex blade of the rotor that occurs in opposition to that of rotation without altering the fundamental design of a standard Savonius rotor. While placing a curtain in front of the returning blade is a potential strategy, its effectiveness depends heavily on the specific design and operating conditions. According the (Deda Altan, 2010) studies on curtain design the optimum angle of position obtained at an angle of β =15° and α =45° from the horizontal. Studies have shown that a wider curtain (ratio of curtain width to rotor diameter exceeding 1.41) can actually decrease performance at higher speeds. Conversely, a narrower curtain might improve performance. The value of curtain plate's size is $\ell_2 = 1.5$m and $\ell_1 = 1$m with at angle of β =15° and α =15° for this study to be optimum because at this position the water from the inlet strikes the advance blade with higher pressure due to this it reduces the negative torque produced by the returning blade.

3.5.9 CAD modeling of the ducted curtain savonius turbine system

When selecting pumps for construction applications, prioritize reliability, readily available repair parts, ease of repair for minimal downtime, and cost-effective installation, operation, and power consumption. The developed CAD models of ducted curtain savonius turbine, Based on the design above the three modeling of the ducted savonius hydrokinetic turbine system modeled as below.

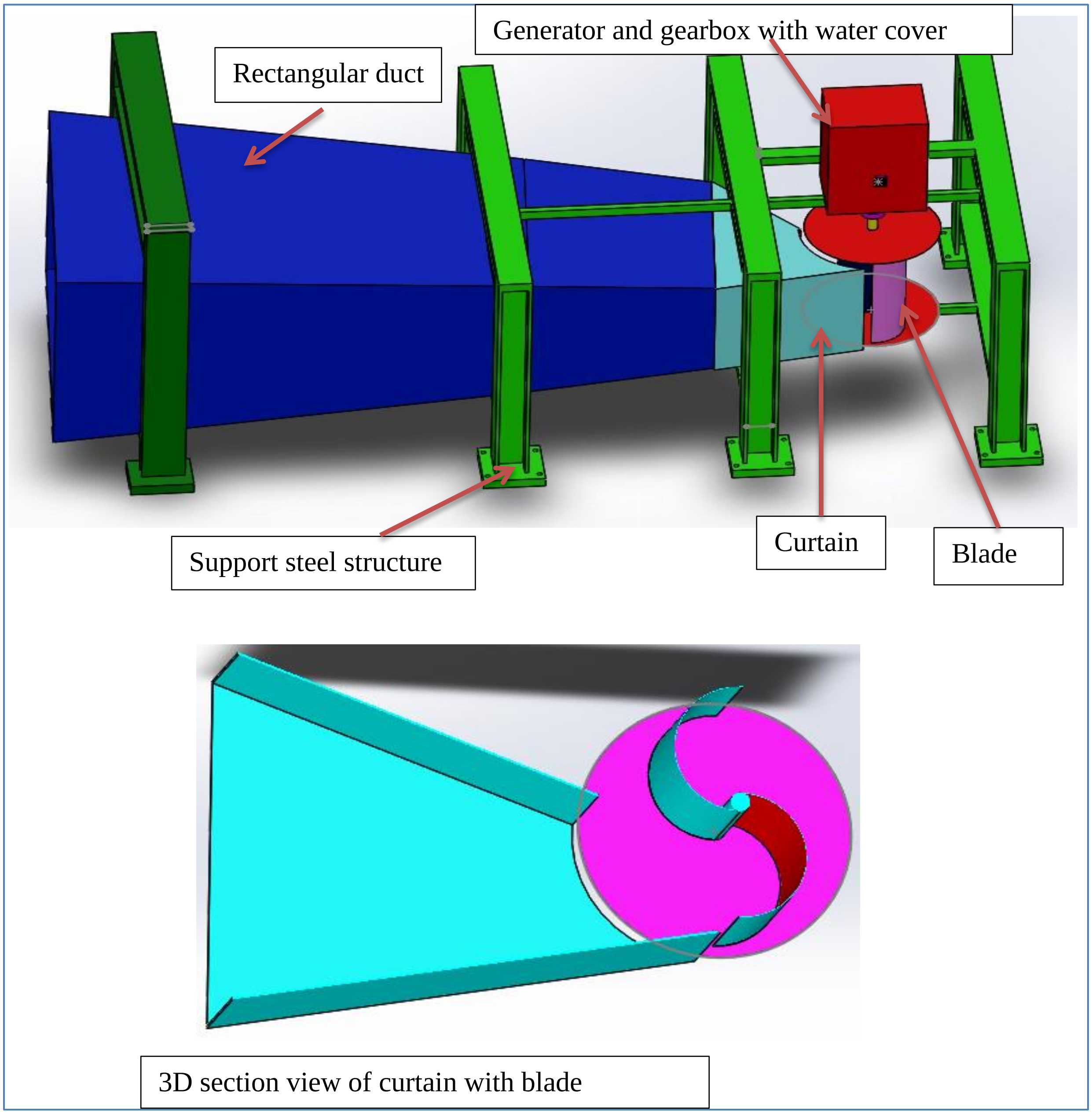

Figure 3.10 3D modeling of ducted curtain hydrokinetic savonius turbine system in solid work

3.5.10 Pump Selection

When selecting pumps for construction applications, prioritize reliability, readily available repair parts, ease of repair for minimal downtime, and cost-effective installation, operation, and power consumption. The power available is take as 10KW and the total head is approximately 50m then by using these two parameters find the standard pump from manufacturer catalogue. From the above comparisons and the suitability of the pump to the site is electric high flow rate centrifugal water pump, their main parameter specifications shown in the table below, and the main catalogue attached to the appendix.

Figure 3.11 Electric High Flow Rate Centrifugal Water Pump

Table 3.2 specification of electric high flow rate centrifugal water pump

Type	Centrifugal Pump
Main applications	Water pumping
Power Supply	Driver Electric motor 220V/240V380/415V 3phase; 50hz/60hz
Maximum drive rating	10KW
Rotational speed	2900RPM
Maximum head	60m
Flow rate range	43 m^3/h

CHAPTER FOUR

NUMERICAL ANALYSIS OF HYDROKINETIC TURBINE

4.1 Introduction

Numerical analysis provides approximate solutions to complex mathematical problems that are often analytically intractable in science and engineering. Computational Fluid Dynamics (CFD) utilizes numerical analysis techniques to simulate and predict fluid flow behavior by solving the governing equations using computational power. In a CFD analysis, various fluid properties like velocity, pressure, viscosity, density, and temperature are calculated simultaneously based on the defined operating conditions, ultimately aiming to provide an accurate representation of the physical phenomenon.

The equation for the Conservation of Mass specified as

$$\frac{\mathrm{D}\rho}{\mathrm{Dt}} + \rho(\nabla . \vec{V}) = 0 \tag{4.1}$$

Where ρ is the density, $\vec{V}$ the velocity and ∇ the gradient operator

$$\nabla = \vec{\imath}\frac{\partial}{\partial x} + \vec{\jmath}\frac{\partial}{\partial x} + \vec{k}\frac{\partial}{\partial x}$$

If the density is constant, the flow is water and assumed to be incompressible ($\frac{\mathrm{D}\rho}{\mathrm{Dt}} = 0$) and the continuity equation reduces to:

$$\left(\nabla . \vec{V}\right) = \frac{\partial u}{\partial x} + \frac{\partial v}{\partial x} + \frac{\partial w}{\partial x} = 0$$

a) Conservation of Momentum (Newton's Second Law)

Conservation of Momentum, which can be referred to as the Navier-Stokes Equation, is given by:

$$\overbrace{\frac{\partial}{\partial x}(\rho\vec{V})}^{I} + \overbrace{\nabla.(\rho\vec{V}\vec{V})}^{II} = -\overbrace{\nabla\rho}^{III} + \overbrace{\nabla.(\tau)}^{IV} + \overbrace{\rho\vec{g})}^{V} \quad (4.2)$$

I: Local change with time II: Momentum convection III: Surface force IV: Diffusion term

V: Mass force

If the fluid assumed incompressible with constant viscosity coefficient, μ the Navier-Stokes equation simplifies to

$$\rho\frac{D\vec{V}}{Dt} = -\nabla\rho + \mu\nabla^2\vec{V} + \rho\vec{g} \quad (4.3)$$

b) Conservation of Energy (First Law of Thermodynamics or Energy Equation)

Conservation of Energy is the first law of thermodynamics,

$$dE_t = dQ + dW \quad (4.4)$$

Where dQ is the heat added to the system, dW is the work done on the system and dE_t is the increment in the total energy of the system.

4.2 Operating parameters of the turbine

The tip speed ratio (TSR) is the ratio of blade tip velocity (tangential velocity) to the free stream velocity of the fluid. It is denoted by λ and written in the equation

$$\lambda = \frac{V_{tip}}{V} = \frac{R\omega}{V} \quad (4.5)$$

Where R and ω denotes the radius and the angular velocity of the rotor

Power coefficient is the ratio of power captured by the rotor to available power of the savonius turbine. Mathematically the power coefficient can be expressed as

$$C_p = \frac{P_{rotor}}{P_{avl}} = \frac{T\omega}{0.5\rho AV^3} \quad (4.6)$$

The power coefficient can be expressed in terms of tip speed ratio

$$C_p = \frac{P_{rotor}}{P_{avl}} = \frac{T\omega}{0.5\rho AV^3} = \frac{T}{0.5\rho AV^2 R} * \lambda \quad (4.7)$$

The torque coefficient is the ratio of turbine torque that the turbine develops and the available torque (the ability of fluid to generate torque).

$$C_m = \frac{T}{0.5\rho A V^2 R} \quad (4.8)$$

Using the above equations of (4.7) and (4.8) the power coefficient and the moment coefficient ar

$$C_p = C_m * \lambda \quad (4.9)$$

4.3 Turbulent CFD Calculations

Turbulent flow presents significantly greater challenges for CFD simulations compared to laminar flow due to its inherent complexity. This stems from the presence of unsteady, three-dimensional, and randomly swirling structures called turbulent eddies. To address this, CFD relies on various turbulence models, including algebraic, one-equation, and two-equation models (like k-ε, k-ω, and q-ω). Two-equation models offer a complete and closed system, making them the simplest complete option in CFD. Among these, the k-ε and k-ω models are particularly popular for simulations, with the choice of turbulence model being crucial, especially at low tip speed ratios (TSRs) due to the complex flow structures in vertical axis hydro turbines (VAHTs). Existing literature frequently employs two-equation turbulence models like k-ε and k-ω for VAHT simulations.

4.4 ANSYS-FLUENT

4.4.1 Model Description

The geometry of the designed savonius turbine created in SolidWork to the specifications found in the potential assessment and Blade design section for rated conditions. This geometry then exported into ANSYS Design-Modeler, where the domain geometry created. The savonius turbine blade geometry models of curtain less blade and with curtain blade are shown below and the rectangular duct flow.

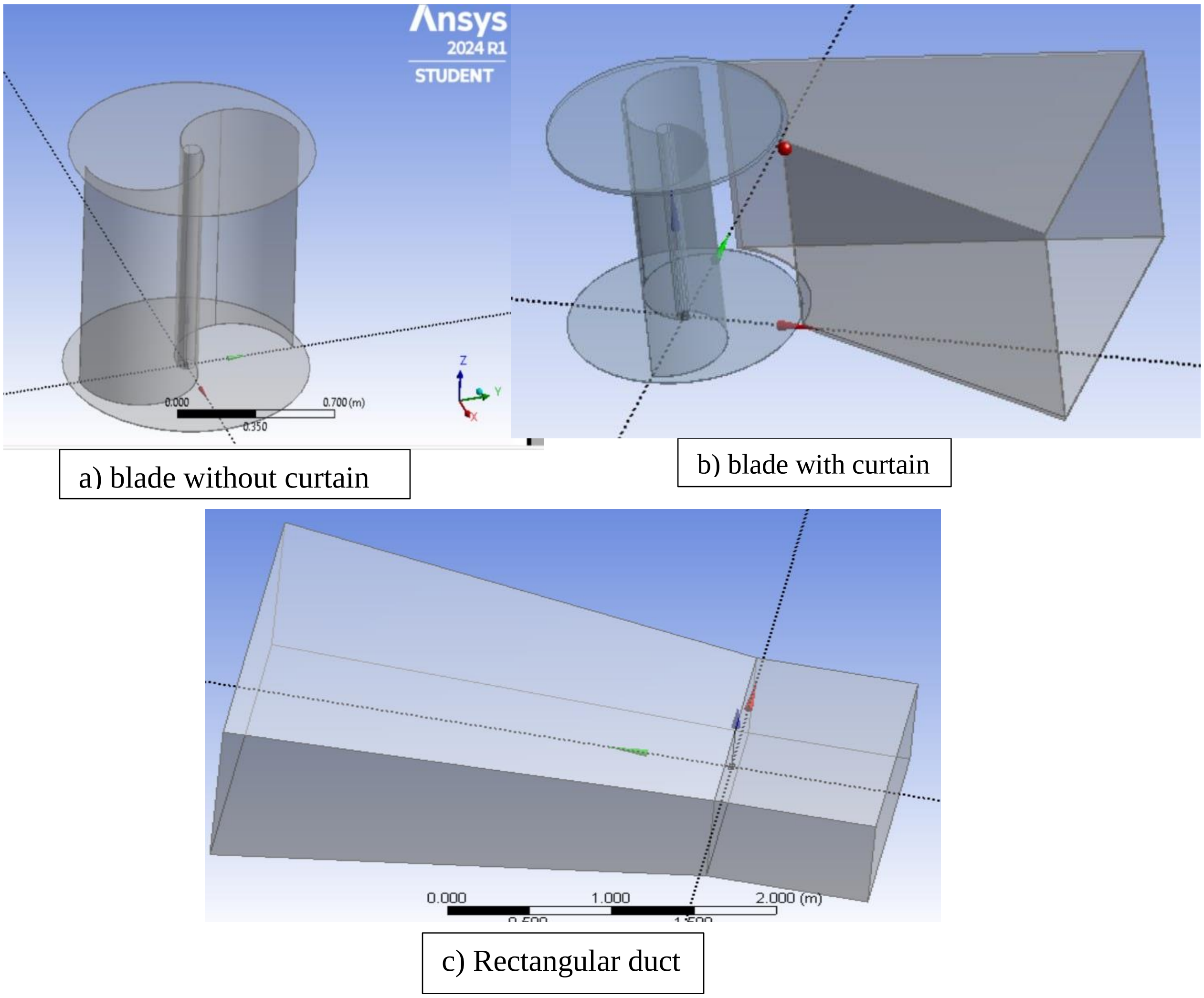

Figure 4.1 Geometrical models of turbine blades and the rectangular duct

4.4.2 Computational domain and boundary conditions

This study investigates turbine performance using Computational Fluid Dynamics (CFD). The computational domain is divided into rotating and stationary zones, with the rotating zone spinning at various tip speed ratios (TSRs) within the stationary zone. Both zones are connected by an interface, and the stationary zone has a rectangular cubic volume while the rotating zone has a cylindrical volume. The turbine design and geometrical parameters are identical for both turbines and are tabulated in the provided table.

Table 4.1 Boundary conditions used for curtain less blade model

No.	Name of boundary	Boundary type
1	Inlet	Velocity inlet
2	Outlet	Pressure outlet
3	Rotating domain	Moving wall
4	Outside domain	Wall symmetry
5	blade	No slip wall

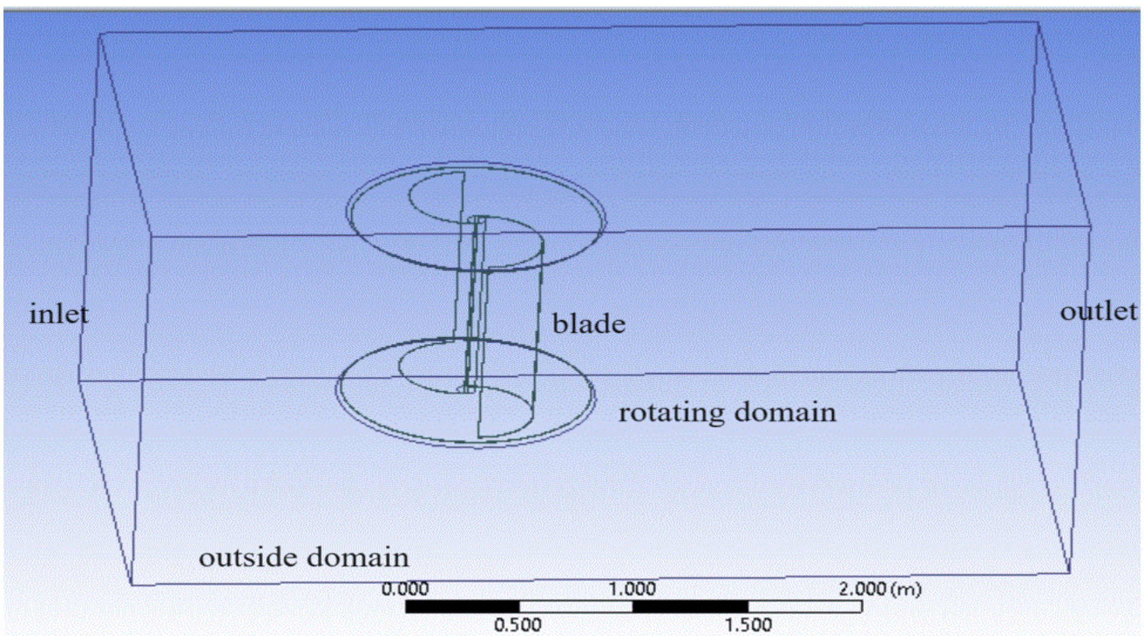

Figure 4.2 Isometric view of the computational domain without curtain

Table 4.2 Boundary conditions used for curtain blade model

No.	Name of boundary	Boundary type
1	Inlet	Velocity inlet
2	Outlet	Pressure outlet
3	Rotating domain	Moving wall
4	Outside domain	Wall symmetry
5	blade	No slip wall
6	curtain	Wall

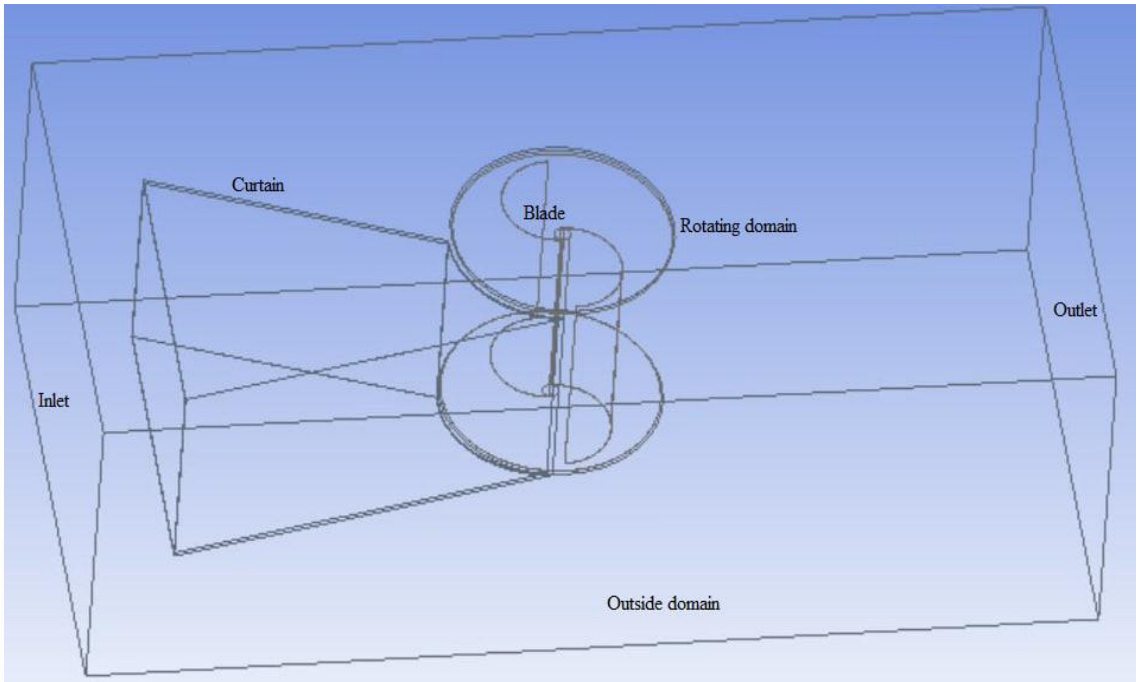

Figure 4.3 Isometric view of the computational domain of blade with curtain

4.4.3 Grid Independence Study

The grid independent limit (GIL) test is the process finding the limit of refinement and the mesh can be considered to the level of limit of grid independence (Munson et al., 2009). The grid independence limit has been achieved by the mesh size has been changed many times. Different refinement levels of mesh for the present work are listed. Refinement level is required for achieving finer mesh near the wall of the rotor as well as the inner fluid zone of the rotor. If the mesh is coarse then results will not be that accurate. Around the blade of the turbine bade is more refined mesh applied to get better result as shown figure below.

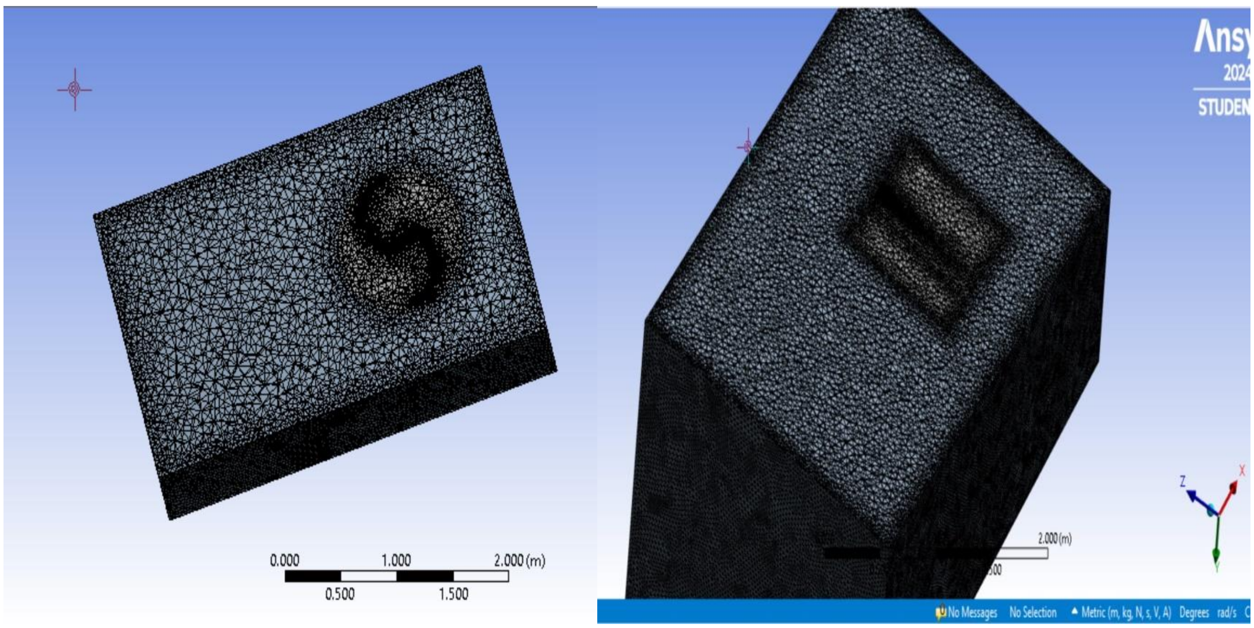

Figure 4.4 the sectional view of refined mesh around the blade

The process of grid independence test has been shown below figure; there are negligible changes in momentum coefficient (C_m) for different numbers of mesh elements so it is decided to conduct the numerical analysis with 750537 mesh elements where the value of moment coefficient value are not that much increasing if the number of elements is increased and the percentage error is less than 5%. So selecting the optimized cell numbers in order to analysis the blade including by considering the computational time.

Table 4.3 the number of elements to moment coefficient for grid independent test

Rotating domain cells	Outside enclosure domain cells	Total cells	C_m
75640	33682	109322	0.00938
357377	73822	431199	0.054
357371	188611	545982	0.084
362162	388375	750537	0.129
1533776	74402	1608178	0.135

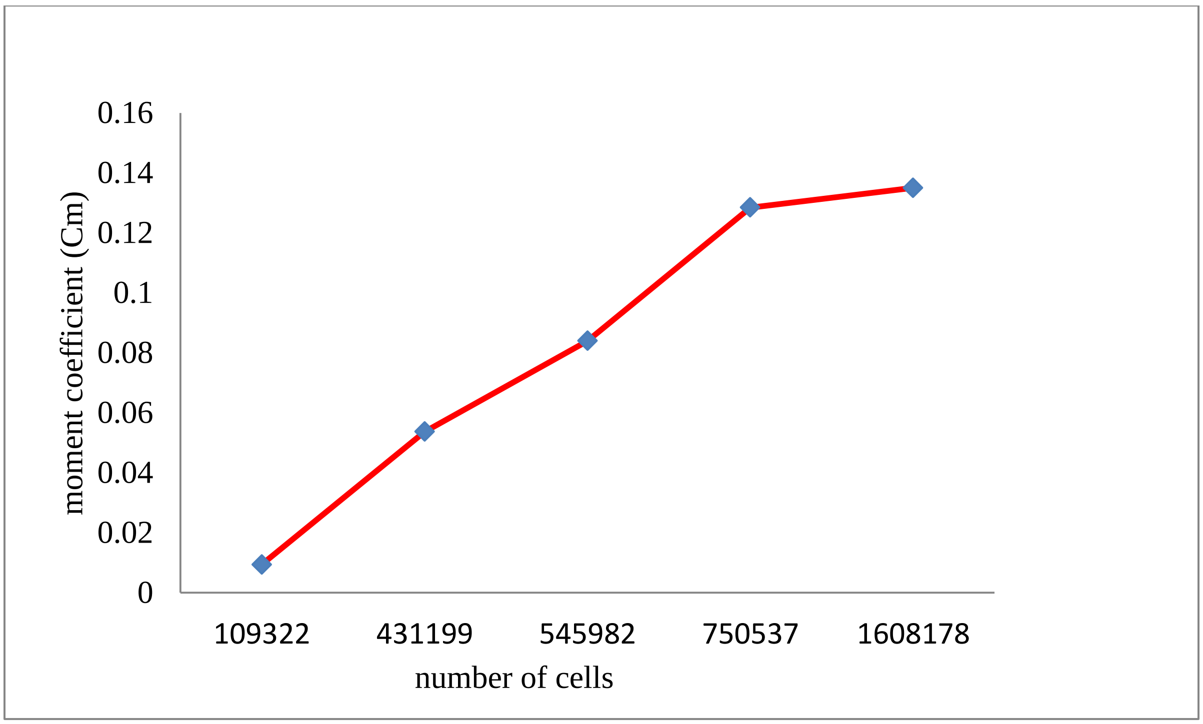

Figure 4.5 the grid independence test

CHAPTER FIVE

RESULTS AND DISCUSSION

This section presents and discussed the results getting from numerical analysis of the site potential assessments in hydrokinetic energy, hydrokinetic turbine design with and without curtain and including the rectangular flow accelerating duct.

5.1 Hydrokinetic Potential of Awash River at Tedecha

5.1.1 The Historical Discharge Data of River

An analysis of the historical discharge data identified representative discharge values.

a) Flow duration curves (FDCs) were used to estimate the average yearly discharge (Qy) for several rivers, enabling the calculation of their average water velocity along their lengths

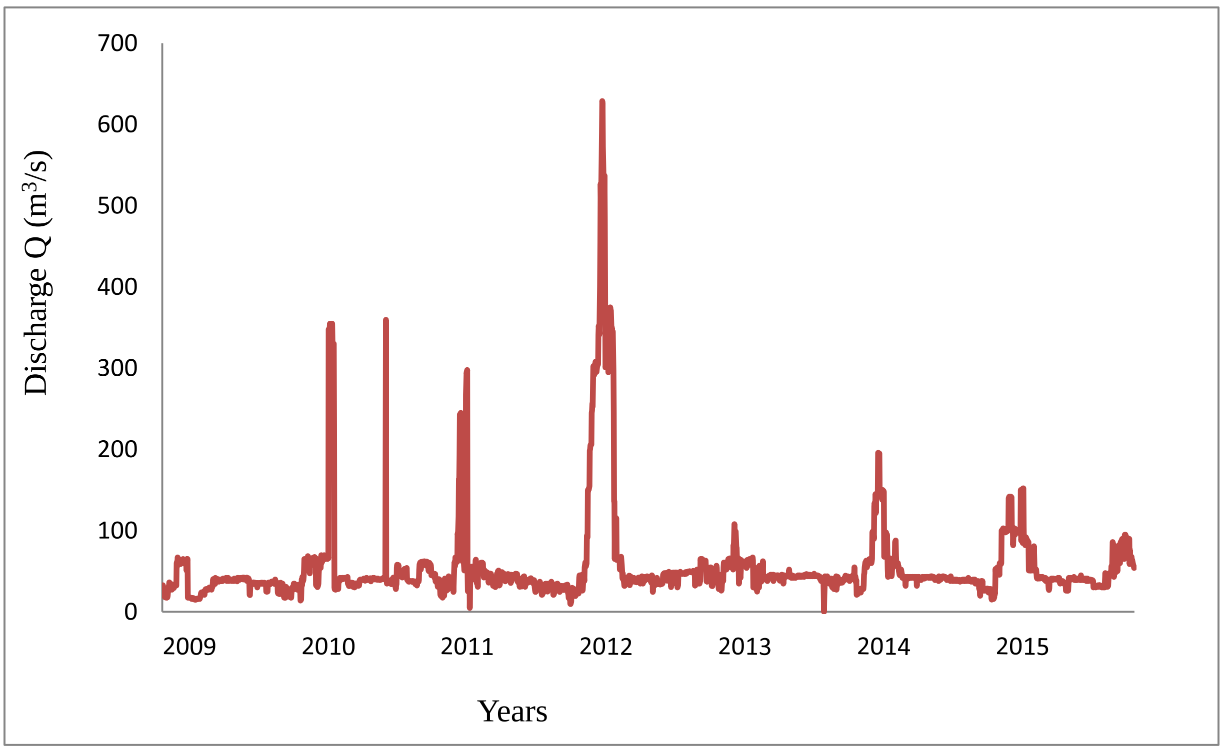

Figure 5.1 yearly average discharge of Awash River

From the figure above the yearly discharge of awash river was higher in 2012EC due to the annual rainfall of the year was higher and also minimum in 2009EC due to lower annual rainfall of the year.

b) The monthly average water velocity was estimated using monthly average discharges (Qm).

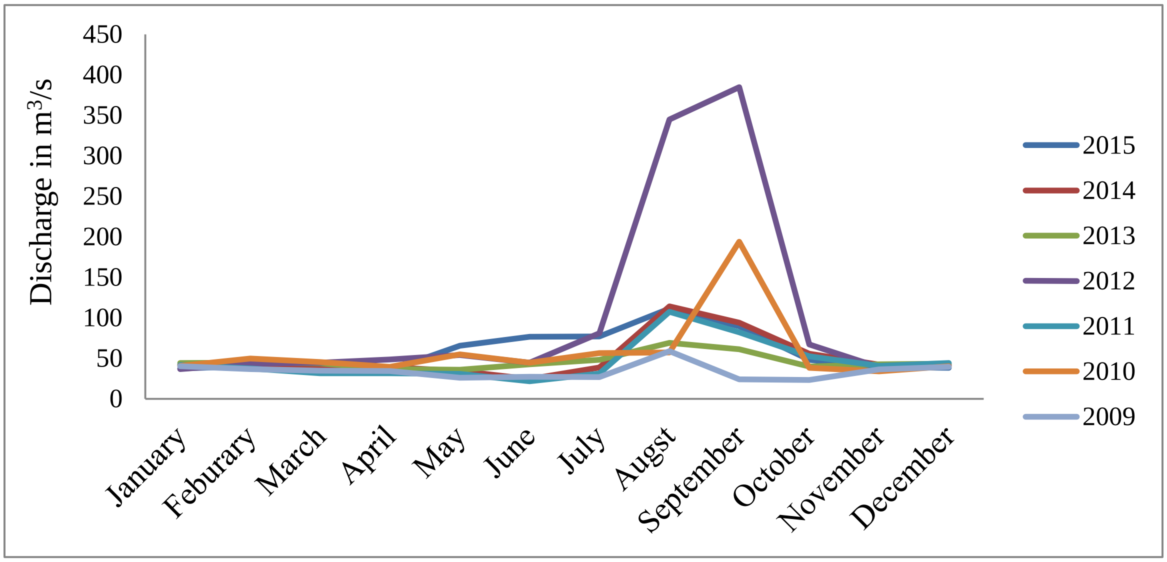

Figure 5.2 monthly average discharge of Awash River

c) To estimate daily average velocity, daily average discharge (Qd) was used. For validation of the hydrodynamic model, direct measurements of depth, width, and velocity were collected.

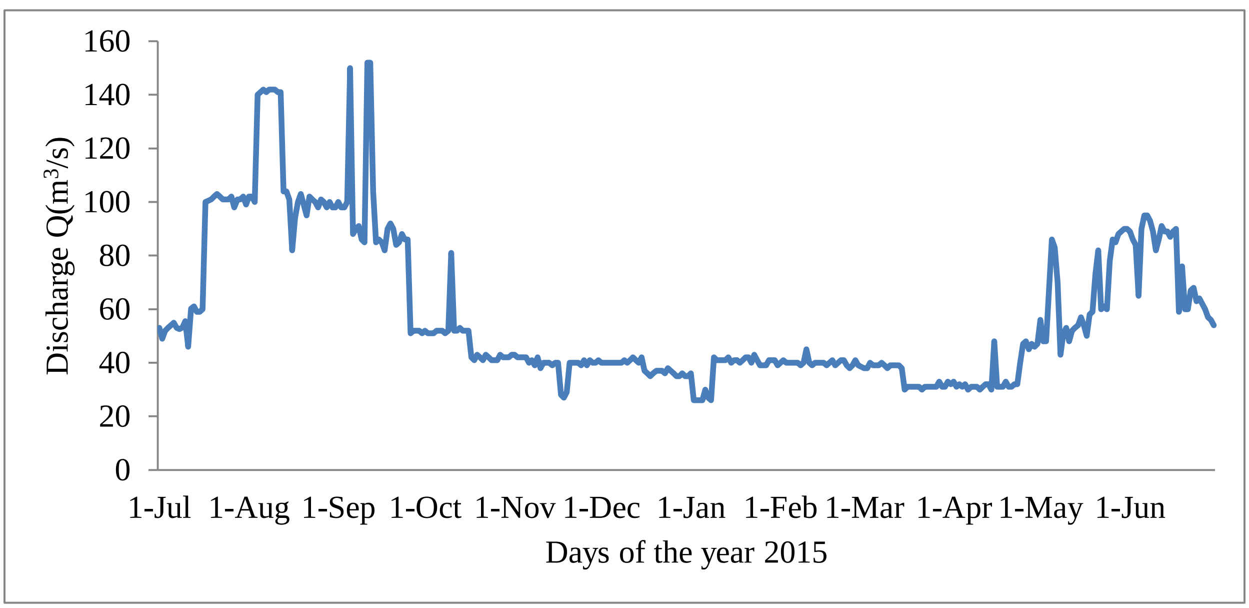

Figure 5.3 daily average discharge of Awash River

With a cut-in flow river speed of 0.5m/s, the minimum stream speed occurs during the dry season (March-April) at 0.98-1m/s, which is sufficient for power generation to start. The maximum-recorded velocity of 3.18m/s occurs in August, corresponding to the maximum (rated) power generation.

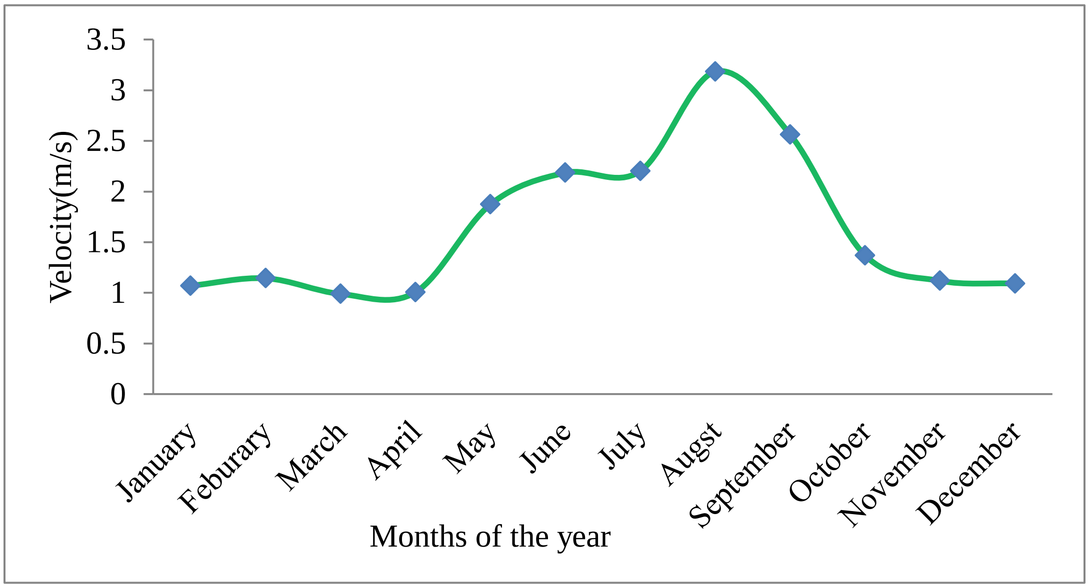

Figure 5.4 Average monthly water velocities

5.1.2 Flow duration curve (FDC)

One technique for analyzing the temporal variability of water flow rate date is flow duration curve. The flow duration curve is a graph that displays the flow rate in cubic meter per second against the percentage time. Conventional hydropower resource assessment is often performed by means of the Flow Duration Curve (FDC), The Flow Duration Curve (FDC) translates daily river discharge values into their corresponding durations, expressed as either the number of days a specific flow is exceeded or as a percentage of the total period. In hydropower plant design, the "firm flow" – the reliable water flow used to determine turbine capacity – is typically set at 20-30% of the total discharge occurrence based on the FDC.

Procedures for calculating the FDC

- ✓ Determine the seven-year mean flow rate
- ✓ Arranging the flow rate in descending order to use the rank order method
- ✓ Rearrange the months based on the rank, then compute the exceeded percentage
- ✓ Create a graph showing the flow rate versus the exceeded percentage

The historical Q_y data FDC plot of the rivers under consideration is shown in Fig below.

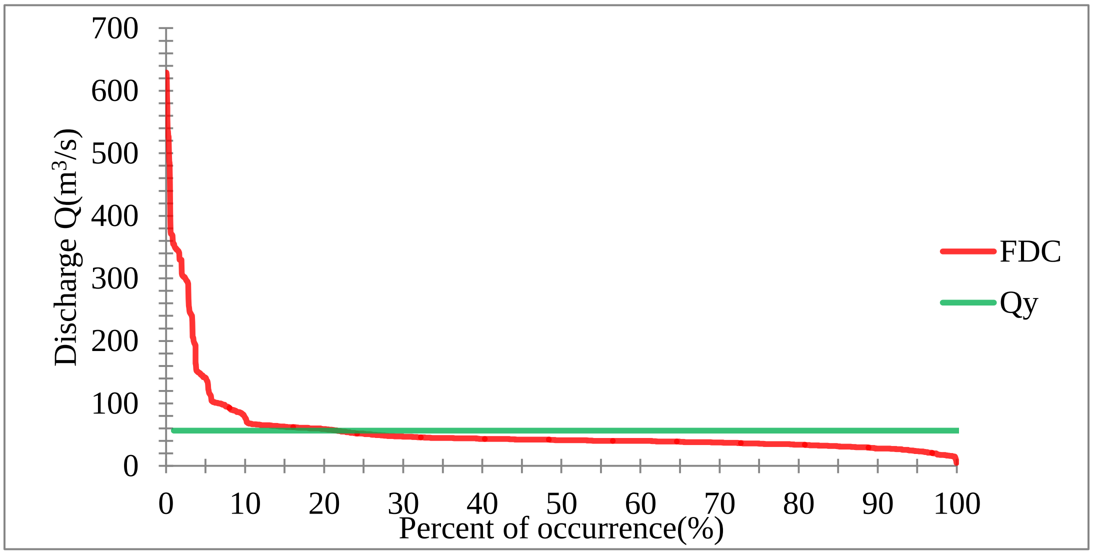

Figure 5.5 FDC of Awash River

The average discharge is 56.377m^3/s, which is found between 20-30% of occurrence so it can be, used the average discharge as a representative discharge.

5.1.3 Site Parameter Measurements

1) Site 1(8°28'34"N 39°10'03"E)

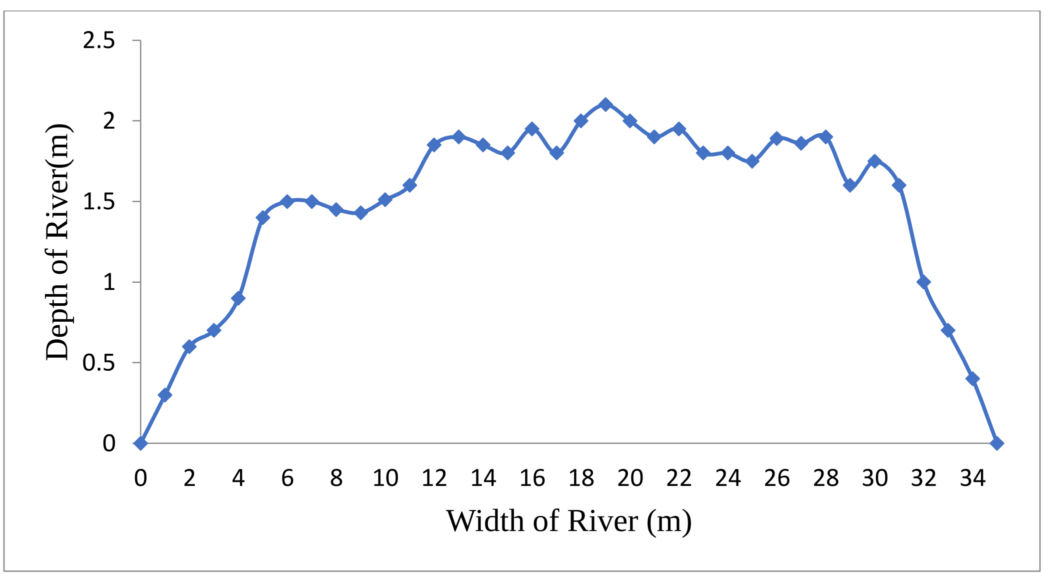

Figure 5.6 River cross section at site1

Table 5.1 the time taken for the floating object covered a distance of 2 meters

Readings	Distance travelled (m)	Time taken (s)	Surface velocity(m/s)	Average velocity(m/s)
1	2	0.91	2.20	1.87
2	2	0.9	2.22	1.89
3	2	0.8	2.50	2.13
4	2	0.93	2.15	1.83
5	2	0.9	2.22	1.89
6	2	0.86	2.33	1.98
7	2	0.92	2.17	1.85
	Average	0.888571429	2.26	1.92

2) Site 2 (8°28'33"N 39°10'16"E)

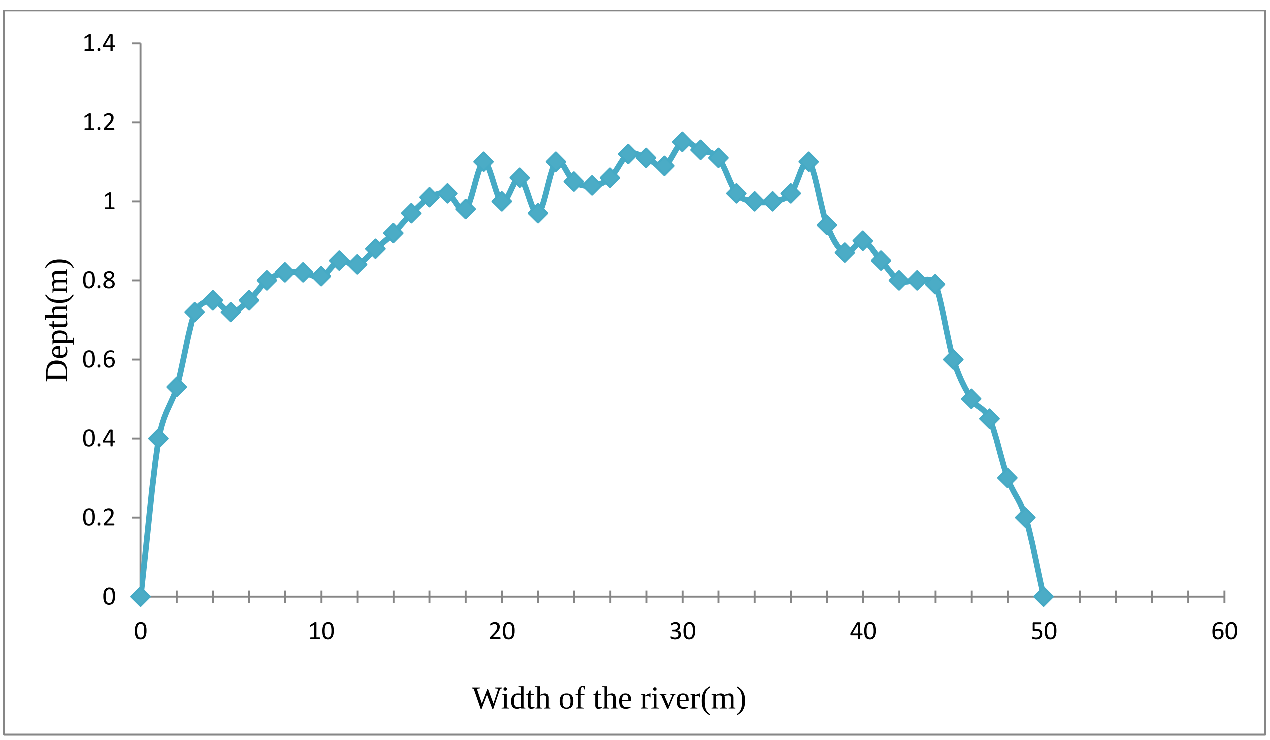

Figure 5.7 River cross section at site 2

Table 5.2 Recorded time taken for the floating object covered a distance of 2 meters

Readings	Distance travelled (m)	Time taken (s)	Surface velocity(m/s)	Average velocity(m/s)
1	2	1.7	1.18	1.00
2	2	1.5	1.33	1.13
3	2	1.3	1.54	1.31
4	2	1.2	1.67	1.42
5	2	1.6	1.25	1.06
6	2	1.23	1.63	1.38
7	2	1.6	1.25	1.06
	Average	1.45	1.41	1.19

3) Site 3 (8°28'33''N 39°10'30''E)

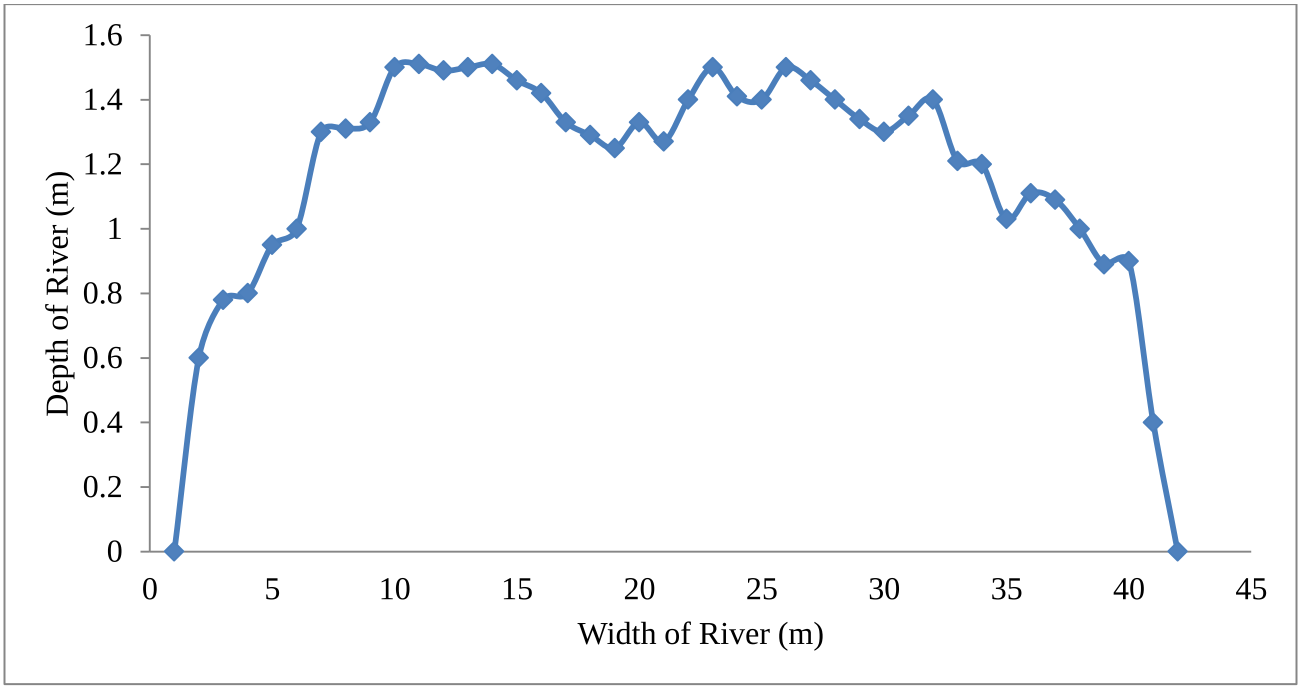

Figure 5.8 River cross section at site 3

Table 5.3 Recorded the time taken for the floating object covered a distance of 2 meters

Readings	Distance travelled (m)	Time taken (s)	Surface velocity (m/s)	Average velocity (m/s)
1	2	1.71	1.17	0.99
2	2	1.63	1.23	1.04
3	2	1.67	1.20	1.02
4	2	1.72	1.16	0.99
5	2	2	1.00	0.85
6	2	1.95	1.03	0.87
7	2	1.83	1.09	0.93
	Average	1.79	1.13	0.96

Among the three sites mentioned above the site one was selected for hydrokinetic savonius turbine because of the flow velocity and the depth of the river is the highest one among other two sites compared and the site is suitable for hydrokinetic turbine installation as well as its location is near to the irrigation lands.

5.1.4 Hydrokinetic Potential of Awash At Site 1

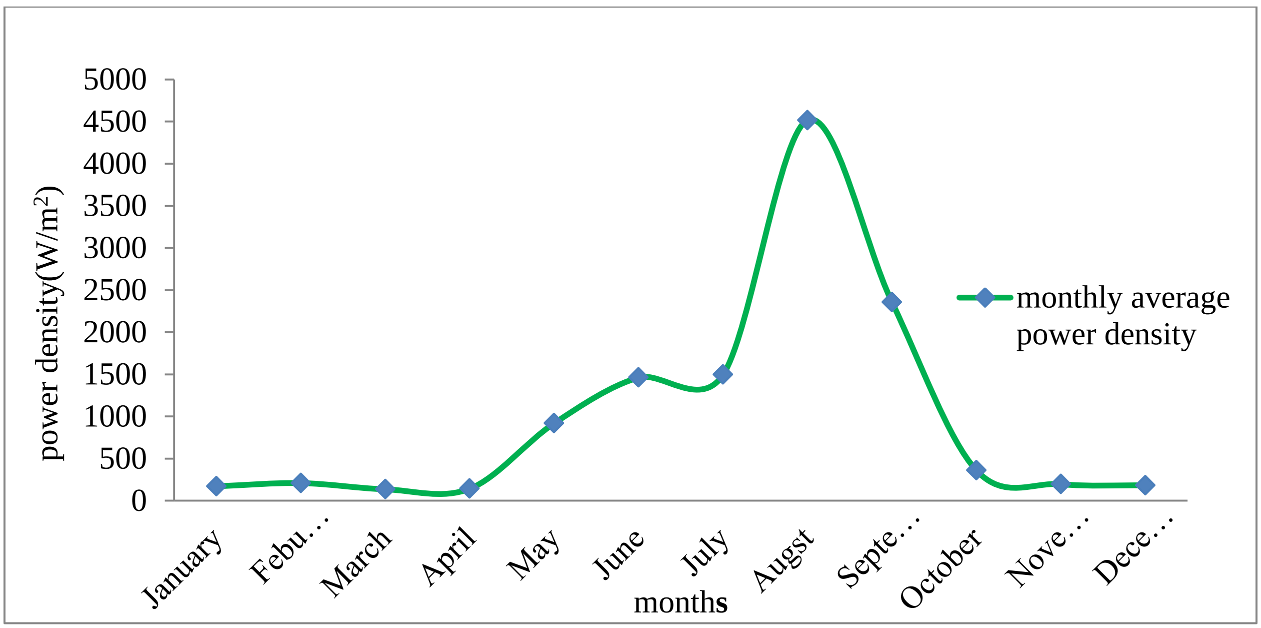

Figure 5.9 monthly average hydrokinetic power density

From the above figure 5.9 shows that the monthly average power density which is the mean annual power available per square meter of swept area of the turbine. The monthly average power density from January to April and October to December is relatively lower value and higher power density in May to September. The maximum monthly average power density is in August with 4500W/m^2.

5.2 Flow analysis on the rectangular duct

In order to accelerate the low velocity of the river to produce more power the flow accelerator rectangular duct designed and the flow velocity on the duct is as shown figure below. From figure 5.1 the pressure distribution along the duct is in decreasing way because of the pressure, energy is transformed in to the velocity energy. During the starting or at the inlet the pressure was higher but gradually it become decreasing.

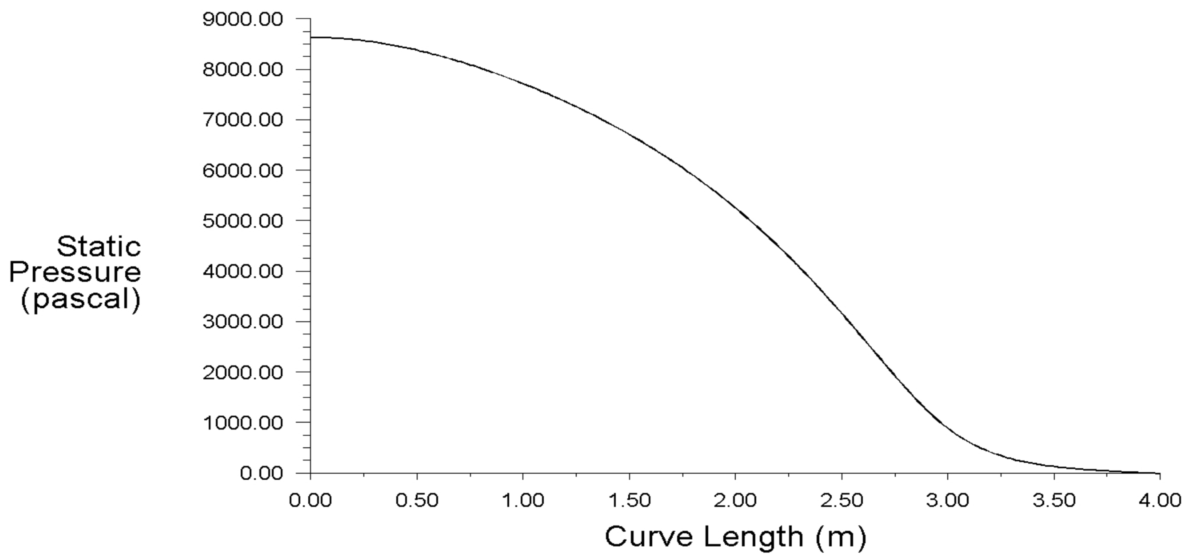

Figure 5.10 the static pressure on the duct flow

From figure 5.11 below, the velocity in the rectangular duct is drastically increasing and achieving the required amount of flow velocity to fulfill the required demand. The velocity at the inlet is free stream velocity with lower velocity 1.92m/s but after traveling, some distances the pressure energy transferred to kinetic energy of the flow velocity and increased to 4.6m/s.

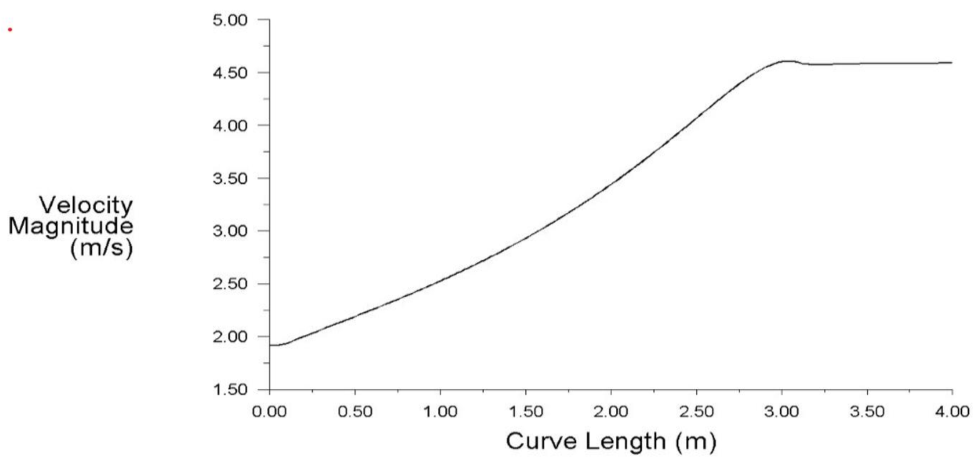

Figure 5.11 the velocity flow through the rectangular duct

The velocity contour is shown the figure 5.12 the velocity contour shows around the inlet the velocity is almost all nears to the free stream velocity and after some distance traveled the velocity is increased. It nears to the walls of the duct the contour velocity is diminished and the velocity around the wall is minimized due to the wall shear. The red color of the contour shows the velocity is higher and dense around the throat of the duct because of the lower velocity area. The reason contours bulge inward in a rectangular duct, like the yellow contour in this image, is because they are showing the velocity magnitude across a two-dimensional slice of the duct. The highest velocity tends to be in the center of the duct, with the velocity reducing as you approach the walls due to friction. This creates a curved profile when represented in a contour plot.

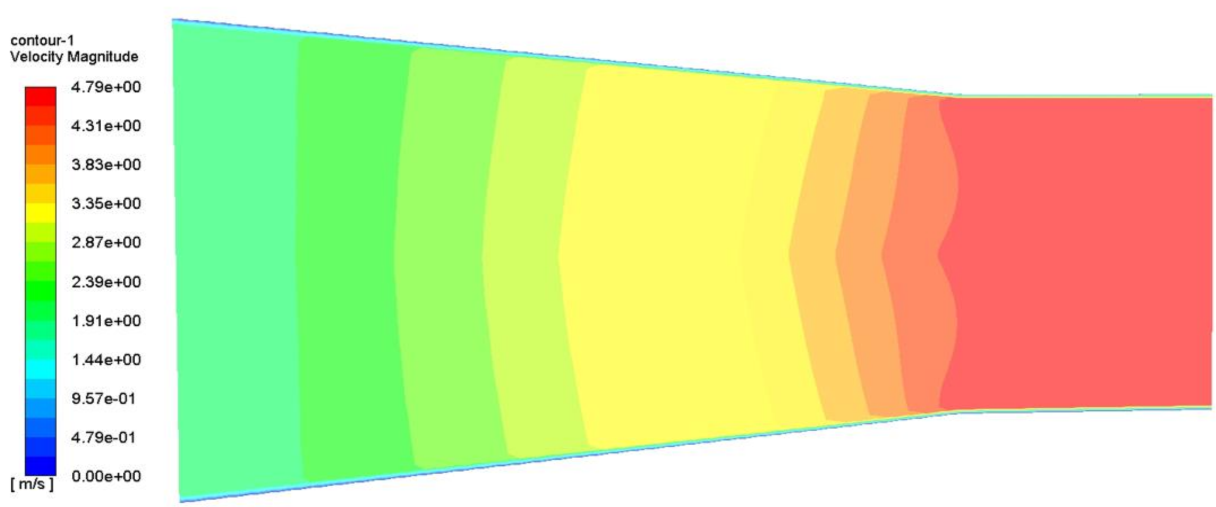

Figure 5.12 the velocity contour of the river flow through the duct

5.3 Power and Torque Analysis

torque and power coefficients (C_m and C_p) are important performance characterstics of the savonius hydrokinetic turbine to studies the performance of the turbine. In this research the average power coefficient and average torque coefficients were investigated as a function of the tip speed ratio for without curtain and curtain turbine that blocks the flow into the returning blade. Figure (5.13) and (5.14) below shows the torque coeefficient and power coefficient with respect to the tip speed ratio. The result shows that with increasing of the tip speed ratio the torque coefficient is decreasing. From this result the curtain used in savonis turbine improves the performance of the turbine by blocking the incoming fluid do not stricks the returning blade. The maximum average torque coefficient provided from with curtain blade is at TSR=0.2 provides the corresponding value C_m=0.38, representing 31% gain in average torque coeffiecient compared to the bar curtain less turbine with the coeffiecient of torque C_m=0.29.

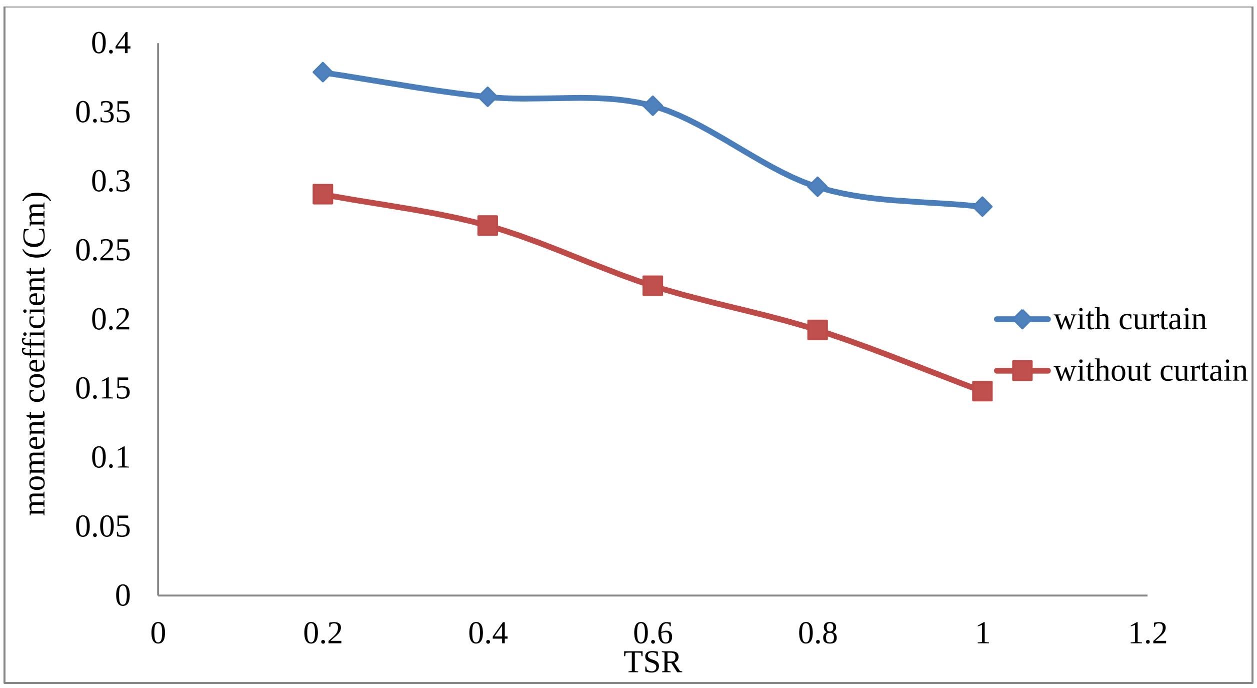

Figure 5.13 the moment coefficient versus the tip speed ratio of curtain and without curtain blade

As depicted in figure (5.14) shown below the power coefficient of without curtain is maximum at TSR=0.8 with C_P =0.15 and the maximum power coefficient for curtain blade is at TSR=1 with C_P =0.28. Therefore, from this value can be decided that with curtain design is more efficient than without the curtain blade.

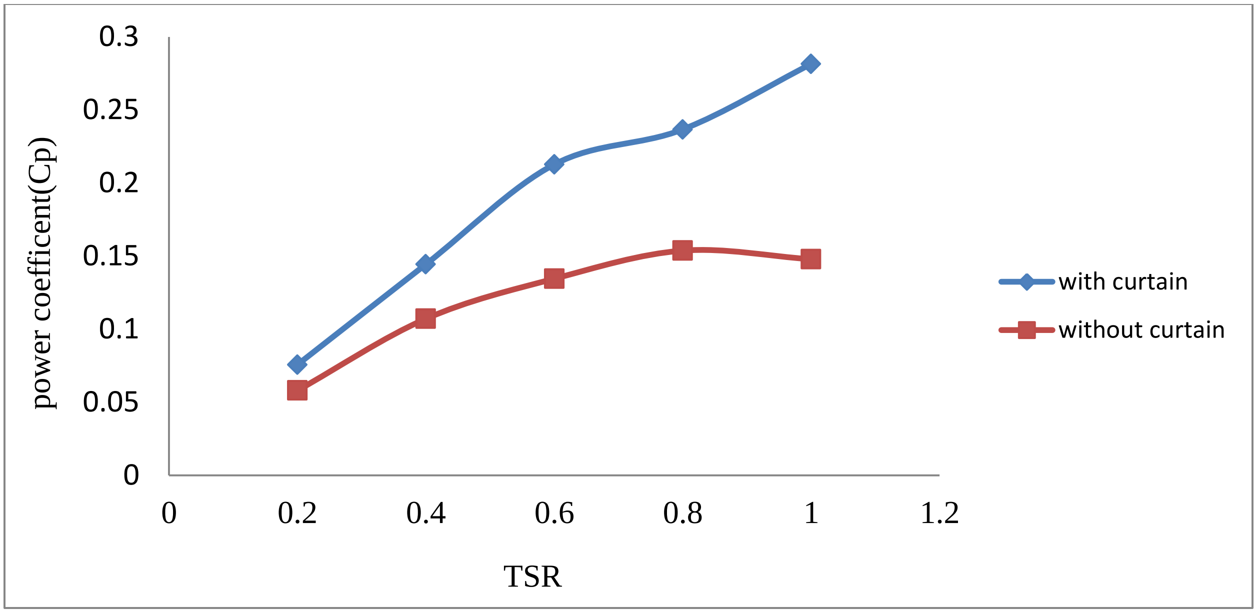

Figure 5.14 the power coefficient versus the tip speed ratio of without curtain blade

5.4 Flow field analysis

From this part, overall analysis of the flow characteristics in the domain of flow and characteristics of the flow includes the critical factors as pressure and velocity investigated based on the graph results. To analysis, the impacts of with curtain and without curtain on the performance of hydrokinetic savonius turbine velocity and pressure contours were analyzed in optimum level.

5.4.1 Pressure variation

From the graph of the pressure contour of with curtain and without curtain blades are shown their differences in the graph. Without curtain graph depicts that the pressure is higher in the concave sides of advancing blades with its convex sides also countered by high pressure this reduce the rotation of the rotor by creating negative torque. Some portions of the convex sides of returning blade affected by high-pressure both of this results in the curtain less blades affected by negative torque. With curtain type higher pressure created on the concave sides of advancing blade with lower on its convex side especially at the tip of the blade and the curtain blocks the convex sides of returning blade from the impacts of higher pressure. From the graph can be concluded that with curtain has more net positive torque effects than without curtain.

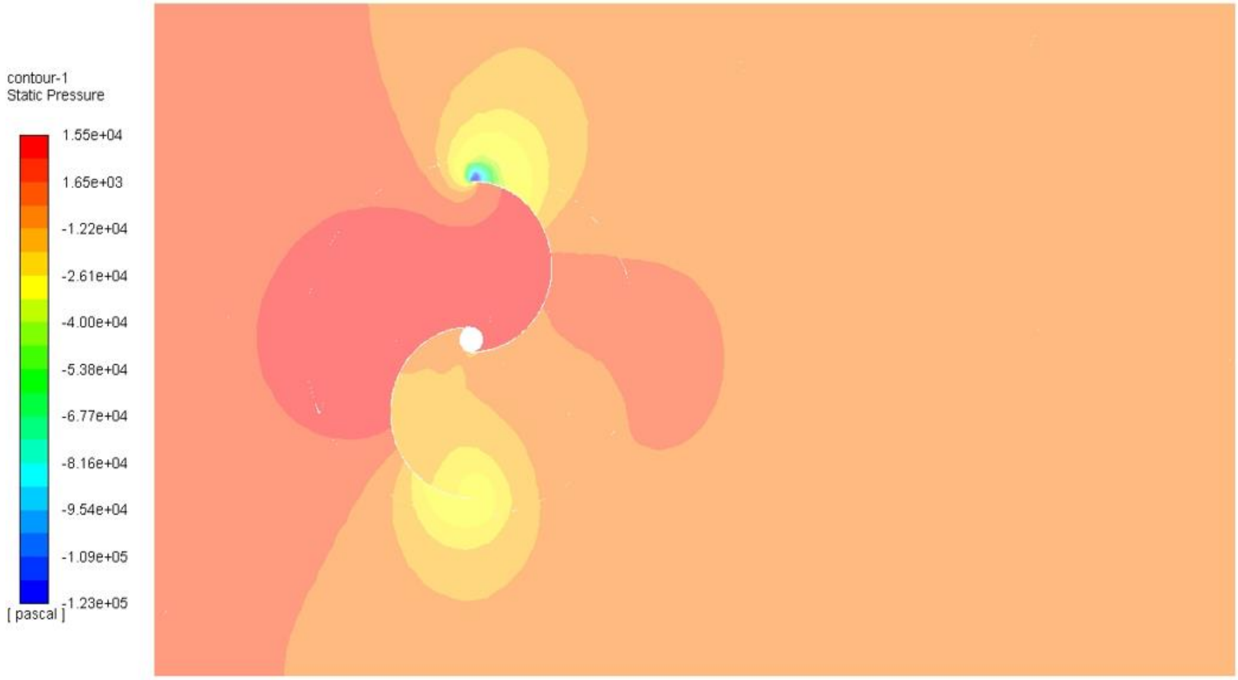

(a) without curtain

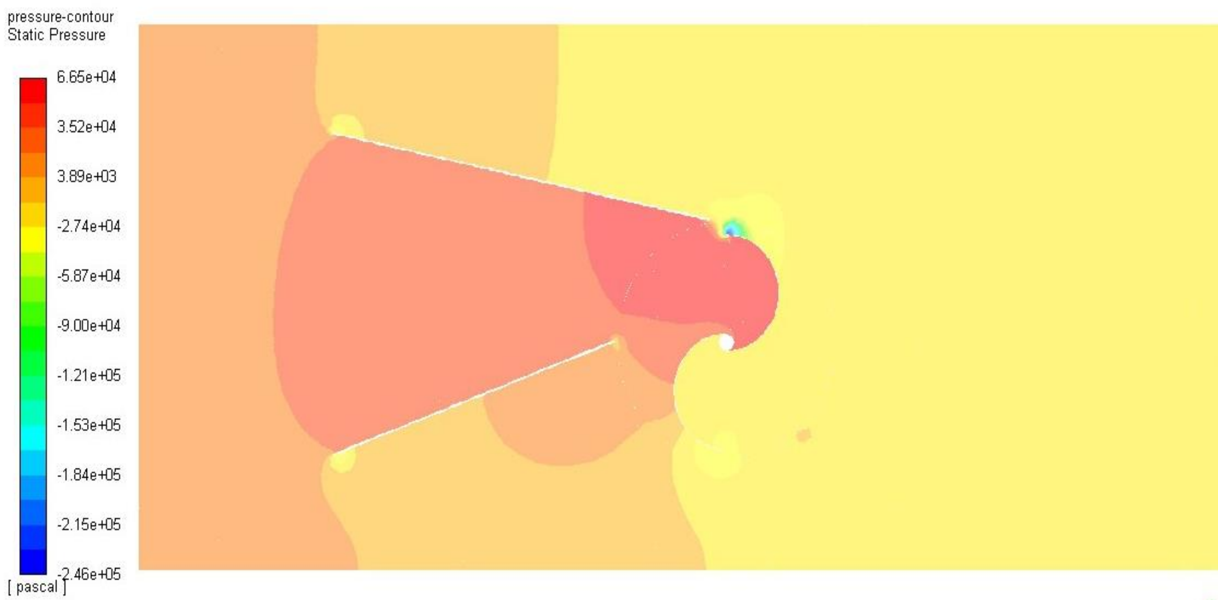

(b) With curtain

Figure 5.15 the pressure contour distribution of with curtain and without curtain

5.4.2 Velocity Variation

The presence of the curtain changes the velocity distribution around the rotor blade compared with the bare turbine, the velocity streamline used for comparison of the hydrodynamic performance of the rotor with without the curtain as shown figure below. From the graph the function of the curtain are analyzing the velocity streamline at the rotor blade. During the starting of rotation, the curtain blocks the direct impact of the streamlines on the returning bade convex sides. This lowered the number of streamline that hits the convex sides of the blade and their velocity lowered compared to a rotor without curtain. This decreases the opposing drag force on the sides of returning blade. In addition, the curtain redirects the incoming free stream velocity towards the convex surface of the advancing blade and leads to an enhancement in the positive torque of the advancing blade.

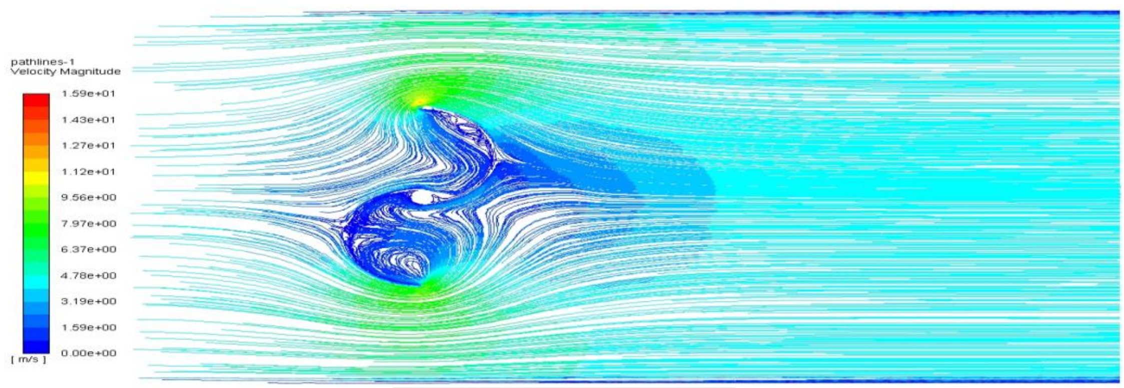

a) Without curtain

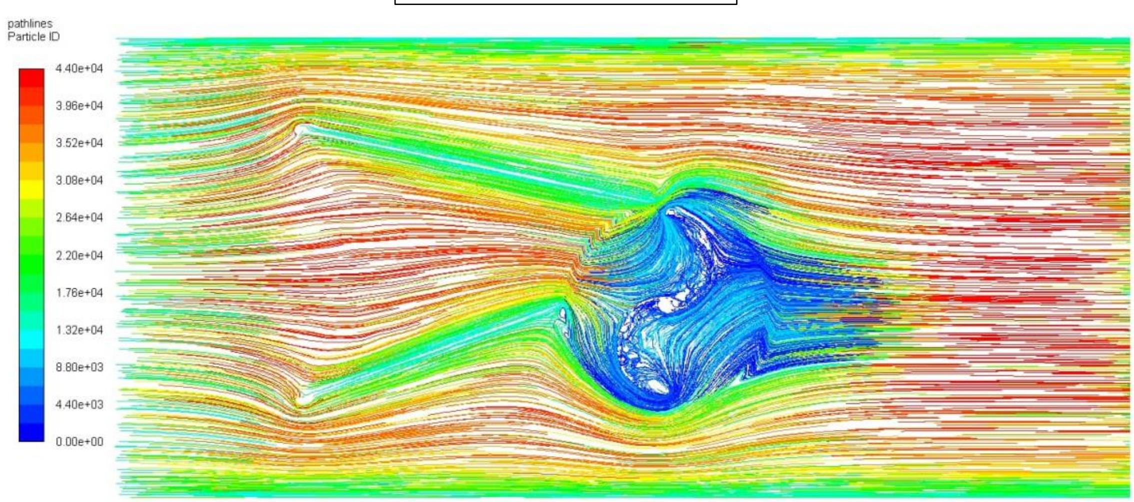

b) With curtain

Figure 5.16 the velocity streamline distribution of with curtain and without curtain

The velocity contour in the figure below shows in curtain less blades at the tip of the blade the velocity is higher but in curtain type the returning blade tip covered by the curtain due to the pressure difference created between the advancing and returning blades this creates positive torque in the rotor and the velocity at blade of advancing side has minimum at the blade wall.

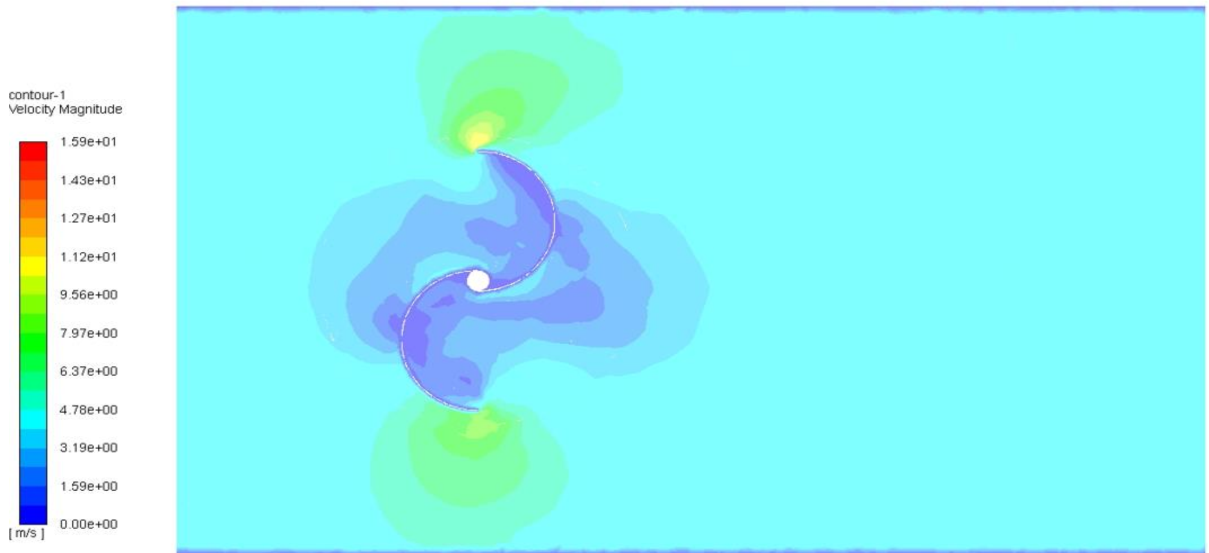

a) Without Curtain

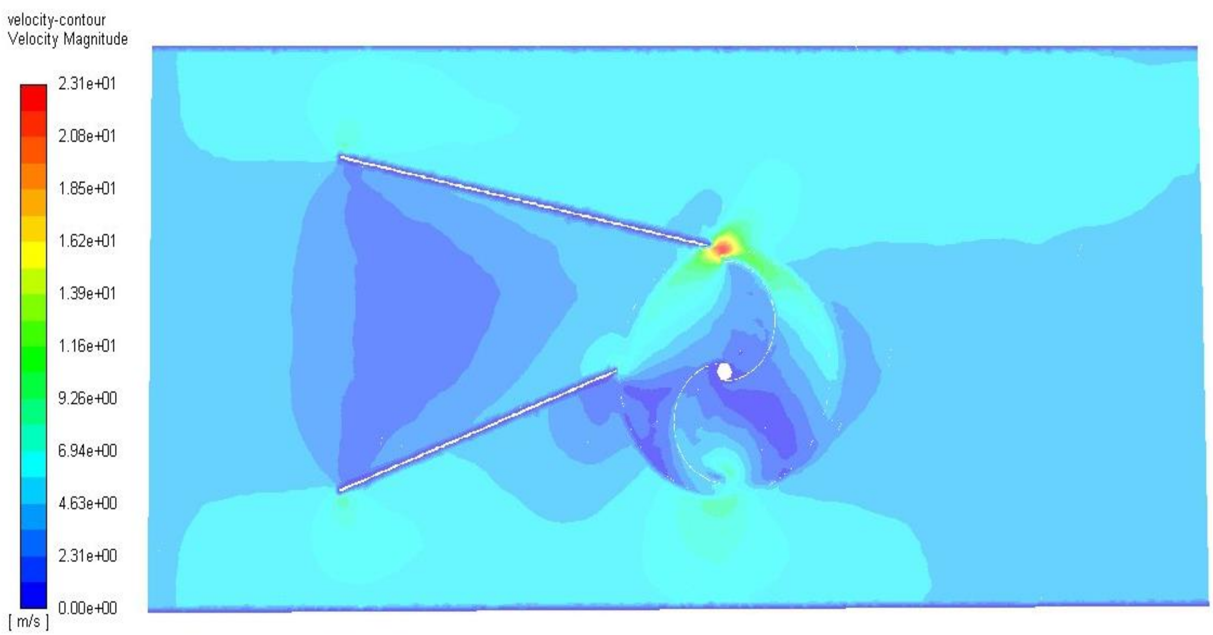

b) With curtain

Figure 5.17 the velocity contour distribution of with curtain and without curtain

The velocity vector shown in figure below in curtain less blade both sides of the returning blade as well as the advancing blades the velocity vector is higher end side of the blade and the flow velocity impacts on the tip sides of the blade. This leads to decrease the rotation of the blade by generating negative torque, but in curtain type, the larger velocity vector at advancing blade sides this helps to generate positive torque.

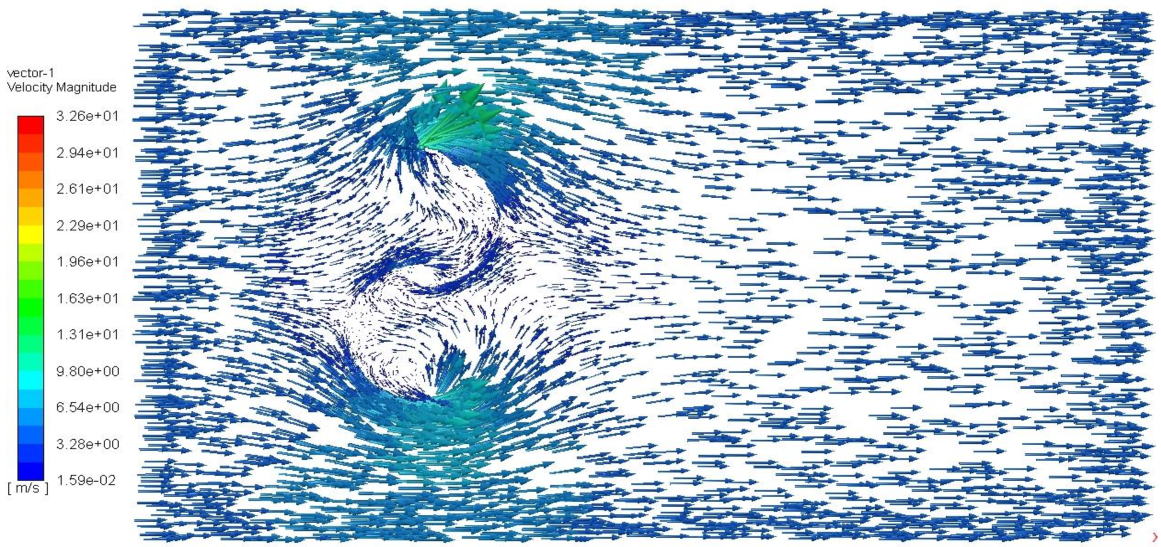

a) Without curtain

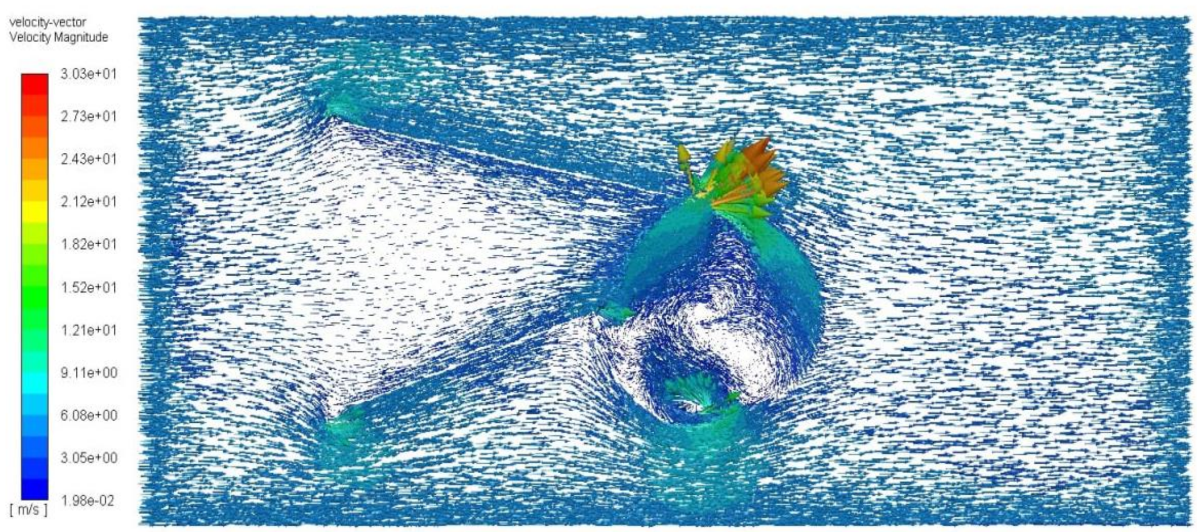

b) With curtain

Figure 5.18 the velocity vector distribution of with curtain and without curtain

CHAPTER SIX

CONCLUSION AND RECOMMENDATION

6.1 Conclusion

This research had manly focused on the potential assessment of Awash River at tedecha in hydrokinetic turbine energy for the application of irrigation, from the assessment three sites was selected for comparison. From the three sites site 1 was selected because of its higher flow velocity, water depth and suitability for installation of the turbine suitable to hydrokinetic turbine installation than other system. From the assessment at site, 1 obtained 1.92m/s flow velocity. This velocity is not large enough for irrigation due to this reason the flow accelerator rectangular duct was designed and increases the velocity from 1.92m/s to 4.6m/s. this velocity enough for energy production for the site.

Based on the velocity increased by the duct and the parameters getting from the site the hydrokinetic curtain savonius turbine components were designed. From the designed the output power of the turbine is 13.6 Kw generated. Based on this power output three-phase AC synchronous STC generator with the rated output power of 15Kw, apparent power of 18.8KVA with 1500 rpm selected and pump type of electric high flow rate centrifugal water pump with maximum power rating of 10Kw were selected.

Numerical analysis comparison of the performance by moment coefficient and power coefficient of with curtain and without curtain savonius blade were done. Based on the numerical results the maximum average torque coefficient provided from with curtain blade is at TSR=0.2 provides the corresponding value C_m=0.38, representing 31% gain in average torque coeffiecient compared to the base curtain less turbine with the coeffiecient of torque C_m=0.29. The power coefficient of without curtain is maximum at TSR=0.8 with C_P =0.15 and the maximum power coefficient for curtain blade is at TSR=1 with C_P =0.28. Therefore, from those above values can be concluded that with curtain design is more efficient than without the curtain blade.

6.2 Recommendation

- ✓ The selected site has a higher in hydrokinetic energy potential so any concerned bodies should studies the potential assessment by using proper measuring devices like water flow meter and other proper devices.
- ✓ Anyone who will be interested in this area should study on the economic and financial feasibility of hydrokinetic energy at the site.
- ✓ Any one-who are interested bodies working on this area and has the potential for experiment you should test the result by making an experiment
- ✓ Flow Rivers so hydrokinetic turbine technology is no practicable still now, so we should do further studies in the area of implementation

REFERENCES

Abebe, N. (2014). Feasibility Study of Small Hydropower Schemes in Giba and WorieSubbasins of Tekeze River, Ethiopia. Journal of Energy Technologies and Policy, 4(8), 8-17.

Akwa JV, Vielmo HA, Petry AP. A review on the performance of Savonius wind turbines. Renew Sustain Energy Rev 2012;16(5):3054–64. https://doi.org/10. 1016/j.rser.2012.02.056.

Behrouzi F, Nakisa M, Maimun A, Ahmed YM. Global renewable energy and its potential in Malaysia: a review of hydrokinetic turbine technology. Renew Sustain Energy Rev 2016;62:1270–81. https://doi.org/10.1016/j.rser.2016.05.020.

Bhattacharyya, S. C. (2019). Energy economics: concepts, issues, markets and governance.Springer Nature

Chaudhari, V. N., & Shah, S. P. (2023). Numerical investigation on the performance of an innovative Airfoil-Bladed Savonius Hydrokinetic Turbine (ABSHKT) with deflector. International Journal of Thermofluids, 17, 100279.

Dos Santos, I. F. S., Camacho, R. G. R., Tiago Filho, G. L., Botan, A. C. B., &Vinent, B. A. (2019). Energy potential and economic analysis of hydrokinetic turbines implementation in rivers: An approach using numerical predictions (CFD) and experimental data. Renewable Energy, 143, 648-662.

Frikha S, Driss Z, Ayadi E, Masmoudi Z, Abid MS. Numerical and experimental characterization of multi-stage Savonius rotors. Energy 2016;114:382–404.https://doi.org /10.1016/j.energy.2016.08.017

Gailiušis, B., Jakimavičius, D., Šarauskienė, D., &Jurgelėnaitė, A. (2017).Assessment of hydrokinetic resources of small and medium-size rivers: the Lithuanian case.Baltica, 23–30.

Golecha, K., Eldho, T. I., &Prabhu, S. V. (2012). Study on the interaction between two hydrokinetic Savonius turbines. International Journal of Rotating Machinery, 2012

Goundar, J. N., Prasad, D., & Ahmed, M. R. (2013, November).Design and performance testing of a ducted savonius turbine for marine current energy extraction.In ASME International

Mechanical Engineering Congress and Exposition (Vol. 56291, p. V06BT07A093).American Society of Mechanical Engineers.

Guta, D. D. (2018). Determinants of household adoption of solar energy technology in rural Ethiopia.Journal of cleaner production, 204, 193-204.

Ibrahim, W. I., Mohamed, M. R., Ismail, R. M. T. R., Leung, P. K., Xing, W. W., & Shah, A. A. (2021). Hydrokinetic energy harnessing technologies: A review.Energy Reports, 7.

Kailash, G., Eldho, T. I., &Prabhu, S. V. (2012). Performance study of modified Savonius water turbine with two deflector plates. International Journal of Rotating Machinery, 2012

Kamoji MA, Kedare SB, Prabhu SV. Experimental investigations on single stage, two stage and three stage conventional Savonius rotor. Int J Energy Res 2008;32: 877–95. https://doi.org/10.1002/er.1399.

Kerikous E, Th´evenin D. Performance Enhancement of a Hydraulic Savonius Turbine by Optimizing Overlap and Gap Ratios. ASME 2019 Gas Turbine India Conf. 2019, vol. 2, American Society of Mechanical Engineers; 2019. https://doi. org/10.1115/GTINDIA2019-2670.

Khan, M. J., Iqbal, M. T., &Quaicoe, J. E. (2006, May). A technology review and simulation based performance analysis of river current turbine systems. In 2006 Canadian Conference on Electrical and Computer Engineering (pp. 2288-2293).

Khan MJ, Iqbal MT, Quaicoe JE.River current energy conversion systems: Progress, prospects and challenges. Renew Sustain Energy Reviews 2008;12:2177–93.

Khan, M. J., Bhuyan, G., Iqbal, M. T., &Quaicoe, J. E. (2009).Hydrokinetic energy conversion systems and assessment of horizontal and vertical axis turbines for river and tidal applications: A technology status review.Applied energy, 86(10), 1823-1835.

Khan, Z. U., Ali, Z., & Uddin, E. (2022). Performance enhancement of vertical axis hydrokinetic turbine using novel blade profile. Renewable Energy, 188, 801-818.

Ladokun, L. L., Sule, B. F., Ajao, K. R., &Adeogun, A. G. (2018). Resource assessment and feasibility study for the generation of hydrokinetic power in the tailwaters of selected hydropower stations in Nigeria. Water Science, 32(2), 338-354.

Mabrouki I, Driss Z, Abid MS. Experimental investigation of the height effect of water Savonius rotors. Int J MechAppl 2014;4:8–12. https://doi.org/10.5923/j. mechanics.20140401.02.

Maldar, N. R., Ng, C. Y., &Oguz, E. (2020). A review of the optimization studies for Savonius turbine considering hydrokinetic applications. Energy Conversion and Management, 226, 113495.).

Mohamed, M. H., Janiga, G., Pap, E., &Thévenin, D. (2010).Optimization of Savonius turbines using an obstacle shielding the returning blade. Renewable Energy, 35(11), 2618-2626.

Mosbahi, M., Ayadi, A., Chouaibi, Y., Driss, Z., &Tucciarelli, T. (2019).Performance study of a Helical Savonius hydrokinetic turbine with a new deflector system design. Energy Conversion and Management, 194, 55-74.

Ngoma, D. H., & Wang, Y. (2018). Hhaynu micro hydropower scheme: Mbulu–Tanzania comparative river flow velocity and discharge measurement methods. Flow Measurement and Instrumentation, 62, 135-142

Olatunji, O. A. S., Raphael, A. T., &Yomi, I. T. (2018).Hydrokinetic energy opportunity for rural electrification in Nigeria.International Journal of Renewable Energy Development, 7(2), 183.

Park, J., Knight, B.G., Liao, Y. et al. CFD-based design optimization of ducted hydrokinetic turbines. Sci Rep 13, 17968 (2023). https://doi.org/10.1038/s41598-023-43724-4

Patel, V., Eldho, T. I., &Prabhu, S. V. (2019). Velocity and performance correction methodology for hydrokinetic turbines experimented with different geometry of the channel. Renewable energy, 131, 1300-1317.

Richard. G. B. And j. K. Nisbett, shigley's , mechanical engineering design, ninth edit. New york: mcgraw-hill, 2011.

R.S. KHURMI J.K. GUPTA, A textbook of Machine Design, 14 edditio., no. I. EURASIA PUBLISHING HOUSE (PVT.) LTD, 2005.

Salleh, M. B., Kamaruddin, N. M., & Mohamed-Kassim, Z. (2019).Savonius hydrokinetic turbines for a sustainable river-based energy extraction: A review of the technology and potential applications in Malaysia.Sustainable energy technologies and assessments, 36, 100554.

Sarauskiene, D., 2017. Assessment of hydrokinetic resources of small and medium-size rivers: The Lithuanian case.Baltica 30, 23–30

Shafei, M. A. R., Ibrahim, D. K., Ali, A. M., Younes, M. A. A., &Abou El-Zahab, E. E. D. (2015). Novel approach for hydrokinetic turbine applications. Energy for Sustainable Development, 27, 120-126.

Shaughnessy, B. M., &Probert, S. D. (1992).Partially-blockedSavonius rotor. Applied Energy, 43(4), 239-249.

Singh, K. V., Bansal, H. O., & Singh, D. (2019).A comprehensive review on hybrid electric vehicles: architectures and components. Journal of Modern Transportation, 27(2), 77–107. https://doi.org/10.1007/s40534-019-0184-3

Singh, O., Saini, G., & De, A. (2024).Hydrodynamic performance enhancement of Savonius hydrokinetic turbine using wedge-shaped triangular deflector in conjunction with circular deflector.Ocean Engineering, 292, 116572.

Song, K., Wang, W. Q., & Yan, Y. (2019).Numerical and experimental analysis of a diffuser-augmented micro-hydro turbine. Ocean Engineering, 171, 590-602.

Talukdar, P. K., Sardar, A., Kulkarni, V., &Saha, U. K. (2018).Parametric analysis of model Savonius hydrokinetic turbines through experimental and computational investigations. Energy Conversion and Management, 158, 36-49.

Tan, K. W., Kirke, B., &Anyi, M. (2021).Small-scale hydrokinetic turbines for remote community electrification. Energy for Sustainable Development, 63, 41-50.

Tigabu, M. T., Guta, D. D., &Admasu, B. T. (2019). Economics of hydro-kinetic turbine for off-grid application: A case study of Gumara River, Upper Blue Nile, Amhara, Ethiopia. International Journal of Renewable Energy Research (IJRER), 9(3), 1368-1375.

Tigabu, M. T., Wood, D. H., &Admasu, B. T. (2020). Resource assessment for hydrokinetic turbines in Ethiopian rivers and irrigation canals. Energy for Sustainable Development, 58, 209-224.)

Tiruye, G. A., Besha, A. T., Mekonnen, Y. S., Benti, N. E., Gebreslase, G. A., & Tufa, R. A. (2021). Opportunities and challenges of renewable energy production in Ethiopia.Sustainability, 13(18), 10381.

Yining,Y.(2020, April). Analysis of the Influence of Camber on Hydrodynamic Characteristics of Airfoil Based on FLUENT. In Journal of Physics: Conference Series (Vol. 1519, No. 1, p. 012020).

Yuce, M. I., &Muratoglu, A. (2015).Hydrokinetic energy conversion systems: A technology status review. Renewable and Sustainable Energy Reviews, 43, 72-82.

Vaz, J. R., Mesquita, A. L., Mesquita, A. L. A., de Oliveira, T. F., & Junior, A. C. P. B. (2019). Powertrain assessment of wind and hydrokinetic turbines with diffusers. Energy Conversion and Management, 195, 1012-1021.

World Bank Ethiopia Electricity Access 2000-2023.www.macrotrends.net. Retrieved 2023-12-23.

https://www.alibaba.com/product-detail/ST-STC-Double-bearing-12-5KVA

https://www.alibaba.com/product-detail/ST-STC-Double-bearing-12-5KVA

APPENDIX

ANSYS fluent results

With curtain moment coefficient

At TSR=0.2

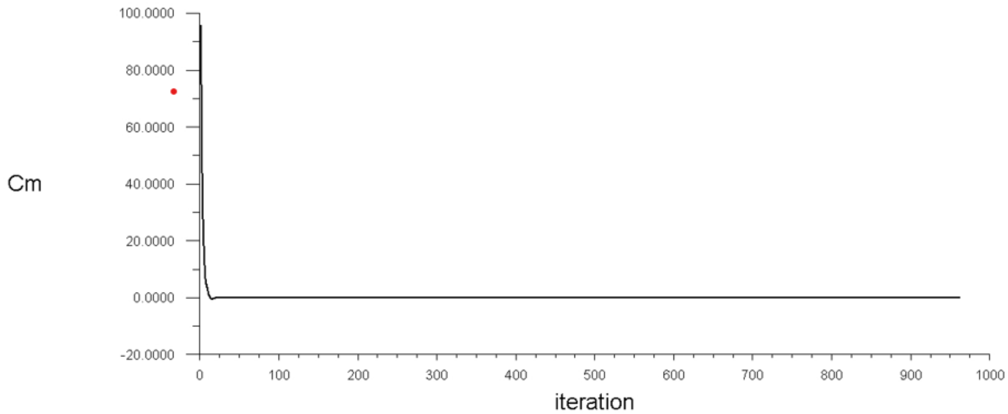

At TSR=0.4

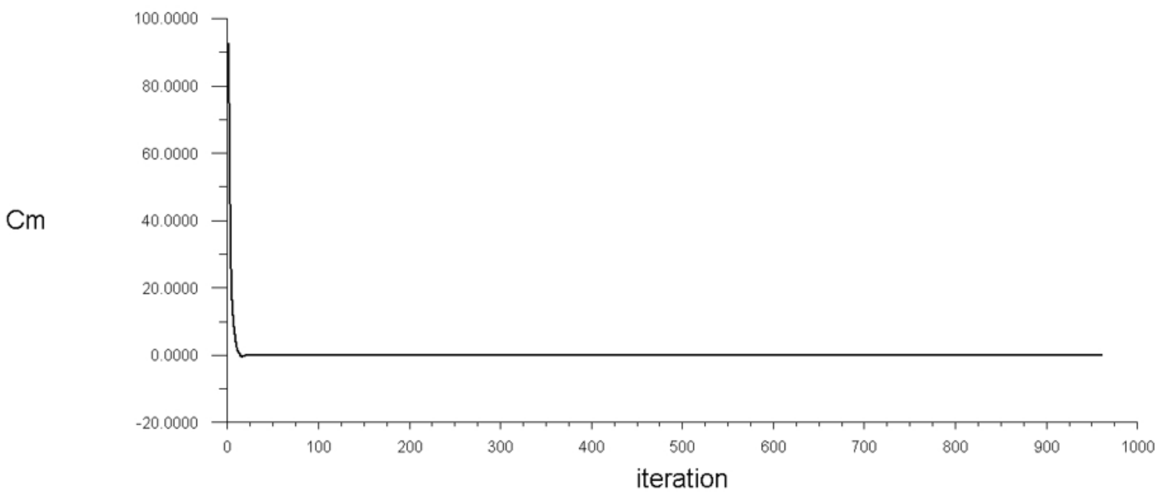

At TSR=0.6

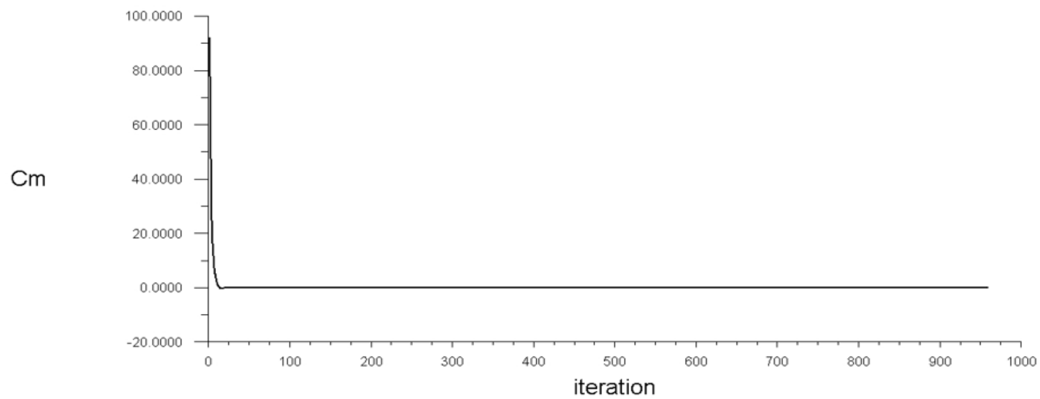

At TSR=0.8

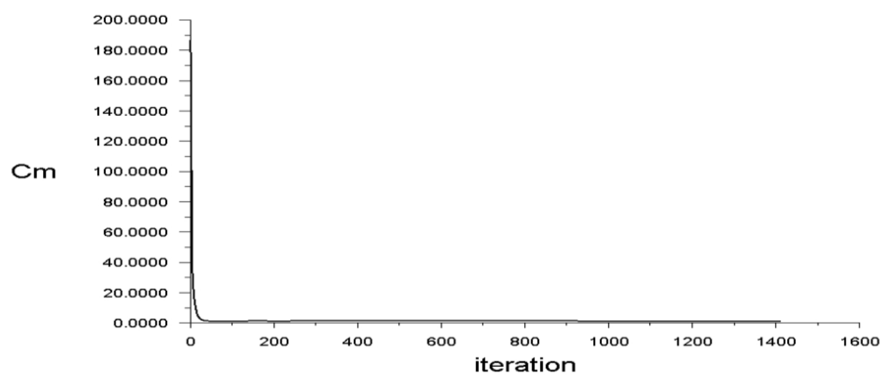

At TSR=1

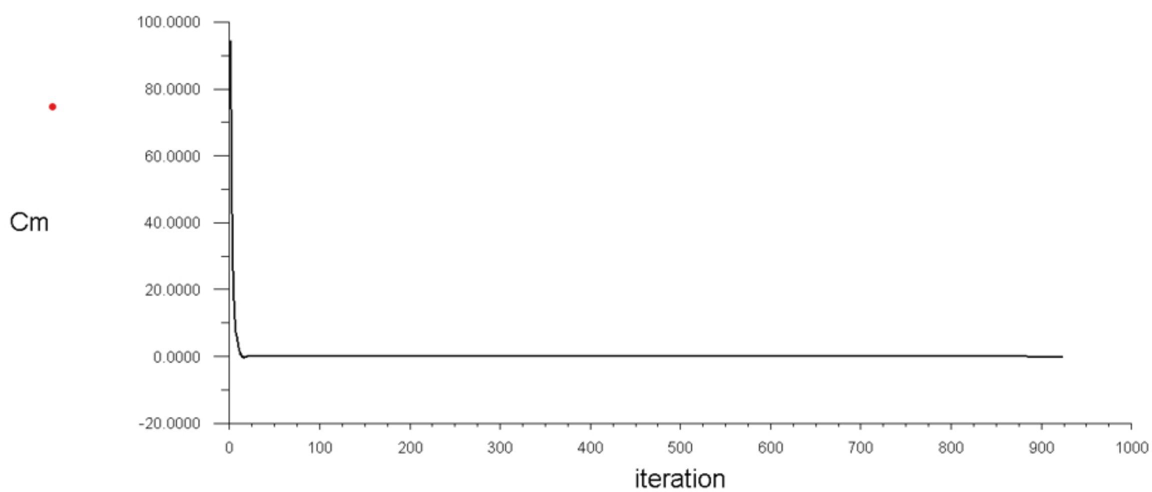

Without curtain moment coefficient

At TSR=0.2

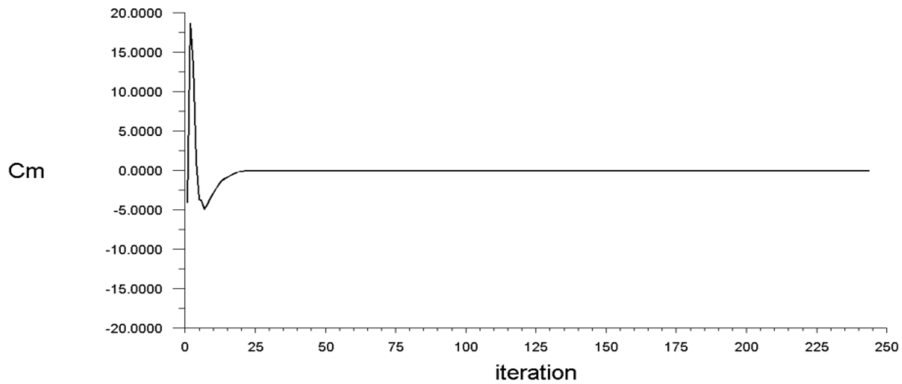

At TSR=0.4

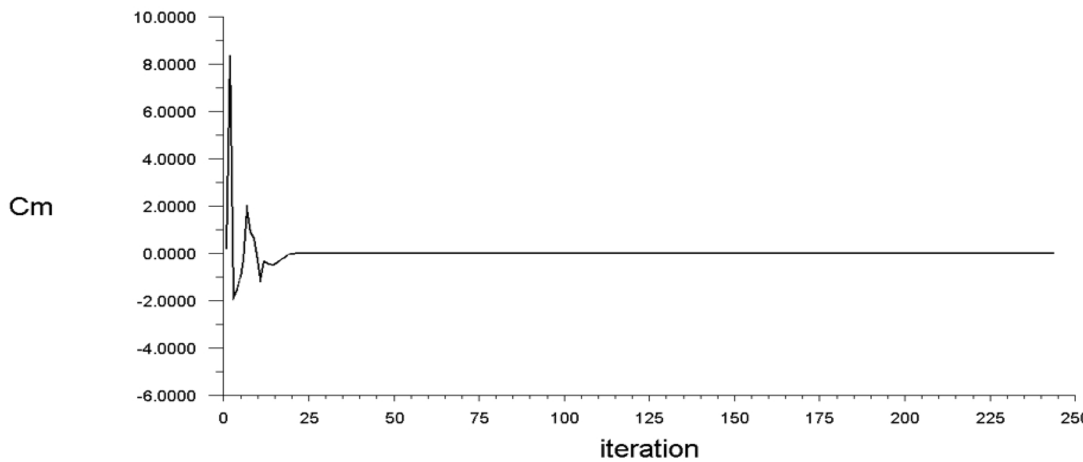

At TSR=0.6

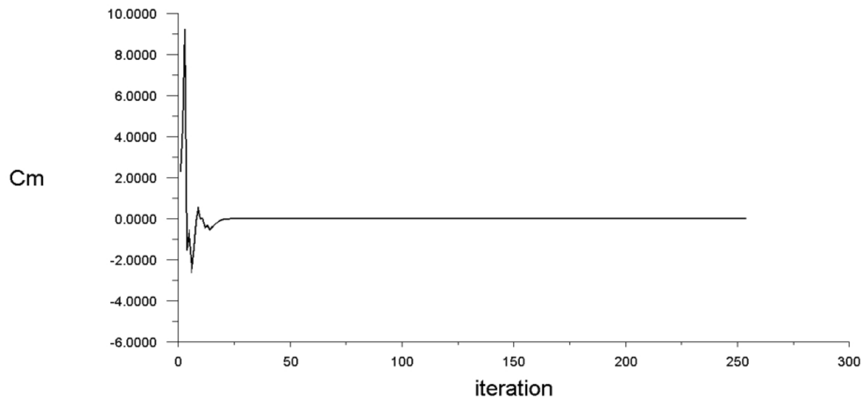

At TSR=0.8

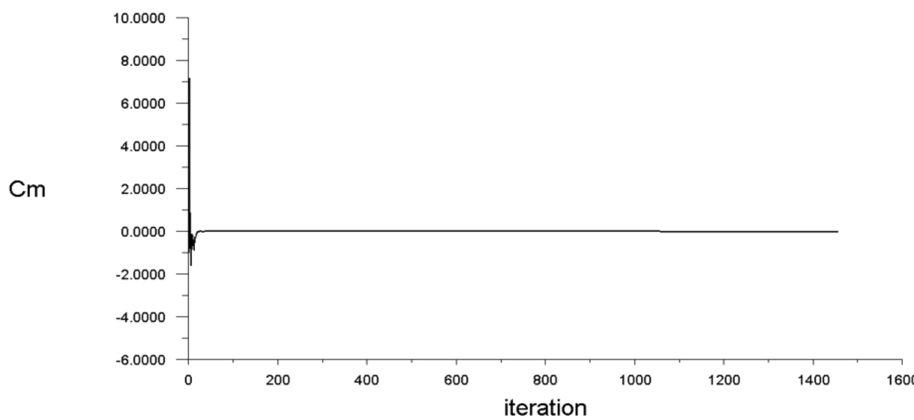

AT TSR=1

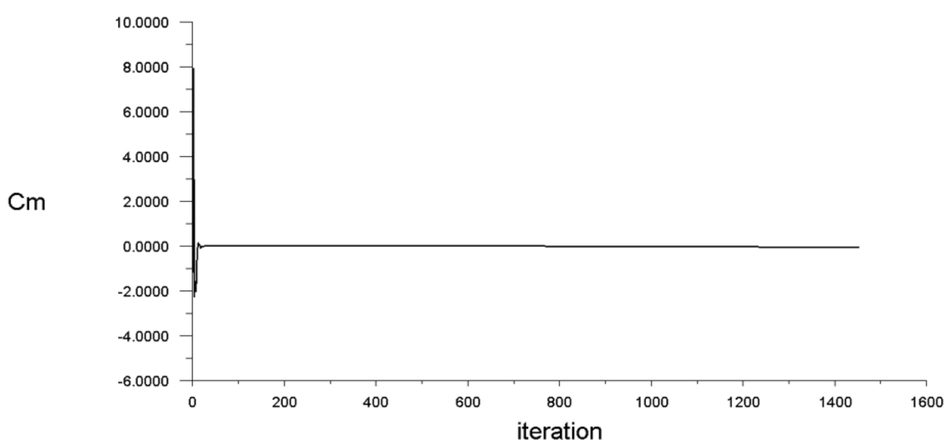

Generator selecting table

Three Phase A.C.synchronous STC alternator:

Model	Rated Output		Power Factor	Speed(rpm)	Pole number	voltage(v)
	Kva	Kw		50Hz/60Hz		
STC-3	3.8	3	0.8	1500/1800	4	110/220 220/380 230/400 240/415 254/440
STC-5	6.3	5	0.8	1500/1800	4	
STC-7.5	9.4	7.5	0.8	1500/1800	4	
STC-10	12.5	10	0.8	1500/1800	4	
STC-12	15	12	0.8	1500/1800	4	
STC-15	18.8	15	0.8	1500/1800	4	
STC-20	25	20	0.8	1500/1800	4	
STC-24	30	24	0.8	1500/1800	4	
STC-30	37.5	30	0.8	1500/1800	4	
STC-40	50	40	0.8	1500/1800	4	
STC-50	62.5	50	0.8	1500/1800	4	

Gear selecting catalogue

SS Module 1

Spur Gears

Specifications	
Precision grade	JIS grade N8 (JIS B1702-1: 1998)
Gear teeth	Standard full depth
Pressure angle	20°
Material	S45C
Heat treatment	—
Tooth hardness	(less than 194HB)
Surface treatment	Black oxide coating

H

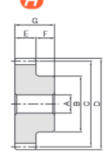

S1

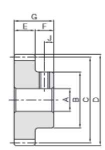

S1T

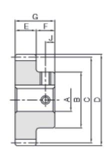

S1K

(H) To order Hardened Plus, please specify Catalog No. + H. Example: SS1-50H

Catalog Number		Module	No. of teeth	Shape	Bore	Hub dia.	Pitch dia.	Outside dia.	Face width	Hub width	Total length	Keyway	Socket head screw	
					AH7	B	C	D	E	F	G	Width × Depth	Size	J
SS1-50	H	m1	50	S1	10	35	50	52	10	10	20	—	—	—
SS1-50A				S1T	8							—	M5	5
SS1-52	H		52	S1	10		52	54				—	—	—
SS1-54	H		54	S1	10		54	56				—	—	—
SS1-55	H		55	S1	10		55	57				—	—	—
SS1-56	H		56	S1	10		56	58				—	—	—
SS1-58	H		58	S1	10		58	60				—	—	—
SS1-60	H		60	S1	10		60	62				—	—	—
SS1-60C				S1K	15							5 x 2.3	M4	5
SS1-62	H		62	S1	10	40	62	64				—	—	—
SS1-64	H		64	S1	10		64	66				—	—	—
SS1-65	H		65	S1	10	40	65	67				—	—	—
SS1-66	H		66	S1	10		66	68				—	—	—
SS1-68	H		68	S1	10		68	70				—	—	—
SS1-70	H		70	S1	10		70	72				—	—	—
SS1-72	H		72	S1	10		72	74				—	—	—
SS1-75	H		75	S1	10		75	77				—	—	—
SS1-76	H		76	S1	10		76	78				—	—	—
SS1-80	H		80	S1	10		80	82				—	—	—
SS1-84	H		84	S1	10		84	86				—	—	—
SS1-85	H		85	S1	10		85	87				—	—	—
SS1-88	H		88	S1	10		88	90				—	—	—
SS1-90	H		90	S1	10		90	92				—	—	—
SS1-95	H		95	S1	10		95	97				—	—	—
SS1-96	H		96	S1	10		96	98				—	—	—
SS1-100	H		100	S1	10		100	102				—	—	—
SS1-110	H		110	S1	15	50	110	112				—	—	—
SS1-120	H		120	S1	15	50	120	122				—	—	—
SS1-150	H		150	S1	20	120	150	152				—	—	—
SS1-200	H		200	S1	20	160	200	202				—	—	—

Allowable torque						Backlash (mm)	Weight (kg)	Catalog Number
Bending strength		Surface durability		Surface durability (H)				
N·m	kgf·m	N·m	kgf·m	N·m	kgf·m			
19.5	1.98	2.32	0.24	10.7	1.09	0.08~0.18	0.22	SS1-50
							0.22	SS1-50A
20.4	2.08	2.52	0.26	11.6	1.18		0.23	SS1-52
21.4	2.18	2.73	0.28	12.5	1.28		0.24	SS1-54
21.8	2.23	2.83	0.29	13.0	1.33		0.25	SS1-55
22.3	2.28	2.94	0.30	13.5	1.38		0.26	SS1-56
23.3	2.37	3.17	0.32	14.5	1.48		0.27	SS1-58
24.2	2.47	3.40	0.35	15.6	1.59		0.29	SS1-60
							0.27	SS1-60C
25.2	2.57	3.64	0.37	16.7	1.70		0.32	SS1-62
26.2	2.67	3.89	0.40	17.8	1.81		0.34	SS1-64
26.6	2.72	4.02	0.41	18.4	1.87		0.35	SS1-65
27.1	2.77	4.15	0.42	18.9	1.93		0.35	SS1-66
28.1	2.86	4.42	0.45	20.1	2.05		0.37	SS1-68
29.1	2.96	4.70	0.48	21.4	2.18		0.39	SS1-70
30.0	3.06	4.98	0.51	22.6	2.31		0.41	SS1-72
31.5	3.21	5.43	0.55	24.6	2.51		0.43	SS1-75
32.0	3.26	5.59	0.57	25.3	2.58		0.44	SS1-76
33.9	3.46	6.23	0.63	28.1	2.87		0.48	SS1-80
35.8	3.66	6.90	0.7	31.1	3.17		0.52	SS1-84
36.3	3.71	7.08	0.72	31.8	3.25		0.53	SS1-85
37.8	3.85	7.62	0.78	34.2	3.48		0.56	SS1-88
38.8	3.95	7.98	0.81	35.8	3.65		0.59	SS1-90
41.2	4.20	8.95	0.91	40.0	4.08		0.64	SS1-95
41.7	4.25	9.15	0.93	40.8	4.16		0.65	SS1-96
43.7	4.45	9.97	1.02	44.4	4.53		0.70	SS1-100
48.6	4.95	12.2	1.24	53.9	5.50		0.87	SS1-110
53.5	5.45	14.7	1.50	64.4	6.57		1.01	SS1-120
68.2	6.96	23.6	2.41	102	10.4		2.23	SS1-150
71.5	7.29	33.6	3.42	144	14.7		4.00	SS1-200

Pump selecting catalogue

型号 Type	流量Flow		扬程 Lift head (m)	转速 Rotation speed (r/min)	功率 Power (kw)
	(m^3/h)	L/s			
15-80	1.5	0.42	8	2800	0.18
20-110	2.5	0.69	15	2800	0.37
20-160	2.5	0.69	32	2900	1.1
25-100	4	1.11	15	2900	0.55
25-125	4	1.11	20	2900	0.75
25-160	4	1.11	32	2900	1.5
25-160A	3.7	1.03	28	2900	1.1
32-100(I)	6.3	1.75	12.5	2900	0.75
32-125(I)	6.3	1.75	20	2900	1.1
32-160(I)	6.3	1.75	32	2900	2.2
32-200(I)	6.3	1.75	50	2900	4.0
40-100	6.3	1.75	12.5	2900	0.75
40-125	6.3	1.75	20	2900	1.1
40-125A	5.6	1.56	16	2900	0.75
40-160	6.3	1.75	32	2900	2.2
40-160A	5.9	1.64	28	2900	1.5
40-160B	5.2	1.53	24	2900	1.1
40-200	6.3	1.75	50	2900	4.0
40-200A	5.9	1.64	44	2900	3.0
40-200B	5.5	1.53	38	2900	2.2
40-250	6.3	1.75	80	2900	7.5
40-250A	5.9	1.64	70	2900	5.5
40-250B	5.5	1.53	60	2900	4.0
40-100(I)	12.5	3.47	12.5	2900	1.1
40-100(I)A	11.2	3.11	10	2900	0.75
40-125(I)	12.5	3.47	20	2900	1.5
40-125 (I)A	11.2	3.11	17.2	2900	1.1
40-160(I)	12.5	3.47	32	2900	3.0
40-160(I)A	11.7	3.25	28	2900	2.2
40-160(I)B	10.5	2.92	22.5	2900	1.5
40-200(I)	12.5	3.47	50	2900	5.5
40-200(I)A	11.7	3.25	44.5	2900	4.0
40-200(I)B	10.5	2.92	35	2900	3.0
40-2501(I)	12.5	3.47	80	2900	11.0
40-250(I)A	11.7	3.25	70	2900	7.5
40-250(I)B	10.5	3.0	60	2900	7.5
50-100	12.5	3.47	12.5	2900	1.1
50-100A	11.2	3.11	10	2900	0.75
50-125	12.5	3.47	20	2900	1.5
50-125A	11.2	3.11	17.2	2900	1.1
50-160	12.5	3.47	32	2900	3.0
50-160A	11.7	3.25	28	2900	2.2
50-160B	12.5	2.92	22.5	2900	1.5
50-200	12.5	3.47	50	2900	5.5
50-200A	11.7	3.25	44.5	2900	4.0
50-200B	10.5	2.92	35	2900	3.0
50-250	12.5	3.47	80	2900	11.0
50-250A	11.7	3.25	70	2900	7.5
50-250B	10.8	3.0	60	2900	7.5
50-100(I)	25	6.94	12.5	2900	1.5
50-100(I)A	22.4	6.22	10	2900	1.1

型号 Type	流量Flow		扬程 Lift head (m)	转速 Rotation speed (r/min)	功率 Power (kw)
	(m^3/h)	L/s			
50-125(I)	25	6.94	20	2900	3.0
50-125(I)A	22.4	6.22	16	2900	2.2
50-160(I)	25	6.94	32	2900	4.0
50-160(I)A	23.4	6.5	28	2900	4.0
50-160(I)B	21.6	6.0	24	2900	3.0
50-200(I)	25	6.94	50	2900	7.5
50-200(I)A	23.4	6.5	44	2900	7.5
50-200(I)B	21.6	6.0	37	2900	5.5
50-250(I)	25	6.94	80	2900	15
50-250(I)A	23.4	6.5	70	2900	11
50-250(I)B	21.6	6.0	60	2900	11
50-315(I)	25	6.94	125	2900	30
50-315(I)A	23.4	6.5	110	2900	22
50-315(I)B	21.6	6.0	93	2900	18.5
65-100	25	6.94	125	2900	1.5
65-100A	22.4	6.22	10	2900	1.1
65-125	25	6.94	20	2900	3.0
65-125A	22.4	6.22	16	2900	2.2
65-160	25	6.64	32	2900	4.0
65-160A	23.4	6.5	28	2900	4.0
65-160B	21.6	6.0	24	2900	3.0
65-200	25	6.94	50	2900	7.5
65-200A	23.4	6.5	44	2900	7.5
65-200B	21.6	6.0	37	2900	5.5
65-250	25	6.94	80	2900	15
65-250A	23.4	6.5	70	2900	11
65-250B	21.6	6.0	60	2900	11
65-315	25	6.94	125	2900	30
65-315A	23.4	6.5	110	2900	22
65-315B	21.6	6.0	93	2900	18.5
65-100(I)	50	13.9	12.5	2900	3.0
65-100(I)A	44.8	12.4	10	2900	2.0
65-125(I)	50	13.9	20	2900	5.5
65-100(I)A	44.8	12.4	16	2900	4.0
65-160(I)	50	13.9	32	2900	7.5
65-160(I)A	46.8	13.0	28	2900	7.5
65-160(I)B	43.2	12.0	24	2900	5.5
65-200(I)	50	13.9	50	2900	15
65-200(I)A	46.8	13.0	44	2900	11
65-200(I)B	43	11.9	37	2900	7.5
65-250(I)	50	13.9	80	2900	22
65-250(I)A	46.8	13.0	70	2900	18.5
65-250(I)B	43	11.9	60	2900	15
65-315(I)	50	13.9	125	2900	37
65-315(I)A	45.8	12.7	105	2900	30
65-315(I)B	43	11.9	93	2900	30
80-100	50	13.9	12.5	2900	3.0
80-100A	44.8	12.4	10	2900	2.2
80-125	50	13.9	20	2900	5.5
80-125A	44.8	12.4	16	2900	4.0
80-160	50	13.9	32	2900	7.5